

**ENVIRONMENTAL
SERVICES, INC.**

524 S. New Hope Road
Raleigh, North Carolina 27610
(919) 212-1760
(919) 212-1707 FAX

www.environmentalservicesinc.com

Site Locations
Proposed GLE Facility
New Hanover County, North Carolina

Project:	ER07155.00
Date:	Oct 07
Drwn/Chkd:	ESL/SS
Figure:	6.1



View of site 31NH800**, facing east



View of site 31NH800** from dirt road, facing west



**ENVIRONMENTAL
SERVICES, INC.**

524 S. New Hope Road
Raleigh, North Carolina 27610
(919) 212-1760
(919) 212-1707 Fax

www.environmentalservicesinc.com

Photos-Site 31NH800**
Proposed GLE Facility
New Hanover County, North Carolina

Project: ER07155.00

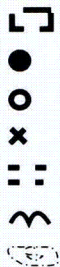
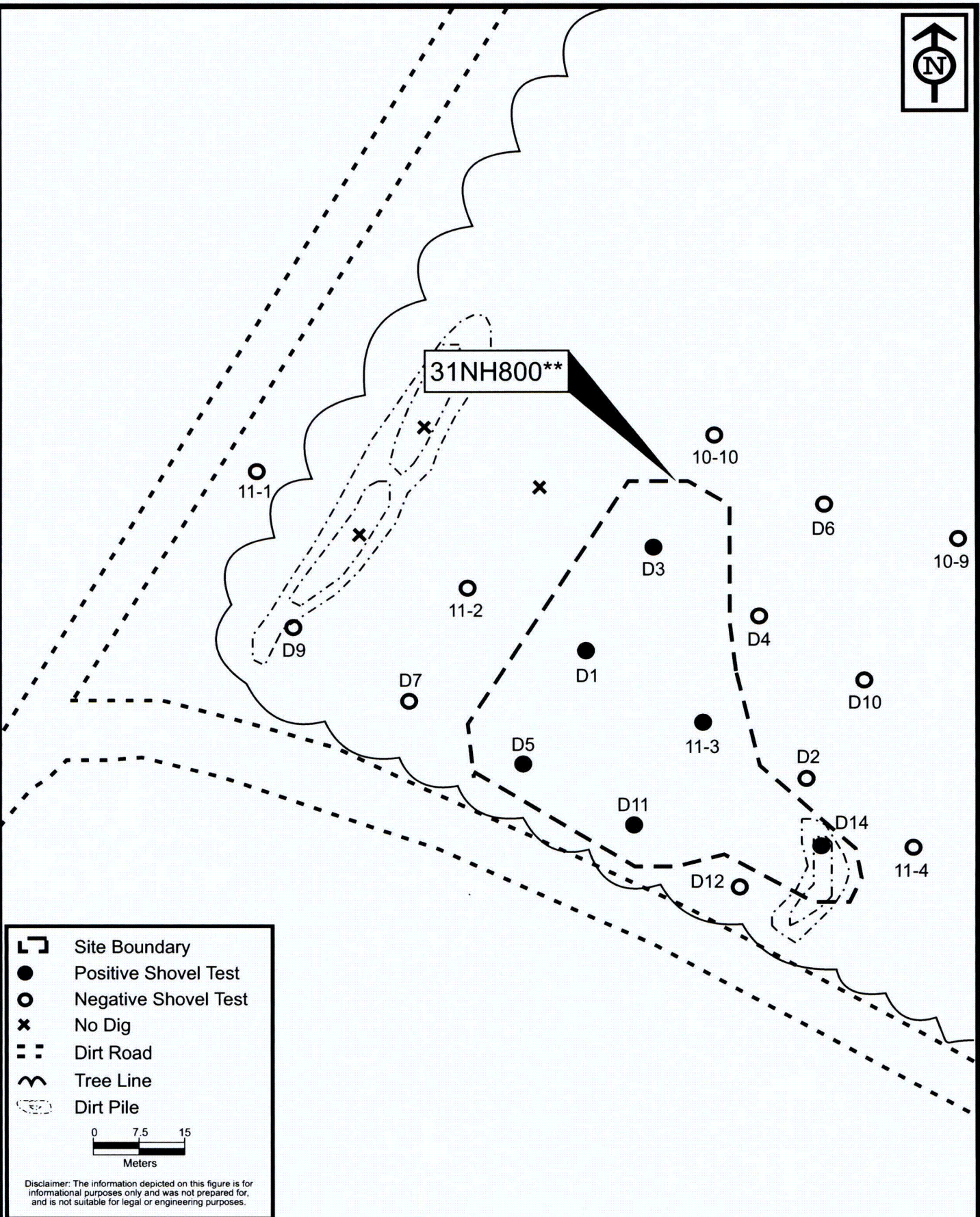
Date: Nov 2007

Drwn/Chkd: MP/SS

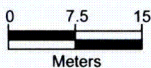
Figure: **6.2**



31NH800**



Site Boundary
Positive Shovel Test
Negative Shovel Test
No Dig
Dirt Road
Tree Line
Dirt Pile



Disclaimer: The information depicted on this figure is for informational purposes only and was not prepared for, and is not suitable for legal or engineering purposes.



ENVIRONMENTAL SERVICES, INC.
524 S. New Hope Road
Raleigh, North Carolina 27610
(919) 212-1760
(919) 212-1707 Fax
www.environmentalservicesinc.com

Site Plan-31NH800**
Proposed GLE Facility
New Hanover County, North Carolina

Project:	ER07155.00
Date:	Nov 2007
Drwn/Chkd:	MP/SS
Figure:	6.3



View of site 31NH801, facing south



View of site 31NH801 from dirt road, facing east

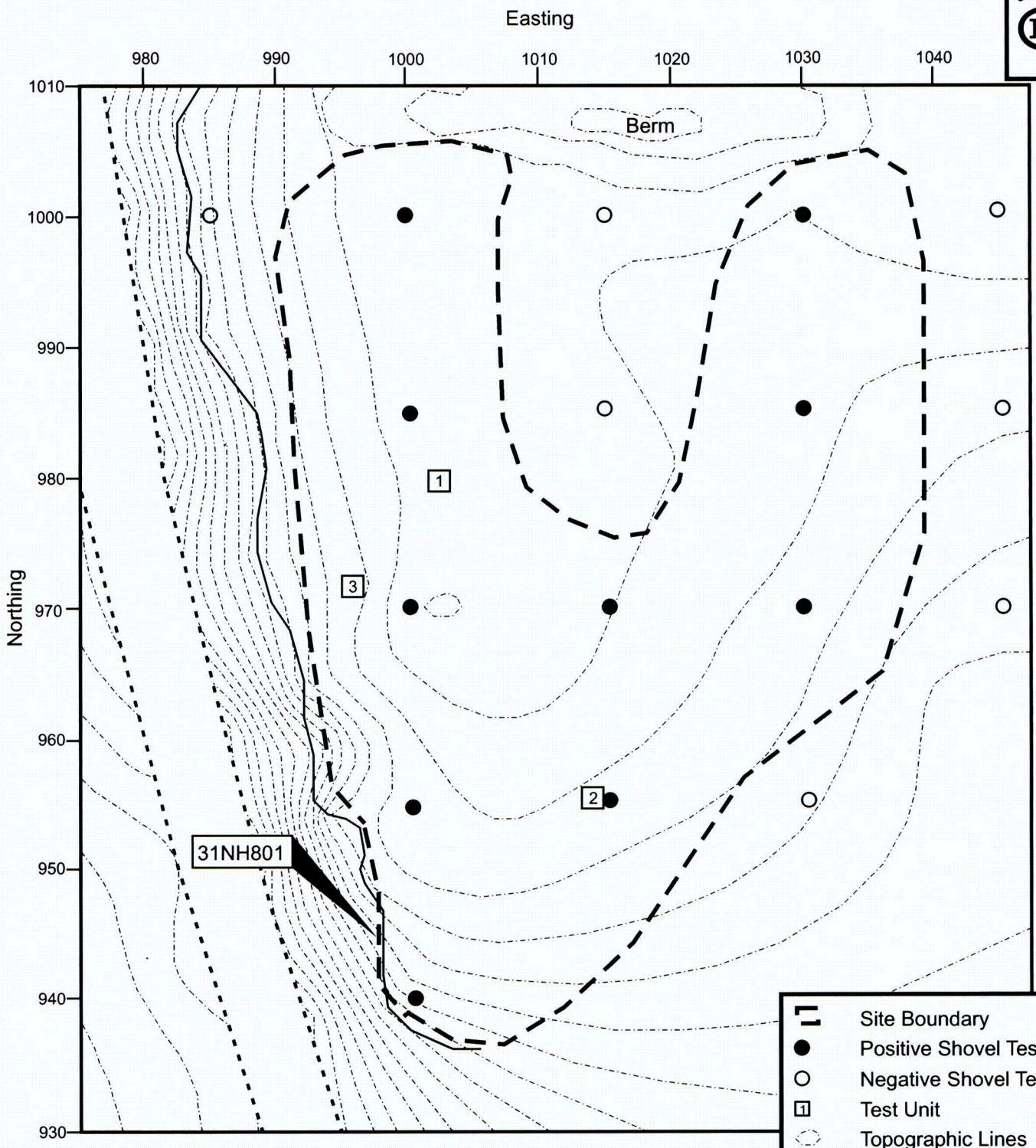



**ENVIRONMENTAL
SERVICES, INC.**


524 S. New Hope Road
Raleigh, North Carolina 27610
(919) 212-1760
(919) 212-1707 Fax
www.environmentalservicesinc.com


Photos-Site 31NH801
Proposed GLE Facility
New Hanover County, North Carolina

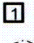
Project:	ER07155.00
Date:	Nov 2007
Drwn/Chkd:	MP/SS
Figure:	6.4





**Site Boundary**


**Positive Shovel Test**

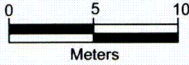
**Negative Shovel Test**

**Test Unit**

**Topographic Lines**

**Dirt Road**

**Bluff Edge**



0 5 10
Meters

Disclaimer: The information depicted on this figure is for informational purposes only and was not prepared for, and is not suitable for legal or engineering purposes.



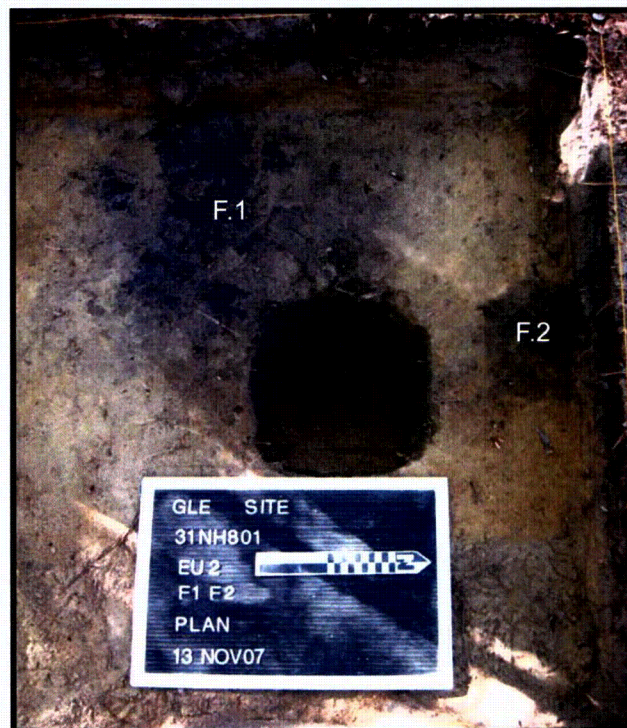
ENVIRONMENTAL SERVICES, INC.
524 S. New Hope Road
Raleigh, North Carolina 27610
(919) 212-1760
(919) 212-1707 Fax
www.environmentalservicesinc.com

Site Plan-31NH801
Proposed GLE Facility
New Hanover County, North Carolina

Project:	ER07155.00
Date:	Nov 2007
Drwn/Chkd:	MP/SS
Figure:	6.5



Typical soil profile for 31NH801



Features 1 and 2, EU 2



**ENVIRONMENTAL
SERVICES, INC.**

524 S. New Hope Road
Raleigh, North Carolina 27610
(919) 212-1760
(919) 212-1707 Fax
www.environmentalservicesinc.com

Photos-Site 31NH801
Proposed GLE Facility
New Hanover County, North Carolina

Project: ER07155.00

Date: Nov 2007

Drwn/Chkd: MP/SS

Figure: **6.6**

Table of Contents

P.1	Introduction.....	P-1
P.2	Conceptual Model.....	P-1
P.2.1	Location and Topography.....	P-1
P.2.2	Hydrogeologic Units.....	P-1
P.2.2.1	Surficial Aquifer	P-2
P.2.2.2	Semiconfining Layer	P-2
P.2.2.3	Principal Aquifer	P-2
P.2.3	Principal Aquifer Groundwater Flow.....	P-2
P.2.4	Hydrogeologic Parameters	P-3
P.2.5	Hydrogeologic Boundaries.....	P-3
P.2.5.1	Recharge	P-4
P.2.5.2	Groundwater/Surface-Water Interaction.....	P-4
P.2.5.3	Groundwater Pumping.....	P-5
P.3	Flow-Model Development and Results.....	P-5
P.3.1	Code Description	P-5
P.3.2	Finite-Difference Grid	P-5
P.3.3	Input Parameters and Boundary Conditions.....	P-6
P.3.3.1	Hydraulic Conductivity	P-6
P.3.3.2	Recharge	P-7
P.3.3.3	Stream Drain Boundaries.....	P-7
P.3.3.4	Effluent Channel River Boundary	P-7
P.3.3.5	Specified-Head Boundary.....	P-8
P.3.3.6	No-Flow Boundary	P-8
P.3.3.7	Pumping Wells.....	P-8
P.3.4	Flow-Model Calibration	P-8
P.3.4.1	Calibration Data Sets	P-8
P.3.4.2	Automated Calibration Procedure	P-8
P.3.4.3	Calibration Error Criteria.....	P-9
P.3.4.4	Flow Calibration Results	P-9
P.4	Model Calibration Update.....	P-10

List of Tables

P-1	Summary of Flow Model Parameters
P-2	Calibration Statistics and Measured and Model Heads

List of Figures

P-1	Location of GE/GNF Site and Hydrogeologic Features and Boundaries.
P-2	Principal Aquifer Goundwater Levels (Nov 1998).
P-3	Principal Aquifer Goundwater Levels (Oct 1999).
P-4	Principal Aquifer Goundwater Levels (Sep 2000).
P-5	Piezometric Head Difference Between the Surficial and Principal Aquifers (9/12/00).
P-6	Estimated Semiconfining-Layer Thickness.
P-7	Estimated Recharge for 9/12/00 Conditions.
P-8	Model Domain and Boundaries.
P-9	Model Finite-Difference Grid.
P-10	Top of Aquifer as Shown by Bain (1970).
P-11	Top of Model Aquifer.
P-12	Bottom of Model Aquifer.
P-13	Model Hydraulic Conductivity Distribution and Pilot Points.
P-14	Calibrated Model Recharge Distribution (11/20/98).
P-15	Calibrated Model Recharge Distribution (10/6/99).
P-16	Calibrated Model Recharge Distribution (9/12/00).
P-17	Measured versus Simulated Heads.
P-18	Calibrated Groundwater Elevations – Site Area, Nov 1998.
P-19	Calibrated Groundwater Elevations – Site Area, Oct 1999.
P-20	Calibrated Groundwater Elevations – Full Domain, Sep 2000.
P-21	Model 2004 Update – Calibration Curve.

Appendix P

Numerical Modeling of Groundwater Flow and Contaminant Transport in the Principal Aquifer at the Wilmington Site

P.1 Introduction

This document describes the development and application of a model to simulate groundwater flow and contaminant transport in the Principal Aquifer at the Wilmington Site. This document is derived from an appendix to the *2000-2001 Comprehensive Report of Organic Compounds in Groundwater* (RTI, 2002) and subsequent model calibration work conducted in 2004 (see **Section P.4**). Simulations for the analysis of the Proposed GLE Facility were performed using average recharge and water levels based on September 2003 data.

The primary goal of the modeling effort was to evaluate the effectiveness of the existing pumping-well network at containing the trichloroethylene (TCE) plumes in the active manufacturing central-eastern areas of the Wilmington Site. Specific additional objectives of the modeling effort included the following:

- Refine the conceptual model describing the Site hydrogeology and the transport of groundwater contaminants
- Develop and calibrate a quantitative, numerical groundwater flow model for the area that is consistent with the Site conceptual model
- Evaluate alternative groundwater-pumping scenarios
- Develop and calibrate a model to simulate the transport of TCE in groundwater
- Use the calibrated numerical flow model and transport models to simulate groundwater flow conditions at the Site and to predict future plume-migration patterns under alternative groundwater-pumping scenarios.

P.2 Conceptual Model

This section describes the conceptual model (i.e., the current qualitative understanding of the geology and hydrogeology of the Site and region and its relationship to the groundwater contamination). The conceptual model is the basis for the development of the quantitative flow and transport models.

P.2.1 Location and Topography

The Wilmington Site is located in northwest New Hanover County in the North Carolina Coastal Plain. Elevations in this region generally range between 0 and 50 feet (ft; 15 meters [m]) above mean sea level (msl). Based on review of the topographic map (**Figure P-1**) and other knowledge of the Site and region, the following features constitute major hydrogeologic boundaries for the groundwater-flow system: the Northeast Cape Fear River, streams (e.g., Ness Creek and Prince George Creek), the low-lying swampy areas, and the on-site effluent channel.

P.2.2 Hydrogeologic Units

The hydrogeologic units of interest in the Site area include the Surficial Aquifer, the semiconfining layer, and the Principal Aquifer.

P.2.2.1 Surfacial Aquifer

The Surfacial Aquifer includes undifferentiated, highly stratified deposits generally between 20 and 50 ft (6 and 15 m) msl. These sediments typically include terraced and barrier beach deposits, fossil sand dunes, and stream channel deposits. The sediment texture varies from medium to fine-grained sands to silts and clays. This aquifer is recharged directly by rainfall, and the water table is generally near the land surface (approximately from 0 to 10 ft [0 to 3 m] below ground). Discharge from the aquifer is into streams, drainage canals, and the low-lying swampy areas surrounding most of the upland areas. In addition, the Surfacial Aquifer recharges groundwater into the underlying Principal Aquifer in some areas.

P.2.2.2 Semiconfining Layer

Relatively less-permeable silty and clayey deposits underlie most of the Surfacial Aquifer and form the semiconfining layer. The semiconfining layer is a heterogeneous, interbedded unit that is not present in all areas. The semiconfining layer appears to be absent to the west and northwest of the Site. For example, a Site investigation indicated that there is no semiconfining layer in the Northwestern Site Sector (RTI, 1998).

P.2.2.3 Principal Aquifer

The Principal Aquifer lies below the Surfacial Aquifer and the semiconfining layer. The Principal Aquifer consists of the upper zones of the Peedee Formation, a Cretaceous-age deposit that includes greenish-gray to dark-gray silt and sand interbedded with semi-consolidated calcareous sandstone and limestone. The upper portion of the Principal Aquifer is generally the most permeable and contains more sand than the lower zones. The unit dips to the southeast (see **Figure 3.4-9**); the Principal Aquifer coincides with the "Sandstone Aquifer" as labeled in this figure.

According to Bain (1970), there is a regional geologic contact that divides the portion of New Hanover County where the Wilmington Site is located (see **Figure 3.4-10**). To the east of this contact, the Principal Aquifer corresponds to the more permeable, upper sandy portion of the Peedee Formation, identified as "Sandstone Aquifer" on the cross section shown in **Figure 3.3-22**. To the west of this geologic contact, the upper Peedee Formation unit pinches out, and the sediment has an increasing silt and clay component and a lower permeability. The semiconfining layer also disappears to the west of this contact, causing the Principal and Surfacial aquifers to essentially become the same hydrogeologic unit with similar properties. Because there is no semiconfining unit, the Principal Aquifer to the west and northwest of the geologic contact is a water-table (unconfined) aquifer rather than a confined aquifer. Although much of the area west of this contact at the Site has not been investigated thoroughly, the pattern has been confirmed for the northwest Site area, where the semiconfining unit is absent and the conductivities are relatively lower than in the eastern Site area (RTI, 1998).

P.2.3 Principal Aquifer Groundwater Flow

Because the focus of the modeling effort is on the Principal Aquifer, Surfacial Aquifer groundwater flow patterns will not be discussed here.

Figure 3.4-10 shows Principal Aquifer water levels collected throughout the Wilmington Site in 2007. As this figure indicates, groundwater flows from upland areas toward the surrounding hydrogeologic boundaries, including streams, the Northeast Cape Fear River, and the low-lying swampy area that surrounds much of the region. The primary input of groundwater to the Principal Aquifer system is recharge from leakage through the overlying semiconfining layer and from direct seepage of rainwater in areas where the semiconfining layer is absent (e.g., west and northwest of the geologic contact in **Figure**

3.3-22). In general, groundwater enters the system through recharge and flows outward toward the hydrogeologic boundaries.

Principal Aquifer water elevations in the area have fluctuated over a range of approximately 10 to 15 ft (3 to 4.5 m) from 1999 through 2007 (**Figure 3.4-11**). Even though the water levels have varied over this range, the resulting groundwater flow patterns have generally been similar throughout this period, as is evident in comparing the water-level contours in **Figures P-2** (relatively high water levels), **P-3** (relatively moderate water levels), and **P-4** (relatively low water levels) from November 1998, October 1999, and September 2000, respectively. The water-level contours in **Figures P-2 through P-4** were generated automatically using a kriging interpolation method; therefore, in some areas, the patterns are somewhat inconsistent with those shown in **Figure 3.4-10**, which was produced manually using hydrogeologic insight (e.g., in the vicinity of the effluent channel). Nevertheless, the contour patterns in the figures are similar, thus demonstrating the general consistency of water-level patterns over time.

P.2.4 Hydrogeologic Parameters

This section describes general information about hydrogeologic parameters that were developed from site-specific data and analyses, as well as through literature research. The approach for estimating the specific model parameter values for the model is presented below in **Sections P.3.3, P.3.4, P.4.3, and P.4.5**.

Estimates for hydraulic conductivity were developed using existing knowledge of the Wilmington Site, including slug tests, grain-size analyses, and pumping tests. Site-wide hydraulic conductivity measurements are shown in **Figure 3.4-12**.

Hydraulic conductivity results from the Wilmington Site indicate that there is a general increasing trend in hydraulic conductivity from the west to east across the Site. For example, slug-test data generated in the Northwestern Site Sector of the Wilmington Site indicate geometric-mean hydraulic-conductivity values of 3 ft/day (0.9 m/day) (RTI, 1998, 1999a). In contrast, pumping tests in pumping well WW-9A in the Eastern Site Sector indicate a hydraulic conductivity in the 40 ft/day (12 m/day) range (RTI, 1996). The average of hydraulic conductivity measurements for the waste treatment (WT) site area (also in located in the Eastern Site Sector, but west of well WW-9A) fall between the ranges measured for the Northwestern and the Eastern Site sectors of the Wilmington Site, with a geometric mean of 16.8 ft/day (5.1 m/day) (RTI, 1999b). This observation agrees with the assessment by Bain (1970) that there is a regional geologic contact dividing the portion of New Hanover County where the Wilmington Site is located, as shown in **Figure 3.3-22**. To the east of this contact, the Principal Aquifer corresponds to the more permeable, upper sandy portion of the Peedee Formation, identified as the "Sandstone Aquifer" on the cross section shown in **Figure 3.4-9**. The conductivity to the east is correspondingly in the upper range of measured values for the Site. To the west of this geologic contact, the older strata of the Peedee Formation outcrop, and these strata have an increasing silt and clay component, and thus, have lower hydraulic conductivities than the upper sandy portion of the Peedee Formation.

The flow modeling includes only steady-state simulations and does not have a temporal component; therefore, aquifer storage properties are not required.

P.2.5 Hydrogeologic Boundaries

The principal hydrogeologic boundaries for the system are recharge, discharge to streams, discharge to the low-lying swampy area, and discharge to the Northeast Cape Fear River. In addition, groundwater flows into and out of an effluent channel crossing the Site. Each of these boundaries is described below.

P.2.5.1 Recharge

Recharge to the Principal Aquifer from the Surficial Aquifer depends on the hydraulic gradient between these aquifers and the thickness and vertical hydraulic conductivity of the semiconfining layer. Because the semiconfining layer is a highly heterogeneous, interbedded geologic unit, the amount of leakage through this layer can vary greatly in different areas. For any given conductivity and thickness of the semiconfining layer, recharge to the Principal Aquifer would increase with the hydraulic head difference between the Surficial and Principal Aquifers. Accordingly, the recharge rate can be estimated using the following form of Darcy's law:

$$\text{Recharge Rate} = K_v (h_{surf} - h_{princ}) / L_{sl}$$

where K_v is the vertical hydraulic conductivity of the semiconfining layer, h_{surf} is the head in the Surficial Aquifer, h_{princ} is the head in the Principal Aquifer, and L_{sl} is the semiconfining layer thickness. An exception to this expression applies if the groundwater level in the Principal Aquifer were below the bottom of the semiconfining layer (e.g., in the immediate vicinity of pumping wells). In this case, h_{princ} should be the bottom of the semiconfining layer rather than the head in the Principal Aquifer (representing a seepage-face boundary where the Principal Aquifer is dewatered).

Figure P-5 shows the difference in the groundwater elevation between the Surficial and Principal aquifers based on data collected on September 12, 2000 (as described above, the bottom of the semiconfining layer is used where the aquifer is dewatered around some of the pumping wells). The Surficial Aquifer water levels are generally higher than the Principal Aquifer levels, with the difference varying between 2 and 18 ft (.6 to 5.4 m). The greatest differences are in the vicinity of the pumping wells, which have lowered the water levels in the Principal Aquifer. Combining the head difference in **Figure P-5** with the estimated thickness of the semiconfining layer (**Figure P-6**) and using an estimated vertical hydraulic conductivity of the semiconfining layer of 0.001 ft/day, the recharge to the Principal Aquifer is estimated to range approximately from 1 to 29 inches (2.5 to 74 centimeters [cm]) per year for the September 2000 time period (**Figure P-7**).

Small head differences between the Principal and Surficial aquifers could indicate relatively effective communication between these units (or even the absence of the semiconfining layer), where head gradients readily dissipate between the aquifers. In such areas, the above estimates of recharge would likely be inaccurate, because a greater volume of groundwater would be able to flow between the aquifers without a large head differential. One example is the Northwestern Site Sector where the semiconfining layer is absent. A calibrated, three-dimensional modeling of the Northwestern Site Sector (RTI, 1999a) suggested a recharge rate of 11.6 inches (29.5 cm) per year, which is about 23% of the annual average rainfall in the Wilmington area of 50 inches (127 cm) per year.

The recharge values developed using the above methodology were applied as initial estimates for the modeling; however, considering the uncertainty of recharge estimates in the Principal Aquifer system, the recharge was varied using an automated flow-model calibration procedure (described in **Section P.3.4**) that minimizes the differences between measured and simulated groundwater elevations. The recharge parameter varied during the model calibration was the conductivity of the Semiconfining Layer.

P.2.5.2 Groundwater/Surface-Water Interaction

At higher elevations in the region, groundwater in the Principal Aquifer does not typically interact significantly with most surface-water features (e.g., streams) because the stream beds are separated from the aquifer by the less-permeable semiconfining layer. However, at lower elevations, surface water has often incised through the semiconfining layer and is in direct connection with the Principal Aquifer;

therefore, the Principal Aquifer groundwater elevations typically are influenced by surface water only at lower elevations.

Due to historical dredging of the original streambed, the effluent channel is the only known exception to this pattern. Much of the original dredged depth of the effluent channel streambed has been filled in with relatively more permeable sandy, alluvial sediments, and the semiconfining layer is thin or absent along much of the dredged length of the effluent channel. Therefore, groundwater can flow more readily between the Principal Aquifer and the effluent channel in the dredged areas. Upstream of the WT area, the effluent channel water level is generally higher than the groundwater elevations, thus indicating a losing stream (surface water seeps into the Principal Aquifer). Downstream of the WT area, the groundwater level is generally higher than the effluent channel water level, thus indicating a gaining stream (Principal Aquifer groundwater discharges into the effluent channel).

The low-lying swampy area surrounding much of the region constitutes an additional major hydrogeologic boundary. Very strong upward vertical gradients in the swampy area (on the order of 0.15 in the Northwestern Site Sector) indicate that this area is a major groundwater-discharge boundary (RTI, 1998).

P.2.5.3 Groundwater Pumping

A system of active pumping wells is maintained across the facility (shown in **Figure 3.4-10**) to provide water for plant processes and to prevent off-site migration of groundwater contamination. The total volume pumped from each well is currently measured twice monthly. The total volume data were time-averaged by dividing the total volume by the total time between measurements. The pumping rates remain within fairly consistent ranges, although maintenance activities or periods of variable water demand can lead to pumping-rate adjustments. Also, the pumping rates are modified occasionally to adjust the control of the contaminant plumes.

P.3 Flow-Model Development and Results

This section describes the development of the groundwater flow model, including the code, the finite-difference grid, input parameters, and boundary conditions.

P.3.1 Code Description

The flow model code, MODFLOW-2000, is a three-dimensional, block-centered, finite-difference numerical model that was developed by the U.S. Geological Survey (USGS; Harbaugh et al., 2000; McDonald and Harbaugh, 1988). MODFLOW-2000 can solve for steady-state and transient conditions. Simulation output includes water balances and heads for each time step and layer. MODFLOW-2000 can handle multiple boundary conditions, including specified head, specified flux, and various mixed-type boundaries. The model can also simulate multiple hydraulic sources and sinks, including recharge, rivers, drains, lakes, pumping wells, injection wells, and evapotranspiration.

P.3.2 Finite-Difference Grid

The model domain includes the Site area of concern and extends outside of this area to include the relevant regional hydrogeologic boundaries for the Principal Aquifer (**Figure P-8**). The boundaries include the low-lying swampy area to the northwest and southwest, the Northeast Cape Fear River to the west, and Prince George Creek to the northwest. The eastern lateral edge of the model is estimated to be perpendicular to the groundwater flow in this area. Because groundwater does not flow perpendicular to flow paths, this eastern edge of the model is established as a no-flow boundary for the flow system.

The spacing of the finite-difference rows and columns is shown in **Figure P-9**. Relatively fine grid spacing is often required for accurate transport modeling; therefore, the established grid spacing is 100 ft (30.5 m) in the area encompassing measured groundwater impacts at the Wilmington Site. In order to decrease computer memory and processing requirements, the grid spacing was increased outside of this area. A coarser grid is adequate in these regions because the contaminant plumes do not extend to these areas, making transport modeling unnecessary. With the spacing described above, the finite-difference grid contains 124 columns and 81 rows, giving a total of 10,044 finite-difference cells.

The design of the model top elevation depends on the location within the model domain. To the east of the geologic contact, the model top corresponds to the top surface of the Principal Aquifer (the bottom of the semiconfining layer). This unit generally dips to the southeast. To the west of the geologic contact, the top of the model corresponds to the land surface because the semiconfining unit is absent in this area and the aquifer is a water-table aquifer. Note that for a simulated water-table aquifer, the top surface is typically the land surface, even though the water level is usually below this level and is determined as part of the simulation. In contrast, for a simulated confined aquifer, the top surface represents the actual top of the aquifer.

Within the Wilmington Site, the model top surface was estimated by interpolating data from well and boring logs across the Site. Outside of the Wilmington Site and to the west of the geologic contact, the top of the model was set to the ground surface elevation based on USGS digital elevation model (DEM) data, which provide surface elevations across the region. Outside of the Wilmington Site and to the east of the geologic contact, the top of the model dips to the east following information from Bain (1970), as shown in **Figure P-10**. **Figure P-11** shows the final model top elevation distribution.

The model includes one layer. To the east of the geologic contact, this layer corresponds to the more permeable and more sandy section of the Principal Aquifer. In this region, this model layer extends 35 ft (11 m) below the top of the Principal Aquifer, which is the typical thickness of the aquifer estimated by Bain (1970). The bottom surface of the layer was derived by subtracting 35 ft (11 m) from Bain's estimated top-of-aquifer surface (**Figure P-10**). To the west of the geologic contact, Bain's surface was extrapolated through the model domain, giving the final bottom elevation distribution shown in **Figure P-12**.

P.3.3 Input Parameters and Boundary Conditions

As discussed in **Section P.2.3**, groundwater generally flows from upland recharge areas outward into discharge areas, including the swampy area, the Northeast Cape Fear River, and streams. This section discusses the model treatment of each of these discharge features and the additional boundaries within the flow-model domain (shown in **Figure P-8**). **Table P-1** summarizes specific values associated with these boundary conditions and includes a brief description of the basis for the values. The remainder of this section describes the estimation of input parameters and boundary conditions in more detail.

P.3.3.1 Hydraulic Conductivity

The model hydraulic conductivity distribution is based on a series of "pilot points" shown in **Figure P-13**. The hydraulic conductivity distribution is determined by interpolating (using a kriging algorithm) between conductivity values at each of these points. **Figure P-13** also shows the calibrated hydraulic conductivity field and the associated values of the conductivity at each of the pilot points. The resulting distribution varies continuously across the domain rather than being constant within areal parameter zones. The conductivity values at the pilot points were adjusted during calibration using the automated calibration procedure described below in **Section P.3.4**. Note that no measurements were performed at the off-site pilot-point locations shown in **Figure P-13**; nevertheless, the model-estimated conductivity

distribution compares well with the measured conductivities at the Site, as is evident when comparing **Figure P-13** with **Figure 3.4-12**.

P.3.3.2 Recharge

Recharge is represented through a recharge boundary in MODFLOW, which delivers a specified flux of groundwater to the top of the model. This recharge boundary extends throughout the model domain. Within the primary area of concern for the model, an initial estimate of the recharge was developed in **Section P.2.5.1**. Outside of this primary area of interest, the recharge was estimated as being constant within a series of recharge zones shown in **Figures P-14, P-15, and P-16**. These figures also show the calibrated recharge distribution resulting from the automated calibration procedure described below in **Section P.3.4**. The zonal recharge values and the semiconfining unit hydraulic conductivity (used to calculate the recharge within the primary area of interest) were adjusted automatically by the calibration routine.

P.3.3.3 Stream Drain Boundaries

As discussed in **Section P.2.5.2**, groundwater from the Principal Aquifer typically discharges to streams only at lower elevations, where the streams have incised through the semiconfining layer. At upper elevations, the semiconfining layer prevents significant interaction between streams and the Principal Aquifer. In this situation, streams can be represented in MODFLOW as drain boundaries. A drain boundary only allows groundwater to leave the system through discharge to the boundary. The rate of flux out of the system through a drain depends on the specified elevation of the drain and the surrounding groundwater piezometric head. If the piezometric head falls below the drain elevation, the boundary becomes inactive, and groundwater does not enter (or leave) the groundwater system through the drain. Likewise, the flux of water leaving the groundwater system increases as the piezometric head increases relative to the drain elevation. Drain elevations were set based on the estimated average elevation of water in the stream beds, which was derived through review of the topographic map and Site observation.

The flux of groundwater out of a drain boundary is also controlled by a conductance parameter, which is linearly proportional to the flux. For the drain boundaries, the conductance was set to a high enough value to allow nearly the maximum amount of flow out of the system. With a high conductance value, the drains are essentially specified head boundaries with the important difference that they only allow flow out of the groundwater system and are inactive if the piezometric head is below the drain elevation.

As **Figure P-8** shows, drain boundaries are specified for three streams to the south and southwest of the Wilmington Site, one stream to the north, and a portion of Prince George Creek along the northern model boundary.

P.3.3.4 Effluent Channel River Boundary

The effluent channel is modeled as a river boundary. This boundary is similar to a drain boundary, as described in **Section P.3.3.3**; however, groundwater can either enter or exit the flow system through river boundaries. If the hydraulic head in the aquifer is greater than the river boundary elevation, groundwater discharges into the river. If the head in the aquifer is less than the river elevation, water from the river recharges the aquifer. This treatment of the effluent channel is based on the interpretation that the effluent channel is a losing stream in its upper reaches and a gaining stream in its lower reaches (as described in **Section P.2.5.2**). The conductance of the effluent channel was varied along its length based on the interpretation that dredging led to caused variable degrees of communication with the Principal Aquifer. In addition, the effluent channel intersects the Principal Aquifer downstream where the conductance values are greatest. The conductance varies from 0.1 ft/day (0.03 m/day) at the channel's eastern edge to 100 ft/day (30.5 m/day) at its western edge. (Note that these values are expressed as the hydraulic

conductivity times the boundary width divided by the boundary thickness. This value is then multiplied by the finite-difference cell length to yield the actual boundary-conductance value.) The elevation of the effluent channel drain boundary was set based on both the topographic map and water elevations measured at effluent-channel stream gauges.

P.3.3.5 Specified-Head Boundary

Specified-head boundaries are used to describe the swampy area, the Northeast Cape Fear River, and much of Prince George Creek, which surround the model domain to the west, south, and much of the north, as shown in **Figure P-8**. The elevation of this boundary was estimated to be 3 ft (0.9 m) msl based on the topographic contour map.

P.3.3.6 No-Flow Boundary

The eastern lateral edge of the model is estimated to be perpendicular to the groundwater flow in this area. Groundwater does not flow perpendicular to flow paths; therefore, this eastern edge of the model is established as a no-flow boundary for the flow system. Also, the bottom of the model was set as a no-flow boundary because there is no evidence of significant interaction between the modeled groundwater flow system and groundwater flow deeper than the lower model boundary.

P.3.3.7 Pumping Wells

The pumping wells were modeled as specified flux boundaries. The pumping rates were estimated from site-specific data, as described in **Section P.2.5.3**.

P.3.4 Flow-Model Calibration

Minimization of the error between the simulated and measured results was achieved using an automated calibration procedure implemented using PEST, a nonlinear parameter estimation software. This method automatically adjusts the calibration parameters until a numerical error criterion (the root mean squared) is minimized. In addition to PEST, calibration curves (x-y plots of the simulated versus the measured heads) and alternative quantitative error criteria were reviewed.

P.3.4.1 Calibration Data Sets

The goal of model calibration is to minimize the differences between measured and simulated values. For the flow model, simulated groundwater elevations were compared with elevations measured during three time periods: November 1998 (**Figure P-2**), October 1999 (**Figure P-3**), and September 2000 (**Figure P-4**). These datasets each included groundwater elevations from all of the active monitoring wells at the Site. In addition, these datasets represent conditions at relatively low, high, and medium groundwater elevations, as described in **Section P.2.3**.

P.3.4.2 Automated Calibration Procedure

The PEST automated calibration procedure was set up to estimate values for the following parameters:

- The hydraulic conductivity at each pilot point location (**Figure P-13**)
- Recharge within the constant-value recharge zones (**Sections P.2.5.1 and P.3.3.2 and Figures P-14, P-15, and P-16**)
- The semiconfining layer hydraulic conductivity within the Site area (**Sections P.2.5.1 and P.3.3.2**).

PEST allows automated calibration and incorporates powerful techniques of regularization. Regularization provides stability to the parameter-estimation process. Regularization involves additional “regularization observations” that constrain and control the direction of the parameter-estimation process. The following regularization constraints were included in the GE/GNF model calibration:

- The differences in hydraulic conductivity between adjacent pilot points were minimized. This constraint allowed the conductivity field to vary smoothly and only to deviate from homogeneity to the extent necessary to calibrate the model. (Note that adjacency between pilot points was determined by constructing a triangulated irregular network [TIN] between the points).
- The differences between adjacent recharge-zone values were minimized. Similar to the hydraulic conductivity, this constraint caused the recharge distribution only to deviate from homogeneity to the extent necessary to calibrate the model.

P.3.4.3 Calibration Error Criteria

Several quantitative error criteria are available, including: (1) mean error (ME), (2) mean absolute error (MAE), (3) root mean squared error (RMS), (4) RMS divided by the range of measured head values, (5) maximum residual, and (6) minimum residual.

The ME is the arithmetic average of the residuals (a residual value is the measured head subtracted from the simulated head at a particular point):

$$ME = \frac{\sum_{i=1}^n h_{meas} - h_{model}}{n}$$

where h_{meas} is a measured head value, h_{model} is the simulated head value, and n is the total number of measurements. The MAE is the mean of the absolute value of the residuals:

$$MAE = \frac{\sum_{i=1}^n |h_{meas} - h_{model}|}{n}$$

The RMS is calculated by squaring the residuals, taking an average of the squared residuals, and then taking the square root of the result:

$$RMS = \sqrt{\frac{\sum_{i=1}^n (h_{meas} - h_{model})^2}{n}}$$

The RMS divided by the range is calculated by dividing the RMS by the overall range of measured head values (the minimum measured head subtracted from the maximum measured head).

P.3.4.4 Flow Calibration Results

Table P-2 provides the quantitative calibration results, including the residual values, ME, MAE, and RMS. All of these values indicate that the modeled heads are very close on average to the measured values, thereby providing an effective calibration to measured results. **Figure P-17** shows a graph of the

modeled versus the measured heads. The plotted values in this figure follow a linear pattern, and there is no clustering of data in particular regions above or below the $x=y$ line, indicating that there is no systematic bias in the calibration results. This figure includes the results of a linear regression of the calibration curve. The slope of the regression line (0.9958) is very close to the ideal result of 1.0. Also, the coefficient of determination, or R^2 error (0.9786), is close to the ideal result of 1.0. The simulated head distributions for the November 1998, October 1999, and September 2000 in **Figures P-18, P-19, and P-20**, respectively, compare well with the contours produced from measurement data shown in **Figures P-2, P-3, and P-4**. (Note that **Figure P-20** shows the head distribution throughout the model domain.) These results collectively indicate that the groundwater flow model accurately represents groundwater flow conditions at the Site.

P.4 Model Calibration Update

The model calibration was updated in 2004 to represent the effects of a new pumping well (RW-4) installed in January 2002 after the initial model development was completed. All of the model setup and parameters were consistent with the previously developed model except for the recharge. The model was calibrated to three sets of groundwater elevation data: one set of data from a time before RW-4 was installed (January 2002) and two sets of data collected after RW-4 became operational (September 2003 and April 2004). These data span a representative range of pumping and groundwater-level conditions for the Site. Results of the calibration are summarized in **Figure P-21** and indicate good agreement between measurements and simulation results. Simulations for the analysis of the Proposed GLE Facility were performed using the modeled recharge condition more representative of average recharge and water levels based on September 2003 data.

Tables

Table P-1. Summary of Flow Model Parameters

Parameter	Value	Basis
Porosity	0.3	Typical value for fine to medium sands.
Recharge	See Figures P-14, P-15, and P-16	See Sections P.2.5.1 and P.3.3.2
Horizontal Hydraulic Conductivity	See Figure P-13	See Sections P.2.4.1 and P.3.3.1
Stream Drain Boundary Elevations	Variable	Topographic Map
Stream Drain Boundary Conductance	100 ft/day ^a (30.5m/day)	Large enough for the drains to act as specified head boundaries. (Expressed as the conductivity * boundary width/boundary thickness. This value is then multiplied by the finite-difference cell length.)
Effluent Channel River Boundary Elevation	Variable	Measured stream gauge elevations; topographic map
Effluent Channel River Boundary Conductance	0.1–100 ft/day ^a (30.5m/day) Between 574 and 957 ft ² /day (175 and 292 m/day)	An increasing trend from east to west, assuming increasing communication with the aquifer (due to the dredged depth and the channel elevation). Calibration to adjust the influence of the effluent channel on flow patterns (Section P.3.3.4)
Elevations of Hydrogeologic Units	Variable	Site boring and well logs; Bain (1970); Topographic map; Geologic interpretation
Swampy-Area Constant Head Elevation	3 ft (0.9 m)	Topographic map

^a Expressed as the conductivity multiplied by the boundary width/boundary thickness. This value is then multiplied by the finite-difference cell length to yield the actual conductance value.

[This page intentionally left blank.]

Table P-2. Calibration Statistics and Measured and Model Heads

Name	Date Measured	Measured Head (ft)	Model Head (ft)	Residual (ft)
BL-1B	11/20/1998	18.32	18.87	-0.55
BL-2B	11/20/1998	18.3	19.41	-1.11
BW-1B	11/20/1998	14.49	16.00	-1.51
BW-2B	11/20/1998	11.78	12.59	-0.81
BW-3C	11/20/1998	5.46	5.85	-0.39
BW-4B	11/20/1998	5.01	5.56	-0.55
BW-5B	11/20/1998	4.94	6.00	-1.06
BW-6B	11/20/1998	5.22	4.98	0.24
BW-7B	11/20/1998	6.69	7.59	-0.90
BW-8B	11/20/1998	12.23	12.29	-0.06
BW-9B	11/20/1998	7.57	8.51	-0.94
CW-1B	11/20/1998	19.95	19.13	0.82
CW-1C	11/20/1998	19.97	19.16	0.81
CW-2B	11/20/1998	26.73	25.34	1.39
CW-3B	11/20/1998	27.91	27.82	0.09
CW-4B	11/20/1998	20.33	20.16	0.17
CW-4C	11/20/1998	18.11	20.27	-2.16
CW-5B	11/20/1998	14.22	14.85	-0.63
CW-6B	11/20/1998	15.05	16.15	-1.10
CW-7B	11/20/1998	4.15	4.32	-0.17
CW-7D	11/20/1998	2.43	4.25	-1.82
CW-8B	11/20/1998	4.39	6.35	-1.96
CW-9B	11/20/1998	11.95	10.79	1.16
DW-1B	11/20/1998	8.24	7.89	0.35
DW-2B	11/20/1998	7.91	7.82	0.09
DW-3B	11/20/1998	6.98	9.18	-2.20
DW-4B	11/20/1998	7.69	9.47	-1.78
DW-5B	11/20/1998	11.48	11.75	-0.27
DW-6B	11/20/1998	12.62	12.09	0.53
DW-7B	11/20/1998	11.37	11.59	-0.22
FW-2B	11/20/1998	22.16	20.89	1.27
FX-1B	11/20/1998	23.1	23.81	-0.71
FX-2B	11/20/1998	22.53	22.87	-0.34
FX-3B	11/20/1998	21.87	21.78	0.09
LF-1B	11/20/1998	12.1	13.23	-1.13
LF-2B	11/20/1998	16.76	18.52	-1.76
LF-2C	11/20/1998	20.76	18.57	2.19
LF-3B	11/20/1998	18.16	18.50	-0.34
LF-3C	11/20/1998	18.07	18.56	-0.49
LF-4B	11/20/1998	17.53	18.84	-1.31
MW-1B	11/20/1998	8.93	9.14	-0.21
MW-2B	11/20/1998	21.07	19.83	1.24
MW-3B	11/20/1998	28.22	28.35	-0.13
MW-3C	11/20/1998	28.2	28.31	-0.11
MW-4B	11/20/1998	28.36	28.37	-0.01
MW-4C	11/20/1998	28.45	28.30	0.15
MW-5B	11/20/1998	23.11	23.35	-0.24
MW-5C	11/20/1998	23.16	23.39	-0.23
OB-1	11/20/1998	18.8	17.63	1.17
OB-10	11/20/1998	7.77	11.09	-3.32

Name	Date Measured	Measured Head (ft)	Model Head (ft)	Residual (ft)
OB-2	11/20/1998	12.99	13.57	-0.58
OB-4	11/20/1998	18.73	23.97	-5.24
OB-6	11/20/1998	5.14	6.17	-1.03
OB-7	11/20/1998	14.97	15.39	-0.42
OB-8	11/20/1998	17.74	16.47	1.27
OB-9	11/20/1998	17.71	16.36	1.35
OW-1B	11/20/1998	6.36	5.57	0.79
OW-2B	11/20/1998	7.03	5.70	1.33
OW-4B	11/20/1998	5.76	5.88	-0.12
PW-10B	11/20/1998	5.33	4.97	0.36
PW-11B	11/20/1998	6.72	5.09	1.63
PW-11D	11/20/1998	6.63	5.15	1.48
PW-12B	11/20/1998	7.03	6.80	0.23
PW-13B	11/20/1998	5.97	5.77	0.20
PW-14B	11/20/1998	5.09	5.27	-0.18
PW-15B	11/20/1998	5.61	3.34	2.27
PW-16B	11/20/1998	5.99	6.26	-0.27
PW-1B	11/20/1998	5.85	6.52	-0.67
PW-1C	11/20/1998	5.77	6.54	-0.77
PW-1D	11/20/1998	4.98	6.55	-1.57
PW-2C	11/20/1998	9.57	9.74	-0.17
PW-2D	11/20/1998	9.15	9.81	-0.66
PW-3C	11/20/1998	11.25	11.36	-0.11
PW-4C	11/20/1998	14.24	13.86	0.38
PW-5C	11/20/1998	20.42	19.54	0.88
PW-6C	11/20/1998	22.16	21.14	1.02
PW-7C	11/20/1998	22.56	21.31	1.25
PW-7D	11/20/1998	22.39	21.31	1.08
PW-8C	11/20/1998	21.81	22.03	-0.22
PW-9B	11/20/1998	8.13	7.96	0.17
BL-1B	10/6/1999	23.51	23.71	-0.20
BL-2B	10/6/1999	24.26	24.24	0.02
BW-1B	10/6/1999	18.17	17.76	0.41
BW-2B	10/6/1999	15.88	15.48	0.40
BW-3C	10/6/1999	9.46	8.90	0.56
BW-4B	10/6/1999	8.36	8.57	-0.21
BW-5B	10/6/1999	8.94	8.92	0.02
BW-6B	10/6/1999	9.29	8.58	0.71
BW-7B	10/6/1999	10.39	10.85	-0.46
BW-8B	10/6/1999	16.31	15.76	0.55
BW-9B	10/6/1999	11.91	11.64	0.27
CAF-16C	10/6/1999	21.77	21.93	-0.16
CAF-17C	10/6/1999	20.84	20.71	0.13
CW-1B	10/6/1999	24.23	23.10	1.13
CW-1C	10/6/1999	24.27	23.16	1.11
CW-2B	10/6/1999	31.61	31.64	-0.03
CW-3B	10/6/1999	33.94	34.10	-0.16
CW-4B	10/6/1999	24.71	24.60	0.12
CW-4C	10/6/1999	24.89	24.77	0.12
CW-5B	10/6/1999	16.5	15.08	1.42

Name	Date Measured	Measured Head (ft)	Model Head (ft)	Residual (ft)
CW-6B	10/6/1999	19.05	18.37	0.68
CW-7B	10/6/1999	7.44	7.90	-0.46
CW-7D	10/6/1999	7.69	7.85	-0.16
CW-8B	10/6/1999	8.91	9.19	-0.28
CW-9B	10/6/1999	17.57	14.75	2.82
DW-1B	10/6/1999	11.76	12.04	-0.28
DW-2B	10/6/1999	11.11	11.76	-0.65
DW-3B	10/6/1999	12.26	12.97	-0.71
DW-4B	10/6/1999	13.48	13.34	0.14
DW-5B	10/6/1999	16.22	15.96	0.26
DW-6B	10/6/1999	18.3	17.14	1.16
DW-7B	10/6/1999	16.18	15.71	0.47
FW-2B	10/6/1999	28.2	27.00	1.20
FX-1B	10/6/1999	28.58	29.41	-0.83
FX-2B	10/6/1999	27.72	28.22	-0.50
FX-3B	10/6/1999	27.02	27.01	0.01
LF-1B	10/6/1999	17.14	17.70	-0.56
LF-2B	10/6/1999	21.48	22.56	-1.08
LF-2C	10/6/1999	23.7	22.60	1.10
LF-3B	10/6/1999	20.69	21.98	-1.29
LF-3C	10/6/1999	21.03	22.06	-1.03
LF-4B	10/6/1999	22.4	22.12	0.28
MW-1B	10/6/1999	13.55	12.38	1.17
MW-2B	10/6/1999	25.78	24.50	1.28
MW-3B	10/6/1999	33.95	34.57	-0.62
MW-3C	10/6/1999	33.93	34.53	-0.60
MW-4B	10/6/1999	34.32	34.77	-0.45
MW-4C	10/6/1999	34.38	34.71	-0.33
MW-5B	10/6/1999	28.68	28.70	-0.02
MW-5C	10/6/1999	28.64	28.74	-0.10
OB-10	10/6/1999	12.59	14.99	-2.40
OB-2	10/6/1999	16.7	17.59	-0.89
OB-4	10/6/1999	31.86	28.15	3.71
OB-5	10/6/1999	19.34	18.86	0.48
OB-6	10/6/1999	10.82	6.94	3.88
OB-7	10/6/1999	20.54	19.77	0.77
OB-8	10/6/1999	20.39	20.04	0.35
OB-9	10/6/1999	16.98	18.71	-1.73
OCW-1C	10/6/1999	9.18	8.93	0.25
OCW-2C	10/6/1999	8.54	8.18	0.36
OCW-3C	10/6/1999	7.39	6.81	0.58
OCW-5D	10/6/1999	15.1	14.59	0.51
OW-2B	10/6/1999	9.06	9.51	-0.45
OW-3B	10/6/1999	9.25	9.41	-0.16
OW-4B	10/6/1999	9.55	9.48	0.07
PW-10B	10/6/1999	8.42	9.14	-0.72
PW-11B	10/6/1999	8.66	9.17	-0.51
PW-11D	10/6/1999	8.7	9.23	-0.53
PW-12B	10/6/1999	10.33	10.61	-0.28
PW-13B	10/6/1999	9.17	9.62	-0.45

Name	Date Measured	Measured Head (ft)	Model Head (ft)	Residual (ft)
PW-14B	10/6/1999	7.27	9.20	-1.93
PW-15B	10/6/1999	9	8.66	0.34
PW-16B	10/6/1999	8.98	9.71	-0.73
PW-1B	10/6/1999	8.98	9.68	-0.70
PW-1C	10/6/1999	8.76	9.68	-0.92
PW-1D	10/6/1999	8.53	9.68	-1.15
PW-2C	10/6/1999	13.88	13.57	0.31
PW-2D	10/6/1999	13.92	13.65	0.27
PW-3C	10/6/1999	16.41	15.34	1.07
PW-4C	10/6/1999	21.27	18.44	2.83
PW-5C	10/6/1999	25.2	25.07	0.13
PW-6C	10/6/1999	26.4	27.20	-0.80
PW-7C	10/6/1999	27.48	27.71	-0.23
PW-7D	10/6/1999	27.58	27.71	-0.13
PW-8C	10/6/1999	27.95	28.37	-0.42
PW-9B	10/6/1999	11.71	11.75	-0.04
WT-13B	10/6/1999	17.48	15.67	1.81
WT-14B	10/6/1999	16.82	15.11	1.71
WT-15B	10/6/1999	17.44	16.26	1.18
WT-16B	10/6/1999	15.54	14.49	1.05
WT-17B	10/6/1999	18.05	16.65	1.40
WT-7B	10/6/1999	21.84	21.49	0.35
WT-7C	10/6/1999	21.85	21.48	0.37
BL-1B	9/12/2000	18.82	20.41	-1.59
BL-2B	9/12/2000	17.98	20.85	-2.87
BW-1B	9/12/2000	16.75	17.29	-0.54
BW-2B	9/12/2000	14.15	14.76	-0.61
BW-3C	9/12/2000	8.7	8.35	0.35
BW-4B	9/12/2000	9.68	7.90	1.78
BW-5B	9/12/2000	7.96	8.32	-0.36
BW-6B	9/12/2000	8.7	7.70	1.00
BW-7B	9/12/2000	9.86	10.10	-0.24
BW-8B	9/12/2000	14.15	14.52	-0.37
BW-9B	9/12/2000	11.69	10.99	0.70
CAF-16	9/12/2000	20.37	20.49	-0.12
CAF-17	9/12/2000	19.28	19.35	-0.07
CW-1B	9/12/2000	21.4	21.11	0.29
CW-1C	9/12/2000	21.41	21.13	0.28
CW-2B	9/12/2000	27.57	27.14	0.43
CW-3B	9/12/2000	28.16	28.47	-0.31
CW-4B	9/12/2000	22.32	22.41	-0.09
CW-4C	9/12/2000	22.41	22.54	-0.13
CW-5B	9/12/2000	15.73	15.00	0.73
CW-6B	9/12/2000	17.22	17.75	-0.53
CW-7B	9/12/2000	7.49	6.59	0.90
CW-7D	9/12/2000	6.68	6.51	0.17
CW-8B	9/12/2000	8.46	8.72	-0.26
CW-9B	9/12/2000	15.24	13.12	2.12
DW-1B	9/12/2000	11	10.88	0.12
DW-2B	9/12/2000	11.07	10.31	0.76

Name	Date Measured	Measured Head (ft)	Model Head (ft)	Residual (ft)
DW-3B	9/12/2000	13.78	10.03	3.75
DW-4B	9/12/2000	13.62	11.09	2.53
DW-5B	9/12/2000	13.86	14.28	-0.42
DW-6B	9/12/2000	13.29	15.11	-1.82
DW-7B	9/12/2000	13.78	14.08	-0.30
FW-2B	9/12/2000	26.5	24.45	2.05
FX-1B	9/12/2000	24.97	25.44	-0.47
FX-2B	9/12/2000	23.82	24.43	-0.61
FX-3B	9/12/2000	23.16	23.47	-0.31
LF-1B	9/12/2000	16.15	17.10	-0.95
LF-2B	9/12/2000	20.6	21.37	-0.77
LF-2C	9/12/2000	23.4	21.40	2.00
LF-3B	9/12/2000	20.17	20.67	-0.50
LF-3C	9/12/2000	20.36	20.74	-0.38
LF-4B	9/12/2000	20.47	20.72	-0.25
MW-2B	9/12/2000	21.57	21.48	0.09
MW-3B	9/12/2000	29.11	28.60	0.51
MW-3C	9/12/2000	29.11	28.57	0.54
MW-4B	9/12/2000	28.57	28.84	-0.27
MW-4C	9/12/2000	28.67	28.81	-0.14
MW-5B	9/12/2000	25.2	25.25	-0.05
MW-5C	9/12/2000	24.93	25.27	-0.34
OB-1	9/12/2000	20.43	20.00	0.43
OB-10	9/12/2000	12.94	14.56	-1.62
OB-2	9/12/2000	13.59	14.35	-0.76
OB-5	9/12/2000	17.48	17.63	-0.15
OB-6	9/12/2000	4.64	6.48	-1.84
OB-8	9/12/2000	20.29	20.21	0.08
OB-9	9/12/2000	20.16	19.97	0.19
OCW-1C	9/12/2000	8.43	8.47	-0.04
OCW-2C	9/12/2000	7.77	7.77	0.00
OCW-3C	9/12/2000	6.68	6.50	0.18
OCW-5D	9/12/2000	13.64	13.69	-0.05
OW-2B	9/12/2000	8.78	8.89	-0.11
OW-3B	9/12/2000	8.59	8.97	-0.38
OW-4B	9/12/2000	8.81	9.06	-0.25
PW-10B	9/12/2000	7.65	8.65	-1.00
PW-11B	9/12/2000	7.75	8.65	-0.90
PW-11D	9/12/2000	7.62	8.72	-1.10
PW-12B	9/12/2000	9.63	9.57	0.06
PW-13B	9/12/2000	9.08	9.21	-0.13
PW-14B	9/12/2000	7.31	8.47	-1.16
PW-15B	9/12/2000	6.81	8.61	-1.80
PW-16B	9/12/2000	8.93	9.25	-0.32
PW-1B	9/12/2000	8.65	9.20	-0.55
PW-1C	9/12/2000	8.76	9.20	-0.44
PW-1D	9/12/2000	7.8	9.20	-1.40
PW-2C	9/12/2000	13.77	11.77	2.00
PW-2D	9/12/2000	13.7	11.85	1.86
PW-3C	9/12/2000	13.62	13.81	-0.19

Name	Date Measured	Measured Head (ft)	Model Head (ft)	Residual (ft)
PW-4C	9/12/2000	15.75	17.19	-1.44
PW-5C	9/12/2000	23.37	23.82	-0.45
PW-6C	9/12/2000	25.2	25.84	-0.64
PW-7C	9/12/2000	26.06	25.54	0.52
PW-7D	9/12/2000	25.91	25.54	0.37
PW-8C	9/12/2000	25.44	25.62	-0.18
PW-9B	9/12/2000	11.45	10.32	1.13
WT-13B	9/12/2000	16.32	15.57	0.75
WT-14B	9/12/2000	15.81	15.02	0.79
WT-15B	9/12/2000	16.41	16.03	0.38
WT-16B	9/12/2000	14.58	14.18	0.40
WT-17B	9/12/2000	16.74	16.40	0.34
WT-20B	9/12/2000	14.46	14.13	0.33
WT-21B	9/12/2000	14.7	14.19	0.51
WT-22B	9/12/2000	16.58	14.36	2.22
WT-7B	9/12/2000	19.81	20.18	-0.37
WT-7C	9/12/2000	19.81	20.18	-0.37

Overall Statistics

Mean Error	0.00
Maximum Error	3.88
Minimum Error	-5.24
Mean Absolute Error	0.77
Sum of Squares	311.39
RMS	1.08
RMS/Range	0.03

Figures



Figure P-1
Location of GE/GNF
Plant Site and
Hydrogeologic Features
and Boundaries

Wilmington Site

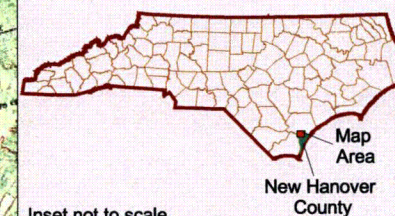
EXPLANATION

Approximate western extent of the semi-confining layer and the more permeable, upper sandy portion of the Pee Dee Formation, after Bain (1970)

- Low-lying swampy area
- GE/GNF effluent channel
- Surface water
- GE/GNF Property Boundary



State of North Carolina



Inset not to scale


Date: 1/22/02



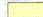


Map No.: 7810003013a

**Figure P-2
Principal Aquifer
Groundwater Levels
(Nov 1998)**

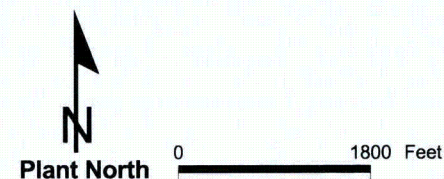
Wilmington Site

Explanation

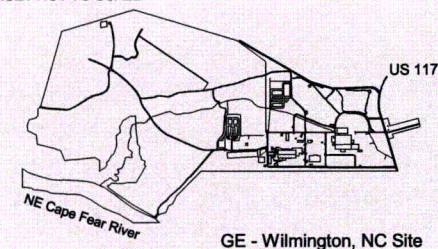
 Groundwater elevation
(ft MSL) (variable color)

-  Road
-  Onsite building
-  Onsite facility
-  GE Property
-  Surface water

Note: Contours were derived through an automatic interpolation procedure (kriging) based on measured elevations.



INSET NOT TO SCALE




Date: 9/9/02



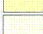


Map No.: 7810003013e

**Figure P-3
Principal Aquifer
Groundwater Levels
(Oct 1999)**

Wilmington Site

Explanation

 Groundwater elevation
(ft MSL) (variable color)

 Road
 Onsite building
 Onsite facility
 GE Property
 Surface water

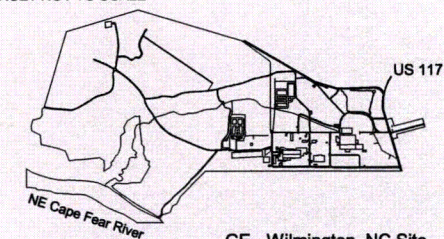
Note: Contours were derived through an automatic interpolation procedure (kriging) based on measured elevations.



Plant North

0 1800 Feet

INSET NOT TO SCALE



GE - Wilmington, NC Site


Date: 9/10/02



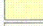


Map No.: 7810003013d

**Figure P-4
Principal Aquifer
Groundwater Levels
(Sep 2000)**

Wilmington Site

Explanation

 Groundwater elevation
(ft MSL) (variable color)

-  Road
-  Onsite building
-  Onsite facility
-  GE Property
-  Surface water

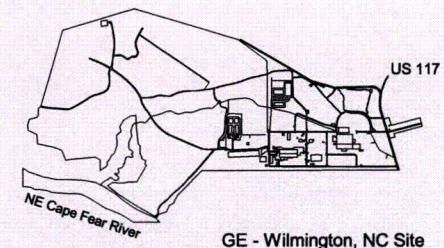
Note: Contours were derived through an automatic interpolation procedure (kriging) based on measured elevations.



Plant North

0 1800 Feet

INSET NOT TO SCALE



GE - Wilmington, NC Site

Date: 9/9/02

Map No.: 7810003013c

**Figure P-5
Piezometric Head Difference
Between the Surficial and
Principal Aquifers (9/12/00)**

Wilmington Site

Explanation

Groundwater elevation
difference between the
surficial and the
principal aquifers
measured on 9/12/00
(feet msl)



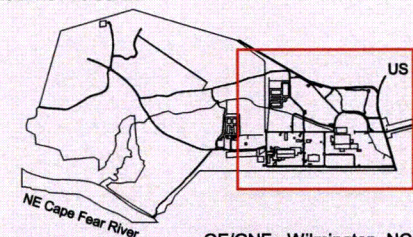
- Pumping well
- Road
- Onsite building
- Onsite facility
- GE Property
- Surface water



Plant North

0 850 Feet

INSET NOT TO SCALE



GE/GNF - Wilmington, NC Site

Date: 9/9/02

Map No.: 7810003013g

Note: The contours show the principal-aquifer groundwater elevation subtracted from the surficial-aquifer elevation. In areas where the bottom elevation of the semiconfining layer was above the principal-aquifer groundwater, the bottom of the semiconfining layer was used.

Figure P-6
Estimated Semiconfining-Layer Thickness

Wilmington Site

Explanation

Estimated semiconfining-layer thickness (ft)



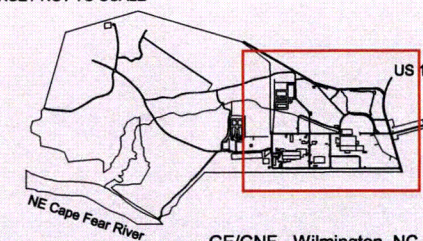
- Pumping well
- Road
- Onsite building
- Onsite facility
- GE Property
- Surface water

Note: Based on boring log data.



0 850 Feet

INSET NOT TO SCALE



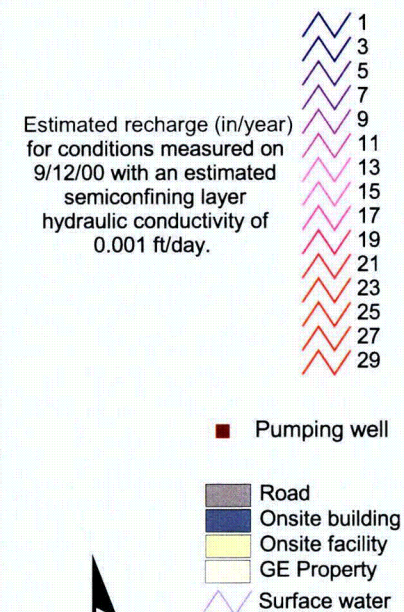
Date: 9/9/02

Map No.: 7810003013f

Figure P-7
Estimated Recharge
for 9/12/00 Conditions

Wilmington Site

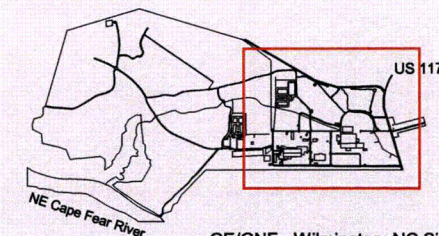
Explanation



Plant North

0 850 Feet

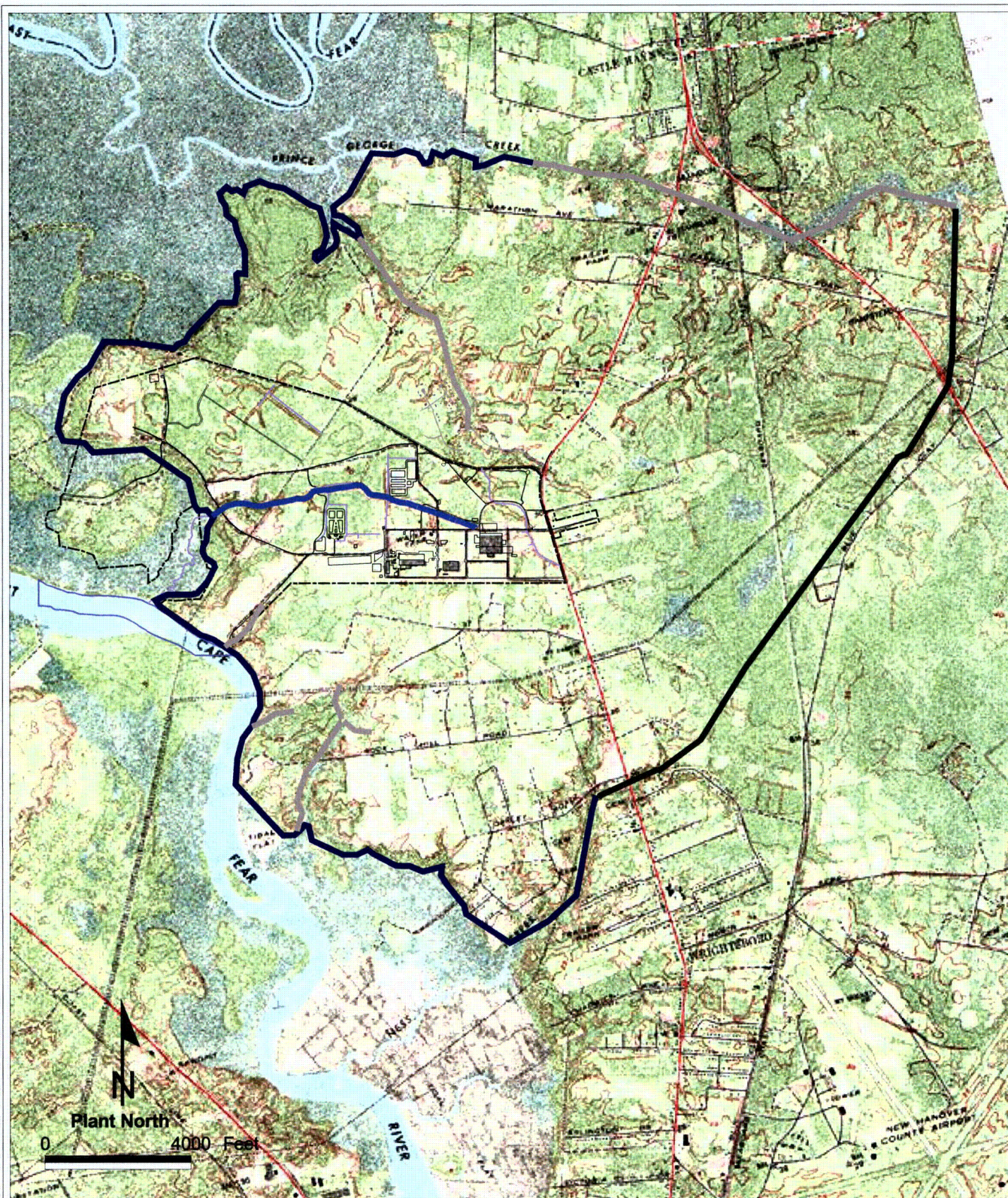
INSET NOT TO SCALE



GE/GNF - Wilmington, NC Site

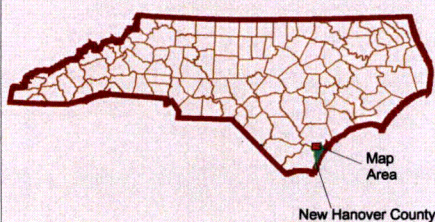
Date: 9/9/02

Map No.: 7810003013h



State of North Carolina

INSET NOT TO SCALE



New Hanover County

Date: 1/26/02

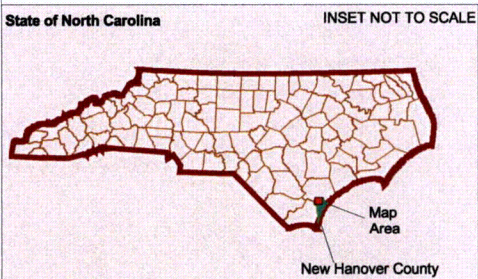
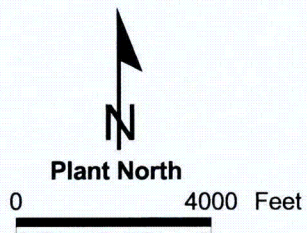
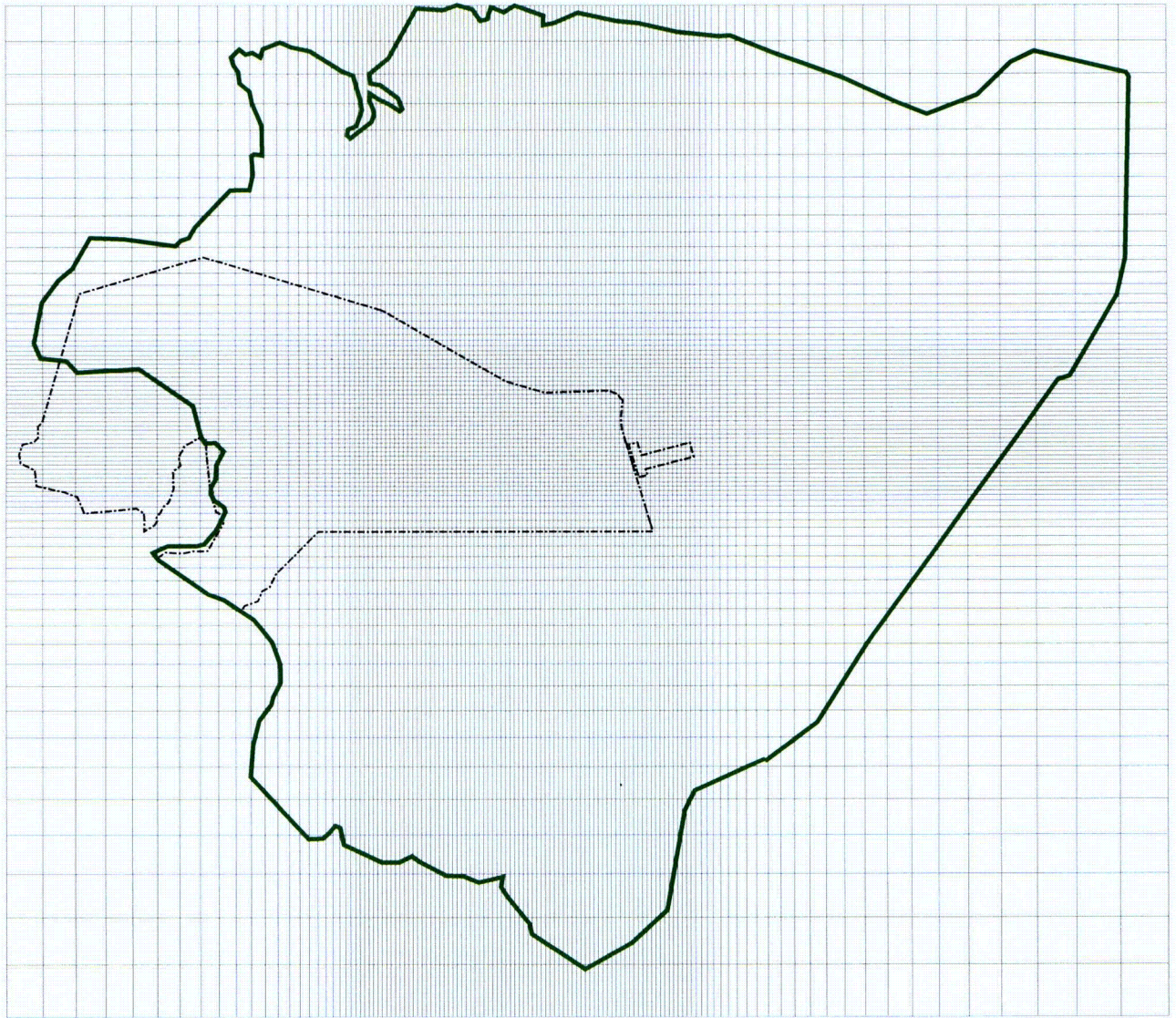
Map No.: 7810003006b

Explanation

- River boundary
- No flow boundary
- Drain boundary
- Constant head boundary
- GE/GNF property boundary
- Low-lying swampy area

Figure P-8
Model Domain
and Boundaries

Wilmington Site




Date: 1/23/02

Map No.: 78100030061

Explanation

Finite-difference grid

 Model domain

 GE/GNF property boundary

Figure P-9

Model Finite-Difference Grid

Wilmington Site

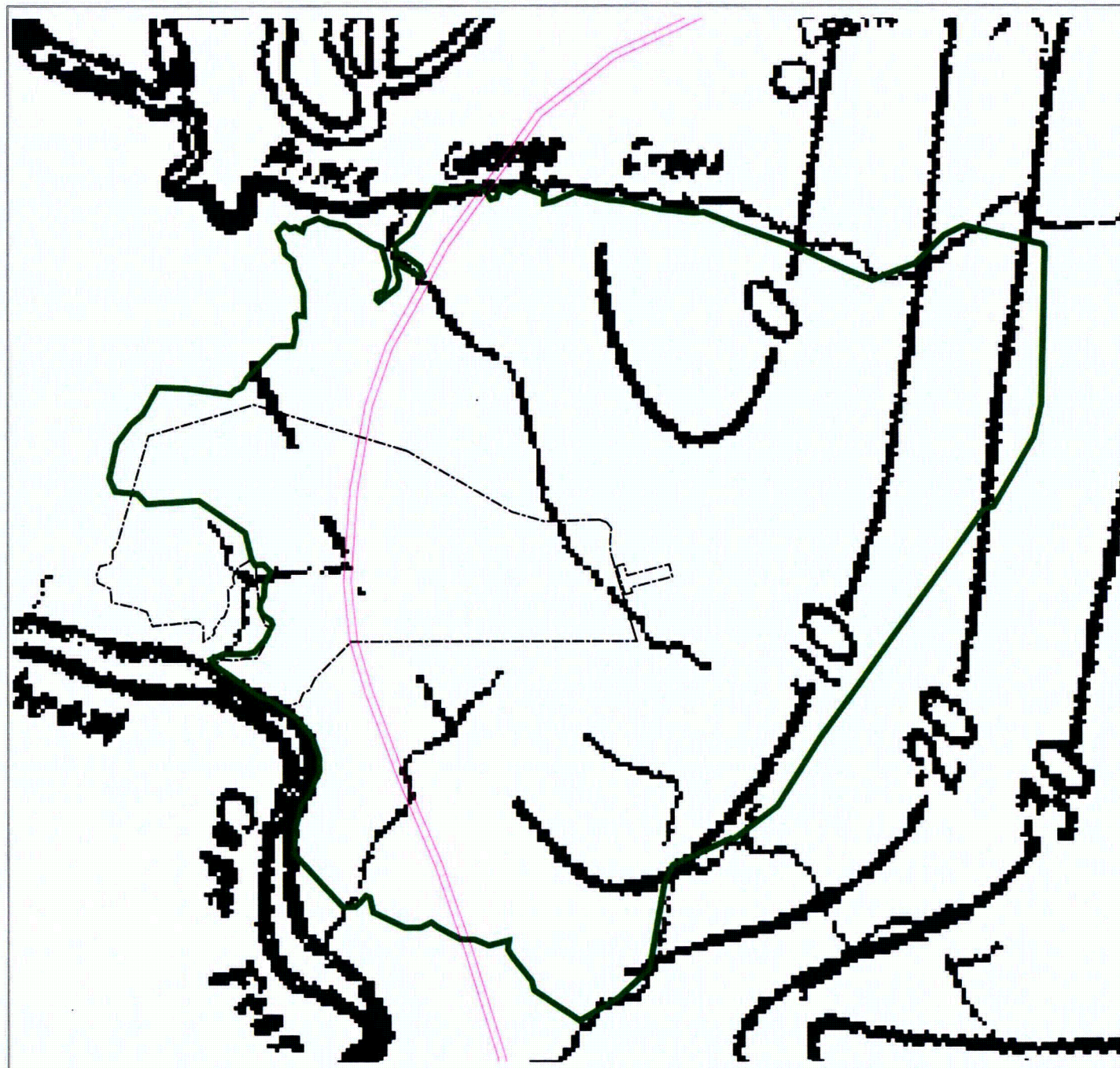




Figure P-10
Top of Aquifer as
Shown by Bain (1970)

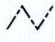
Wilmington Site

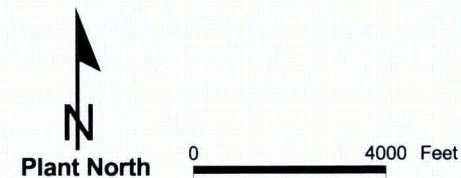
Explanation

Contours shown are the upper surface of the sandstone aquifer as presented by Bain (1970). The units are feet.

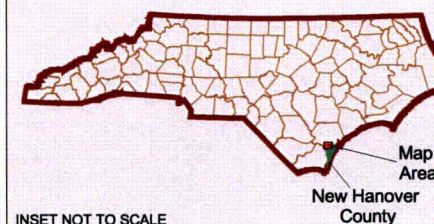
 Approximate western extent of the semi-confining unit.

 Model extent

 GE/GNF property boundary



State of North Carolina



INSET NOT TO SCALE

Date: 8/28/01


Map No.: 7810003006c

Figure P-11
Top of Model Aquifer

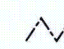
Wilmington Site

Explanation

Contours shown are the upper surface of the simulated aquifer.
 The units are feet msl.

 Approximate western extent of the semi-confining layer.

 Model extent

 GE/GNF property boundary

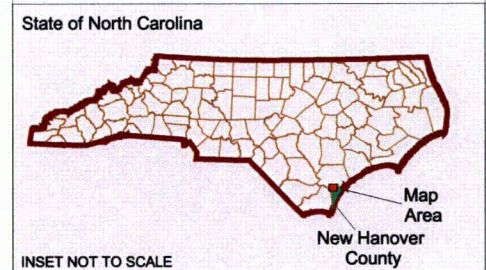
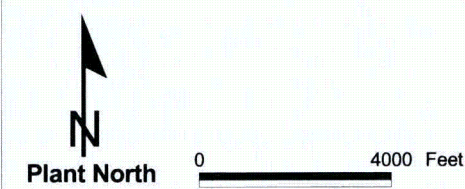
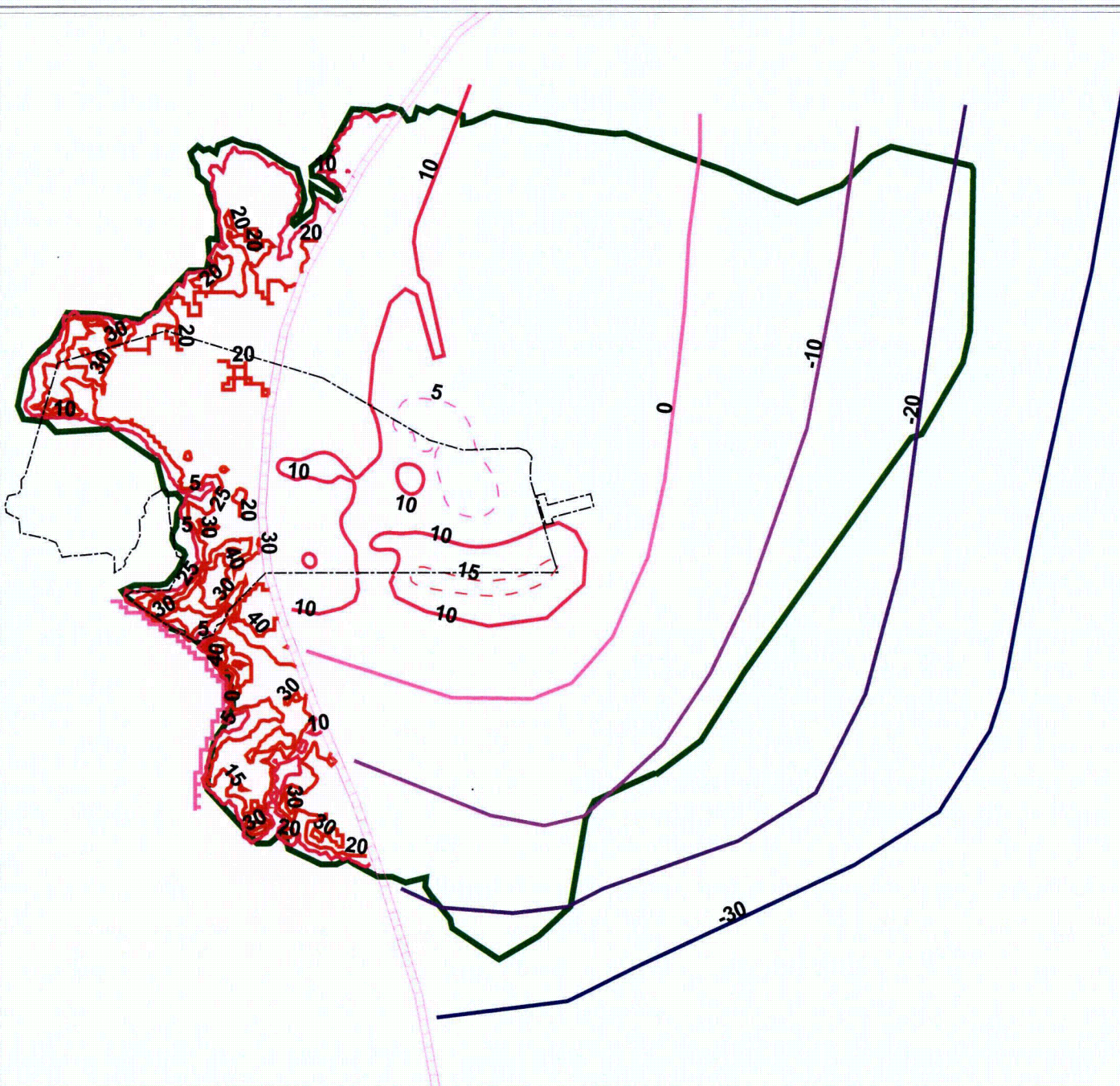



Figure P-12
Bottom of Model Aquifer

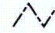
Wilmington Site

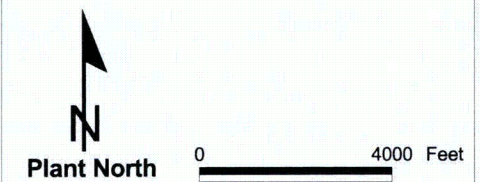
Explanation

Contours shown are the lower surface of the simulated aquifer. The units are feet.

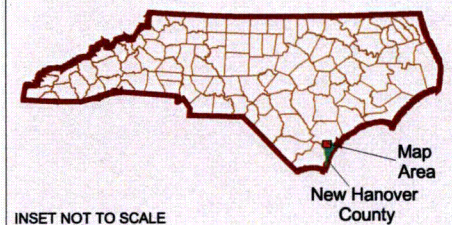
 Approximate western extent of the semi-confining layer.

 Model extent

 GE/GNF property boundary



State of North Carolina



INSET NOT TO SCALE

Date: 8/28/01

Map No.: 7810003006e

Figure P-13 Model Hydraulic Conductivity Distribution and Pilot Points

Wilmington Site

Explanation

Hydraulic conductivity
contours (ft/day)



Pilot point used to estimate the hydraulic conductivity field (labels beside pilot points are the id and estimated conductivity ((ft/day))

GE/GNF property boundary

Model extent

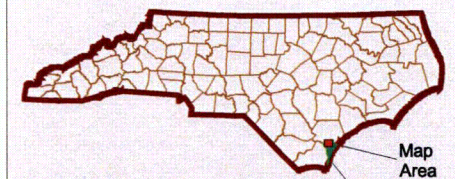
Note: Conductivity values next to the pilot points are computer generated. The only hydraulic conductivity measurements available were made within the site property (see Figure B-8).



Plant North

0 3600 Feet

State of North Carolina



INSET NOT TO SCALE

Date: 9/9/02

Map No.: 7810003006f

**Figure P-14
Calibrated Model
Recharge Distribution
(11/20/98)
Wilmington Site**

Explanation

Recharge zones (in/yr)



Calculated recharge (in/yr)



GE/GNF property boundary

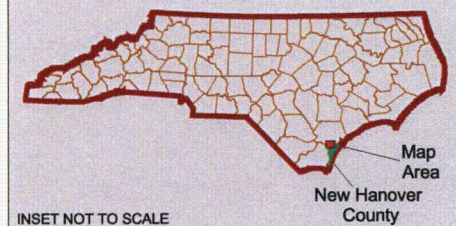
Model extent



Plant North

0 3600 Feet

State of North Carolina



INSET NOT TO SCALE

Date: 10/4/01

Map No.: 7810003006h

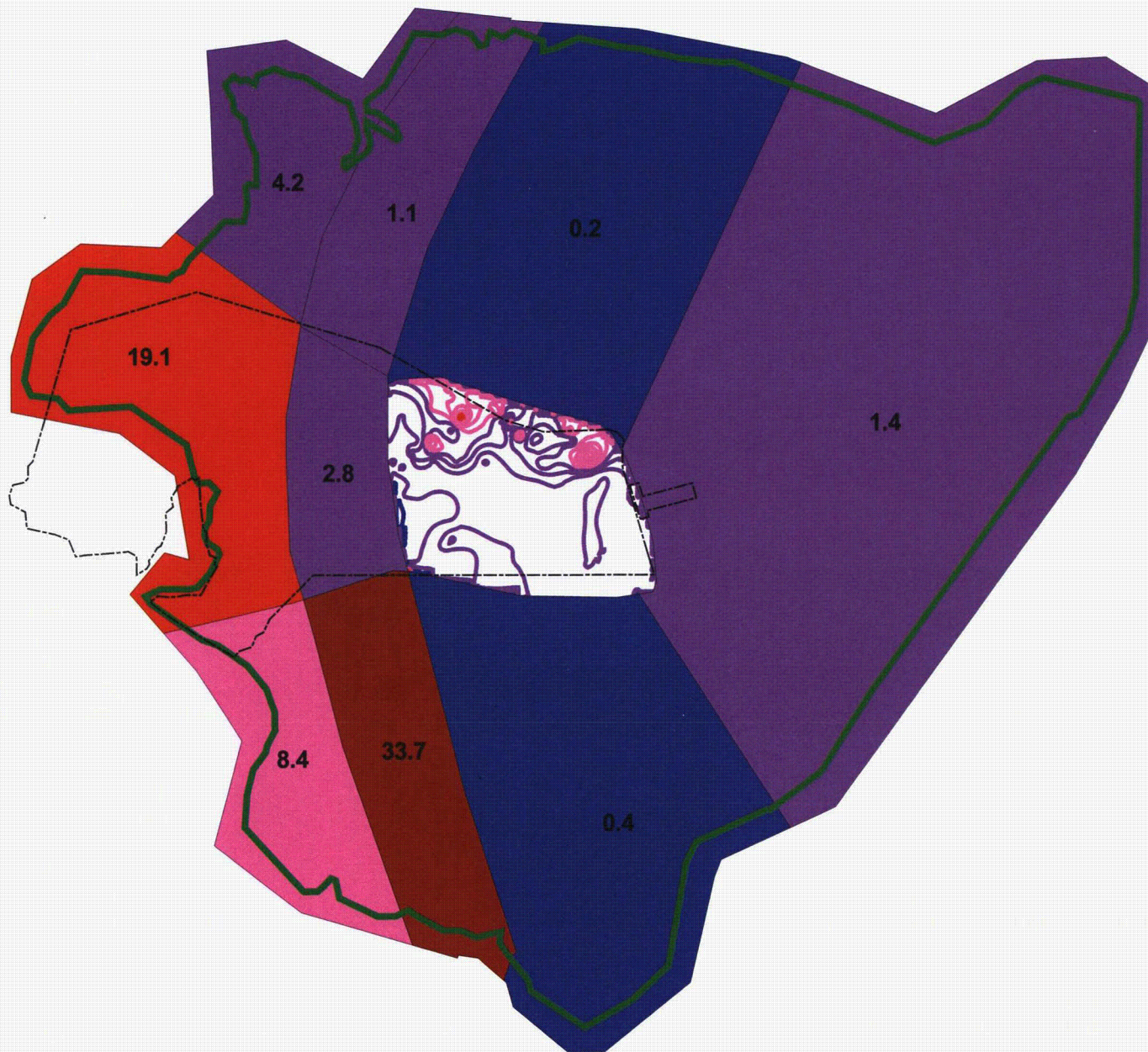


Figure P-15
Calibrated Model
Recharge Distribution
(10/6/99)

Wilmington Site

Explanation

Recharge zones (in/yr)



Calculated recharge (in/yr)



GE/GNF property boundary

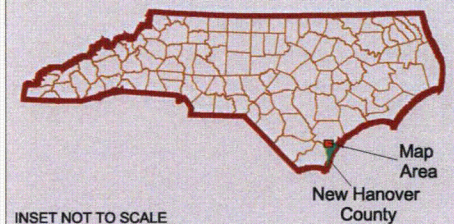
Model extent



Plant North

0 3600 Feet

State of North Carolina



INSET NOT TO SCALE

Date: 10/4/01

Map No.: 7810003006g

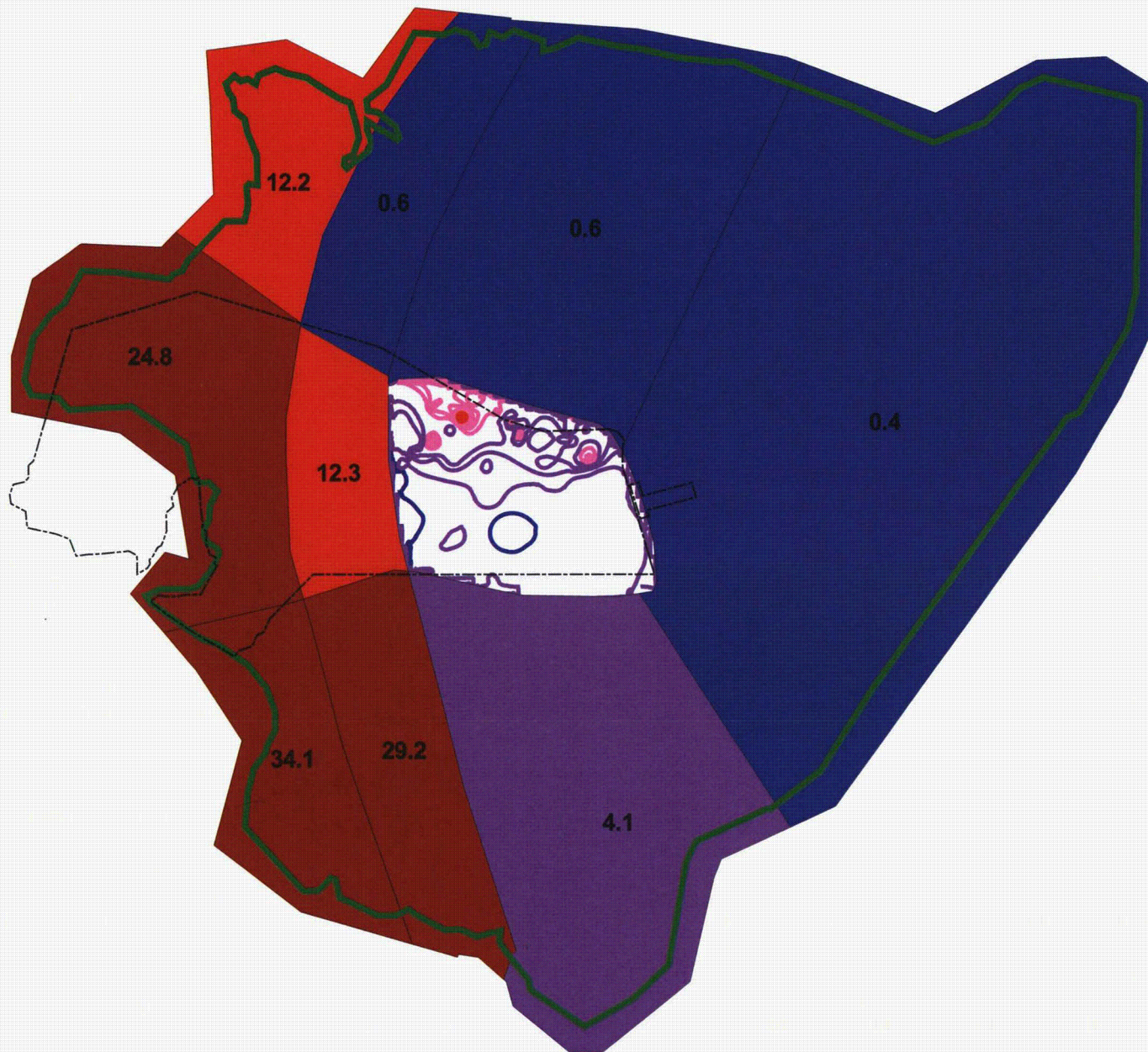


Figure P-16
Calibrated Model
Recharge Distribution
(9/12/00)
Wilmington Site

Explanation

Recharge zones (in/yr)



Calculated recharge (in/yr)



GE/GNF property boundary

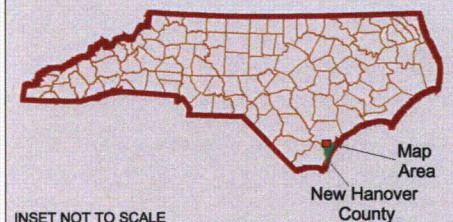
Model extent



Plant North

0 3600 Feet

State of North Carolina



INSET NOT TO SCALE

Date: 10/4/01

Map No.: 7810003006i

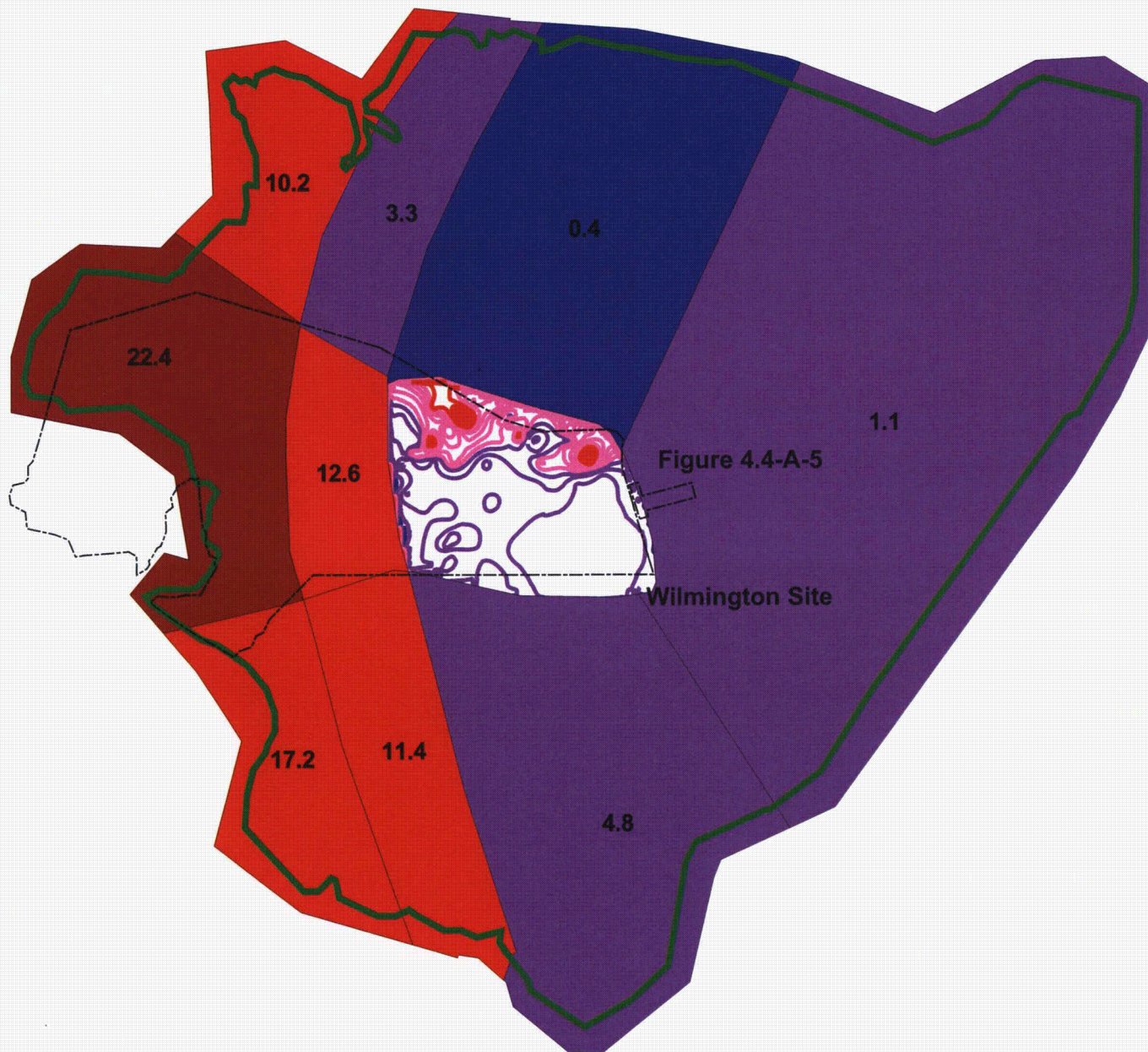


Figure P-17 Measured versus Simulated Heads

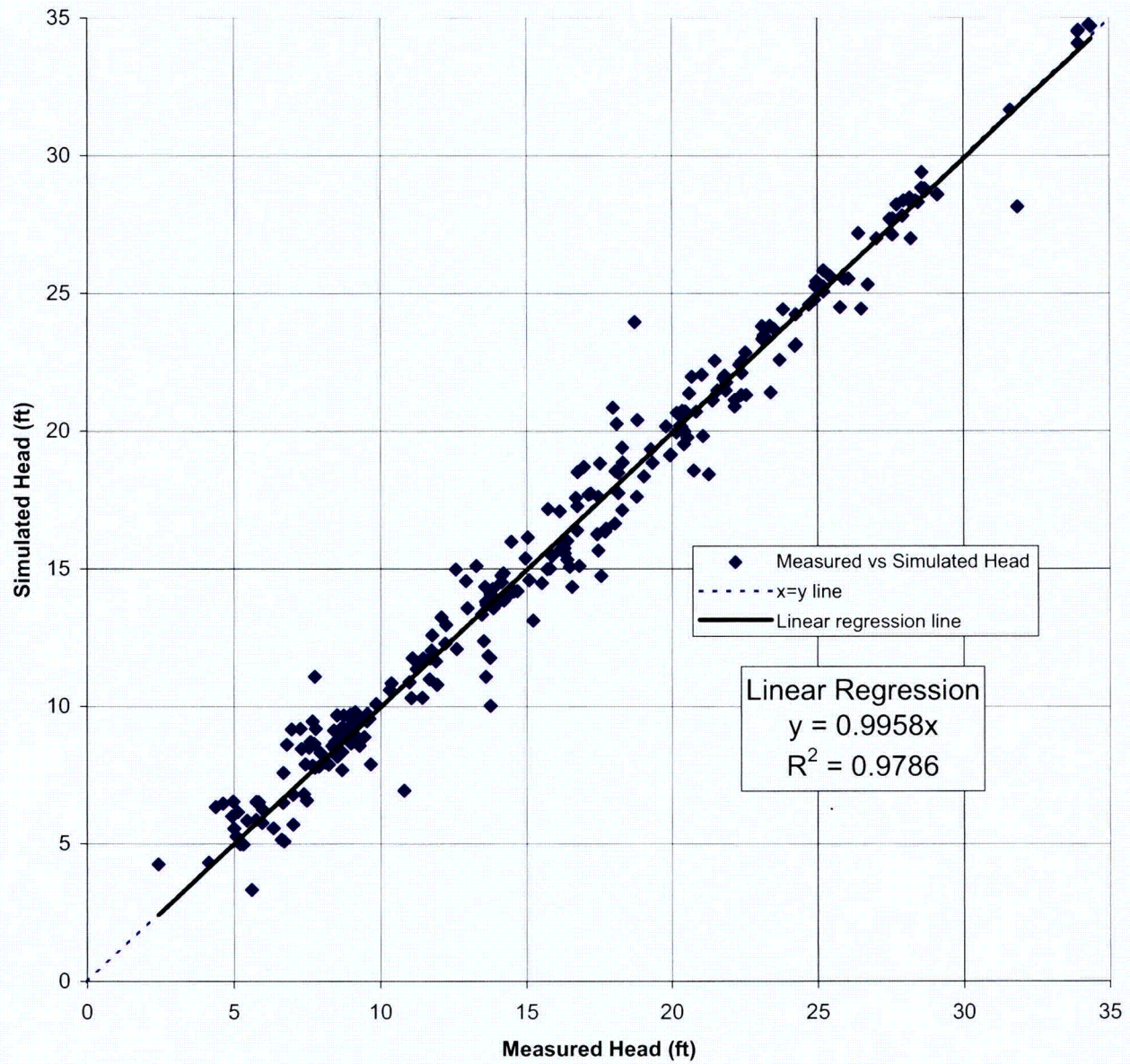








Figure P-18
Calibrated Groundwater
Elevations – Site Area
Nov 1998

Wilmington Site

Explanation

 Groundwater elevation
 contour (ft msl)
 (variable color)

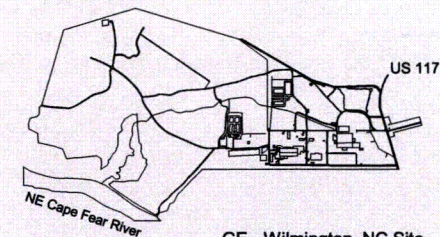
 Road
 Onsite building
 Onsite facility
 GE Property
 Surface water



Plant North

0 1800 Feet

INSET NOT TO SCALE




Date: 9/4/02



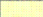
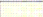

Map No.: 7810003013I

Figure P-19
Calibrated Groundwater
Elevations – Site Area
Oct 1999

Wilmington Site

Explanation

 Groundwater elevation
 contour (ft msl)
 (variable color)

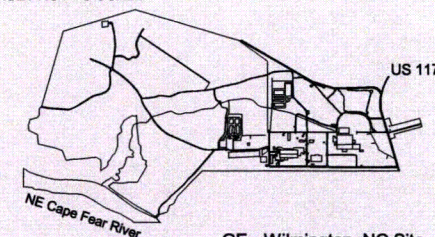
 Road
 Onsite building
 Onsite facility
 GE Property
 Surface water



Plant North

0 1800 Feet

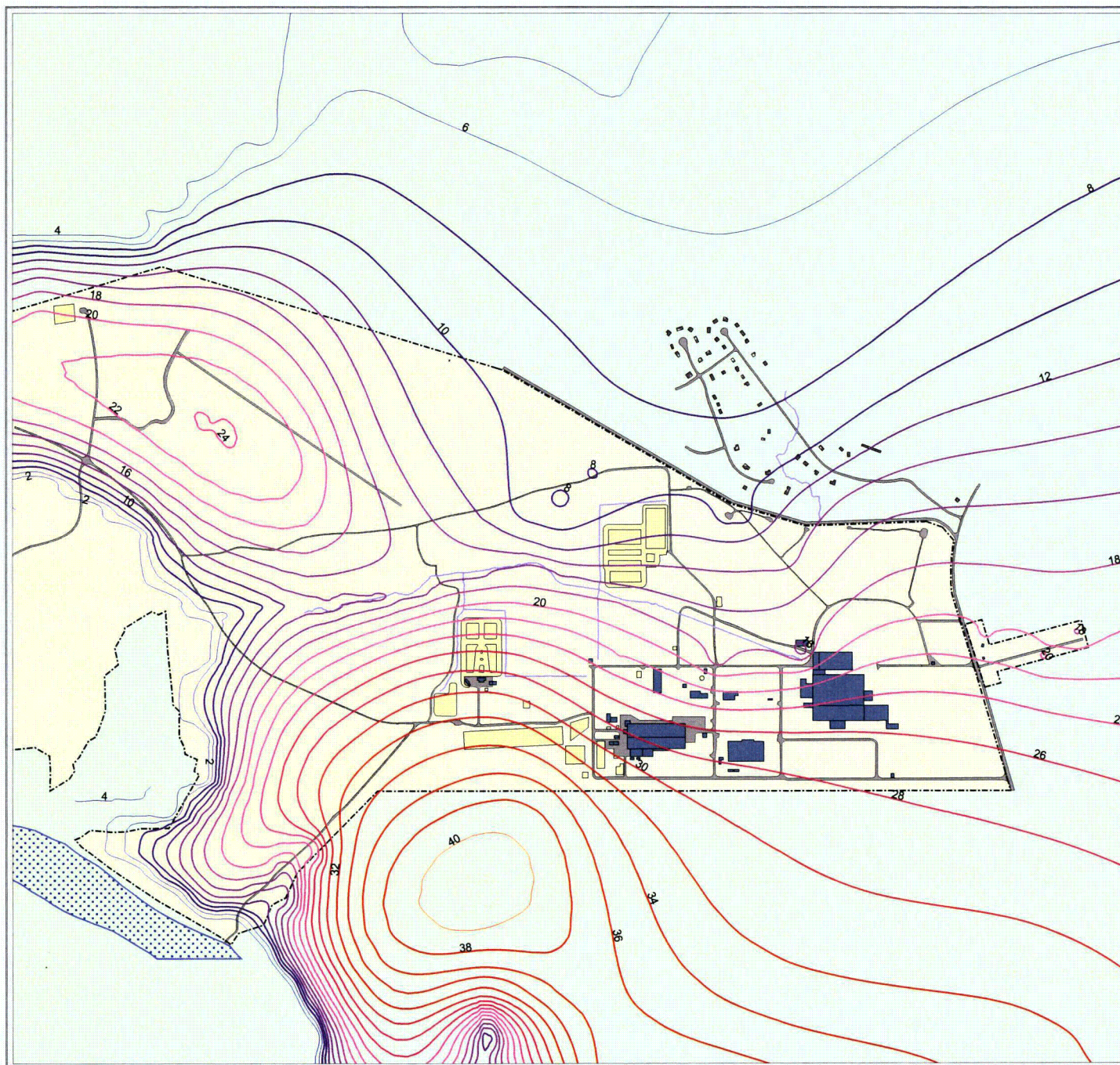
INSET NOT TO SCALE

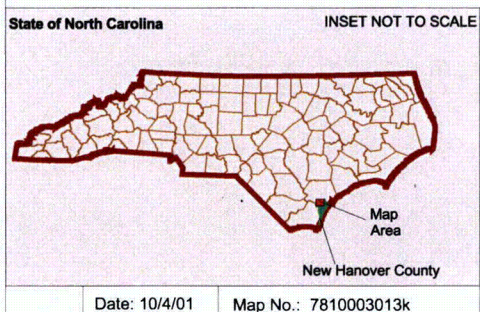
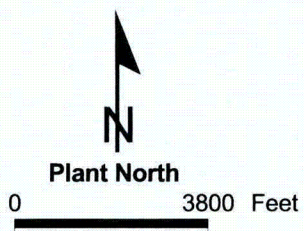
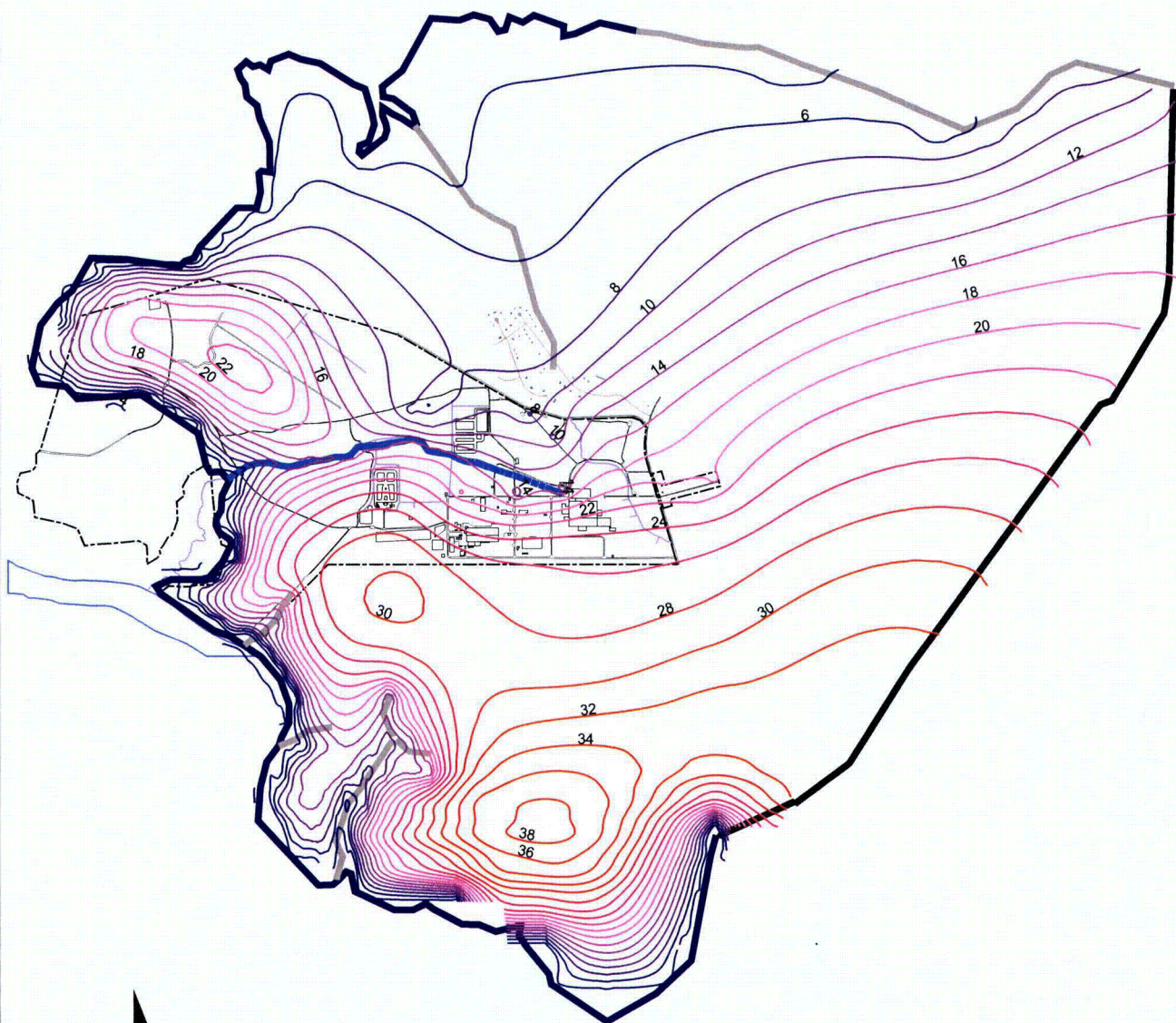


GE - Wilmington, NC Site

Date: 10/4/01

Map No.: 7810003013m





Explanation

- Groundwater elevation contour (ft msl) (variable color)
- River boundary
- No flow boundary
- Drain boundary
- Constant head boundary
- GE/GNF property boundary

Figure P-20
Calibrated Groundwater
Elevations – Full Domain
Sep 2000

Wilmington Site

Figure P-21 Model 2004 Update – Calibration Curve

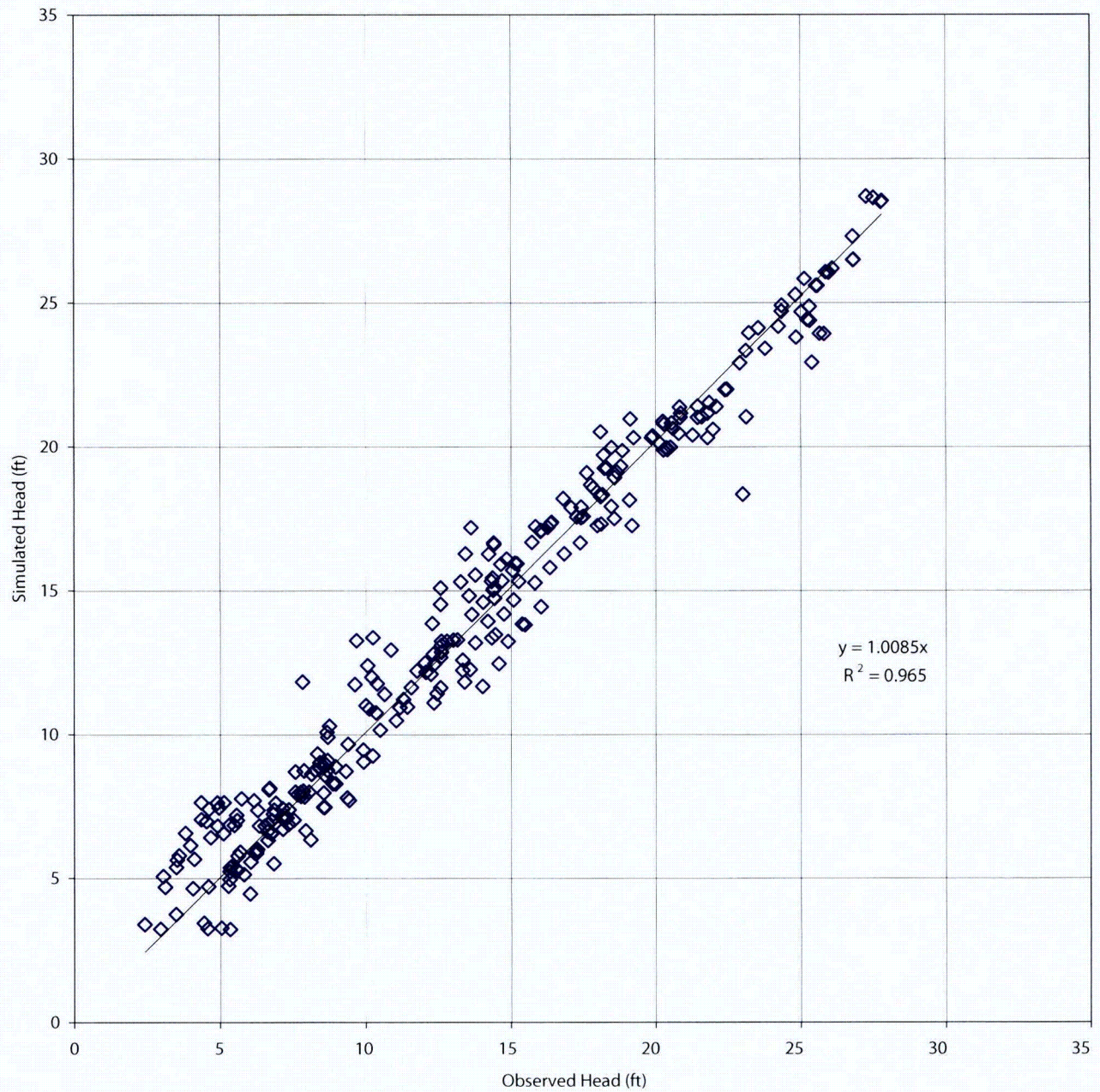


Table of Contents

Q.1	Fugitive Dust	Q-1
Q.2	Off-Road Construction Equipment.....	Q-1
Q.3	Motor Vehicles	Q-1

List of Tables

Q-1	Key Assumptions Used for Proposed GLE Facility Construction Air Emissions Estimates
Q-2	Estimated Air Emissions for Proposed GLE Facility Construction Sources

[This page intentionally left blank.]

Appendix Q

Air Emissions from Proposed GLE Facility: Construction Sources

Q.1 Fugitive Dust

Construction of facilities the scale of the Proposed GLE Facility commonly produces fugitive dust emissions that potentially could have a temporary impact on air quality in the vicinity of the construction project. The fugitive dust emissions from the Proposed GLE Facility construction site were estimated. The estimates were derived following standard practices for applying fugitive dust emission factors developed for regulatory agencies to estimate PM emissions from construction activities when the area and duration for a construction project are known (WRAP, 2004). The key assumptions used for the estimates are summarized in **Table Q-1**, and the estimated fugitive dust emissions are presented in **Table Q-2**. Actual fugitive dust emissions levels from construction of the Proposed GLE Facility are expected to be lower than the values that were estimated using the general emissions factors. Fugitive dust emissions at the GLE construction site (i.e., GLE Facility site) are expected to be naturally mitigated by the high annual precipitation for the area in which the Proposed GLE Facility would be located (see **Section 3.6.2.2** of this Report, *Precipitation [Climate]*). In addition, regular use of water spray trucks and other fugitive dust-suppression practices that are planned to be used during construction (see **Section 5.6** of this Report, *Air Quality [Mitigation Measures]*) would further mitigate fugitive dust emissions at the GLE construction site.

Q.2 Off-Road Construction Equipment

The air emissions resulting from operation of the off-road construction equipment at the GLE construction site were estimated. The key assumptions used for the estimates are summarized in **Table Q-1**. Equipment-specific emissions factors were developed for the assumed equipment mixes using the U.S. Environmental Protection Agency's (EPA's) NONROAD emission factor model (U.S. EPA, 2004a). The estimated air emissions are presented in **Table Q-2**.

Q.3 Motor Vehicles

The motor vehicle traffic impacts projected to occur during the construction of the Proposed GLE Facility are discussed in **Section 4.2.2.1** of this Report (*Site Preparation and Construction [Proposed Action]*). Based on the motor vehicle trip estimates for the Proposed GLE Facility construction phase presented in **Section 4.2.2.1**, the air emissions resulting from these motor vehicle trips were estimated. The key assumptions used for the estimates are summarized in **Table Q-1**. Applicable emissions factors selected from existing factors developed using EPA's MOBILE vehicle emission factor model were used to predict the motor vehicle emissions associated with the Proposed GLE Facility construction phase. The estimated air emissions are presented in **Table Q-2**. Because motor vehicles are mobile sources, the emission estimates do not represent the emissions to the atmosphere from any one location (e.g., the GLE construction site or any other given point). Instead, the estimated emissions represent the incremental increase in air emissions to the atmosphere from all automobiles and trucks traveling along the same roadway routes that would be used by the automobiles and trucks traveling to and from the GLE construction site.

[This page intentionally left blank.]

Tables

**Table Q-1. Key Assumptions Used for Proposed GLE Facility Construction
Air Emissions Estimates**

Air Emission Source	Assumption Parameter	Assumption Value
General assumptions	Construction period	3 years
	Total number of construction days per year	260 days/year
	Hours per construction day	10 hours/day
	Total number of construction workers	300 to 500 workers during initial 3 years of construction, with total daily number varying depending on the construction activities
	Operating day schedule	Project site access road construction: Month 1 Project site preparation: Month 2 through Month 6 Buildings and general construction: Month 7 through Month 36
	Average number of on-site workers per construction day	375 workers ^a
Fugitive dust sources	Emission factors	Access road construction and project site preparation: 0.42 ton/acre/month Buildings and general construction activities: 0.11 ton/acre/month
Off-road construction equipment	Off-road equipment mix for site preparation and road construction	4 Dozers 4 Loaders 2 Graders 2 Compactors/rollers 1 Excavator 1 Water truck 1 Paver (on-site part time)
	Off-road equipment on-site during buildings and general construction	1 Crane 4 Tractors/loaders 4 Forklifts 4 Aerial lifts 2 Air compressors
	Emission factors	Equipment-specific factors for equipment mix using EPA's NONROAD emission factor model
Motor vehicles (automobiles, SUV, pickup trucks)	Average number of construction worker vehicle trips per work day	375 trips
	Average number of visitor vehicle trips per work day	20 trips
	Average vehicle miles traveled per trip	10 miles
	Emission factors	NC DAQ factors developed using EPA's MOBILE6 vehicle emission factor model

(continued)

**Table Q-1. Key Assumptions Used for Proposed GLE Facility Construction
Air Emissions Estimates (continued)**

Air Emission Source	Assumption Parameter	Assumption Value
Motor vehicles (heavy-duty, diesel haul trucks and tractor trailers)	Average number of truck shipments to or from Proposed GLE Facility per day	30 Local trucks, including dump trucks, concrete trucks, waste hauling trucks, and other trucks from local construction material suppliers. 5 Long-haul trucks from equipment and material suppliers ^c
	Average vehicle miles traveled per trip per day	Local trucks = 20 miles ^b Long-haul trucks = 520 miles ^c
	Emission factors	NC DAQ factors developed using EPA's MOBILE6 vehicle emission factor model

^a Basis for assumption is average of construction worker employment estimates for the initial 3 years of construction.

^b Basis for assumption is each local trip consists of two 10-mile segments.

^c Long-haul trucks are considered to be tractor-trailer trucks that travel to and from facilities outside of the Wilmington area, such as the facilities listed in **Table 4.2-2** and other facilities nationwide, depending on the type of material shipped.

Table Q-2. Estimated Air Emissions for Proposed GLE Facility – Construction Sources^a

Air Emission Source	Average Daily Construction Air Emissions Resulting from On-site Construction Activities				
	CO	NO _x	SO ₂	VOC	PM
Fugitive dust					1,500 lb/day
Off-road construction equipment	188 lb/day	45 lb/day	0.2 lb/day	8 lb/day	30 lb/day
Air Emission Source	Annual Construction Air Emissions Resulting from On-site Construction Activities				
	CO	NO _x	SO ₂	VOC	PM
Fugitive dust					194 ton/yr
Off-road construction equipment	41 ton/yr	5 ton/yr	< 0.1 ton/yr	0.8 ton/yr	4 ton/yr
Motor Vehicles	Average Daily Off-site Motor Vehicle Air Emissions Resulting from Construction Traffic to and from Proposed GLE Facility				
	CO	NO _x	SO ₂	VOC	PM
Automobiles	66 lb/day	11 lb/day	0.1 lb/day	12 lb/day	1 lb/day
Heavy-duty diesel trucks	36 lb/day	43 lb/day	0.2 lb/day	2 lb/day	5 lb/day

^a Estimates based on assumptions presented in Table Q-1.

[This page intentionally left blank.]

Tables of Contents

R.1	Construction Air Emissions Dispersion Modeling	R-1
R.2	AERMOD Site-Specific Input Data	R-1
R.3	AERMOD Model Emission Source Assumptions.....	R-2
R.4	AERMOD Receptor Grid Layout.....	R-4
R.5	AERMOD Modeling Results.....	R-4

List of Tables

R-1	AERMOD Site-Specific Input Parameter Values Used for Proposed GLE Facility Construction Ambient Air Dispersion Modeling
R-2	AERMOD Predicted Maximum Fenceline Air Pollutant Concentrations Due to Proposed GLE Facility Onsite Construction Activities

List of Figures

R-1	Wind rose for Wilmington International Airport based on 1992 through 1996 meteorological data used in construction dispersion modeling.
R-2	Receptor grid patterns used for AERMOD modeling of the air emissions due to construction activities.
R-3	Annual average concentration isopleths for PM ₁₀ due to construction activities.
R-4	Annual dry deposition rate isopleths for PM ₁₀ due to construction activities.
R-5	Annual wet deposition rate isopleths for PM ₁₀ due to construction activities.
R-6	Annual total deposition rate isopleths for PM ₁₀ due to construction activities.

[This page intentionally left blank.]

Appendix R

Air Emissions Dispersion Modeling from Construction Phase of Proposed GLE Facility Using AERMOD Model

R.1 Construction Air Emissions Dispersion Modeling

Air emissions dispersion modeling was performed to predict ambient air concentrations from the on-site air emissions released during the Proposed GLE Facility construction phase. The U.S. Environmental Protection Agency's (EPA's) **AMS/EPA Regulatory Model (AERMOD)** was used for the modeling. This computer model uses steady-state Gaussian plume air dispersion algorithms to estimate air pollutant concentrations and deposition values at receptor sites up to a distance of 31 miles (50 kilometers [km]) from the air emissions source (U.S. EPA, 2006a). The AERMOD was used to estimate concentrations and deposition values of particulate matter (PM) with aerodynamic diameters less than 10 μm (PM₁₀) at receptors due to construction activity. The AERMOD can be used to model both wet and dry PM₁₀ depletion from a plume. Dry deposition is removal of pollutants from the air due to gravitational settling; wet deposition occurs when precipitation removes pollutants from the air and deposits them on the ground. The AERMOD area depletion algorithm was selected for the dispersion modeling because it is an optimized method for calculating dry PM removal from the plume when modeling area sources (U.S. EPA, 2006b).

The AERMOD was also used to estimate concentrations of gaseous carbon monoxide (CO), nitrogen oxides (NO_x), sulfur dioxide (SO₂), and volatile organic compounds (VOCs) at the Wilmington Site fence line due to off-road construction equipment and other motor vehicles operating at the GLE construction site (i.e., GLE Facility site) and along the proposed North access road. Plume depletion was not included in the calculations involving gaseous air emissions.

R.2 AERMOD Site-Specific Input Data

Application of AERMOD to a given emission source scenario requires the input of Site-specific surface and upper air meteorological data (e.g., wind speeds and directions). The model also requires input values for Site-specific factors related to the air emission dispersion characteristics of the landscape surrounding the emission source. These parameters are surface-roughness length, albedo, and Bowen ratio. Surface-roughness length relates to the height of obstacles on the land surface around the emission source affecting the wind flow and is expressed as the height at which the mean horizontal wind speed is zero. Albedo is the fraction of incoming solar radiation that is reflected by the land surface around the emission source. The Bowen ratio is an indicator of surface moisture in the land surface around the emission source and is expressed as the ratio of sensible heat flux to latent heat flux. The values used for these AERMOD input parameters vary by the type of landscape (e.g., urban, deciduous forest, coniferous forest, swamp, cultivated land, grassland, water) and the season of the year.

The normal variability of weather conditions in the vicinity of the Proposed GLE Facility was represented using a 5-year period of surface meteorological data from the National Climatic Data Center's Integrated Surface Hourly Data (ISHD) collected at the Wilmington International Airport station (Station 13748). This airport weather station is approximately 4.5 miles (7.2 km) from the Proposed GLE Facility location and is considered to be representative of the local meteorological conditions at the GLE construction site. Upper air meteorological data are not collected at the Wilmington International Airport station; therefore, upper air data collected at the Charleston International Airport station (Station 13880), about 150 miles (241 km) southwest of the Wilmington Site, were used for the required AERMOD inputs. This station was chosen over other stations in the region where upper air data are collected because of its general

proximity and similar site conditions to those at the Wilmington International Airport. The meteorological data used for modeling were for the years 1992 through 1996 because this time period was the most recent data available for which surface and upper air data from the two weather stations coincided. **Figure R-1** shows the wind rose based on data used for dispersion modeling of air emissions from the GLE construction site. The collected surface and upper air meteorological data were integrated into the appropriate combined surface and profile meteorological input files using the AERMOD's Meteorological Preprocessor (AERMET).

The *AERMET User's Guide* specifies seasonal values for surface roughness length, albedo, and Bowen ratio by land-cover type and season (U.S. EPA, 2004c). To select the appropriate parameter values to use for modeling the GLE construction site, four distinct land sectors in a 1.86-miles (3-km) radius around the GLE construction site were identified based on a general qualitative judgment of the extent of existing land development and the amount of open water within the circle formed by the selected radius. For each sector, the land-cover types and area percentages of those types within in the sector were obtained from the 2001 National Land Cover Dataset (NLCD) (USGS, 2003). Because land-cover type affects the atmospheric dispersion properties, individual surface-roughness length, albedo, and Bowen ratio values were selected for each of the four sectors around the GLE construction site. The land-cover categories used for the NLCD do not correspond directly to EPA's land-cover category descriptions used for AERMET; therefore, professional judgment was used to cross-reference the NLCD categories with the AERMET categories. Each parameter was considered individually because land cover affects each of these parameters differently. Separate seasonal parameter values were determined for each sector. These values were calculated as the average of the applicable seasonal value listed in the *AERMET User's Guide* for the land-cover category (cross-matched to the corresponding NLCD land-cover categories identified for the sector) weighted by the area of coverage in the sector. **Table R-1** presents the land-cover area weighted average surface roughness length, albedo, and Bowen ratio values developed for the GLE construction site and used as input for the AERMET modeling. Because Wilmington, NC, has a much higher than average annual rainfall (approximately 57 inches/year [1448 mm/year]) than the average for most of the country (approximately 31 inches/year [787 mm/year]) (NOAA, 2002, 2004), wet condition values were used for the Bowen ratio.

R.3 AERMOD Model Emission Source Assumptions

The GLE construction site is assumed to have the same boundaries as the Proposed GLE Facility (see **Figure R-2**). The AERMOD was run using a unitized emission rate (1 g/sec) to obtain the unitized concentration and deposition rates for each receptor location. Then, the corresponding unitized concentration and deposition rate values were multiplied by site-specific air pollutant emission factors to obtain predicted concentration and deposition values at each receptor location. The site-specific emission factors were based on the assumptions and emissions estimates for construction-related fugitive dust and vehicle emissions described in **Section 4.6.2.1.1** of this Report (*Site Preparation and Construction Air Emissions Sources*).

The GLE construction site was modeled as an area source with uniform emissions because the entire 100 acres (40.5 hectares [ha]) for the Proposed GLE Facility is expected to be cleared and graded as part of the initial site preparation. Off-road construction equipment was assumed to move over the entire GLE construction site. Construction motor vehicle traffic was assumed to use the proposed North access road to access the GLE construction site from N.C. Highway 133 (NC 133, also known as Castle Hayne Road). The access road was assumed to be unpaved during the site preparation stage of construction and later paved for the general construction stages. Assumptions made for the dispersion modeling were consistent with the emission estimate assumptions presented in **Table R-1**.

Fugitive dust emissions produced by wind erosion of the open spaces on the cleared GLE construction site were assumed to be of minor significance and not included in the AERMOD dispersion modeling for several reasons. First, based on a review of wind speed and precipitation data for the GLE construction site (**Section 3.6.2.2**) and EPA's AP-42 emission factors for wind-blown dust (U.S. EPA, 2006a), it was concluded that the potential for significant amounts of fugitive dust emissions at the GLE construction site due to wind erosion is small on an annual basis. Second, significant portions the GLE construction site would likely only be fully exposed to the wind for a relatively short periods of time during the overall construction phase before the construction of the building foundations and hard surfacing of the open storage and parking areas begins. Third, the large number of days per year with precipitation that is expected to occur at the GLE construction site would reduce the number of potential days for wind erosion to occur. Finally, the trees surrounding the GLE construction site and bordering the proposed North access road would serve as a wind break along portions of the exposed soil areas, further reducing the potential for wind blown dust from the site.

Emissions from the GLE construction site were assumed to occur only during daylight construction hours; therefore, AERMOD was set up with an assumed 10-hour daily work schedule (6 a.m. to 4 p.m.) from Monday through Friday. Short-term emission rates were calculated using the highest stage-specific emission rate for each source. This method produces the most conservative, short-term emission estimates. Annual emission values calculated weighting by the number of months for each stage of construction. The first year is expected to have the highest overall annual emissions and can be considered conservative for long-term average dispersion results. Twenty-four hour emission rates were estimated to be the same as those from the construction period having the highest emission rate for each source, and thus were considered conservative. The emission levels of PM_{10} due to road construction, clearing, grading of the site, and construction traffic were calculated assuming that a standard dust-suppression work practice is implemented of watering the GLE construction site and unpaved access road twice per day to keep particulate emissions to a minimum.

PM_{10} emission factors were used for the AERMOD dispersion modeling of the Proposed GLE Facility construction activities. Using EPA precedent (U.S. EPA, 1999), PM_{10} emissions were assumed to be distributed so that 60% had aerodynamic diameters between 10 μm and 2.5 μm , and 40% had aerodynamic diameters less than 2.5 μm ($PM_{2.5}$).

Wet and dry PM depositions were considered separately for 24-hour deposition flux values because 24-hour values must be added for each day at each receptor. The wet deposition values were zero for most time periods because wet deposition occurs only during precipitation events. Also, the maximum values for wet deposition are 2 to 3 orders of magnitude less than the maximum values for dry deposition.

Dispersion of the air emissions from the motor vehicles (e.g., worker automobiles, trucks) on the proposed North access road was also included in the AERMOD modeling of the Proposed GLE Facility construction air quality impacts. **Appendix Q** describes the assumptions made for emission calculations.

The AERMOD-predicted concentration at any given receptor location is the sum of the impacts from all on-site sources operating during the modeled Proposed GLE Facility construction phase. For example, the annual average PM concentration at a receptor location is the sum of the modeled annual average location-specific concentration due to GLE construction site emissions and the proposed North access road emissions. The same calculation procedure was made for annual average PM deposition rates. Twenty-four hour PM concentrations and deposition rates were summed for the construction-day scenario on which the combination of construction activities were judged to be the highest total daily PM emission rate during the initial 3-year construction period.

R.4 AERMOD Receptor Grid Layout

Two sets of receptor grids were created in the AMS EPA Regulatory Model (AERMOD) at both on-site and off-site receptor locations around the Proposed GLE Facility for the purpose of assessing ground-level ambient concentrations from air emissions release during construction of the Facility. The first grid is a standard polar receptor grid created along 16 radials (i.e., 22.5-degree radials) originating from a point within the Proposed GLE Facility footprint and continuing outward to an endpoint distance of 31 miles (50 kilometers). Receptors were placed at the following distances (meters) along these radials: 350, 400, 500, 600, 700, 800, 900, 1000, 1500, 2000, 2500, 3000, 3500, 4000, 4500, 5000, 5500, 6000, 6500, 7000, 7500, 8000, 8500, 9000, 9500, 10000, 11000, 12000, 13000, 14000, 15000, 16000, 17000, 18000, 19000, 20000, 25000, 30000, 35000, 40000, 45000, and 50000. A second site-specific receptor grid was created along the entire perimeter length of the Wilmington Site property boundary (i.e., fenceline). These receptors were placed every 7.5 degrees. **Figure R-2** shows the relative receptor locations for polar and fenceline grids used for the AERMOD dispersion modeling of the Proposed GLE Facility construction activities. Dispersion of the particulate matter (PM) emissions generated during construction was modeled using both receptor grids. Dispersion of motor vehicle gaseous emissions was modeled using only the fenceline receptor grid.

R.5 AERMOD Modeling Results

The AERMOD model predicted maximum ambient air concentrations at the Wilmington Site property boundary (i.e., fenceline) due to air emissions from the Proposed GLE Facility on-site construction activities are presented in **Table R-2**. The maximum concentration at the fenceline represents the highest potential exposure location to the general public due to air emission sources associated with the Proposed GLE Facility construction activities. This is because these air emission sources would be on-site, ground-level sources (e.g., motor vehicle engine exhaust), and air concentrations from ground-level emission sources decrease with distance from the source location. General public access onto the Wilmington Site is and will continue to be restricted, thus preventing general public exposure to concentrations greater than the maximum concentration at the fenceline.

The Proposed GLE Facility would be located in a region for which the air quality is in attainment with all National Ambient Air Quality Standards (i.e., NAAQS) (see **Section 3.6.3.1**). Compliance with ambient air quality standards is determined by long-term ambient air quality monitoring at predetermined monitoring station locations using methods and analysis procedures established by the regulatory agencies. These ambient standards are not intended to be used for direct assessment of localized air quality impacts from individual, temporary emission sources such as construction projects. However, comparison of the predicted AERMOD concentrations with ambient air quality standards as presented in **Table R-2** provides an order-of-magnitude measure of the potential incremental contribution to ambient pollutant levels in the vicinity of emissions of the Proposed GLE Facility produced by the on-site construction activities.

The PM₁₀ concentrations predicted by the AERMOD modeling of the Proposed GLE Facility construction activities include the contributions of fugitive dust and the PM₁₀ vehicle emissions. **Figure R-3** shows isopleths of annual average concentration of PM₁₀ due to construction activities. The maximum off-site annual average concentration of PM₁₀ due to construction activities is predicted by the AERMOD model to be 3.5 µg/m³ and occurs at the fenceline to the northeast (45-degree radial) of the GLE construction site. The maximum on-site annual average concentration of PM₁₀ is predicted to be 12.3 µg/m³. This predicted fenceline maximum PM₁₀ concentration is one order-of-magnitude lower than the ambient air quality standard of 50 µg/m³. The maximum off-site 24-hour average concentration value for PM₁₀ is predicted to be 114 µg/m³, which would occur at the fenceline to the northeast (52.5-degree radial), which

is less than the ambient air quality standard of $150 \mu\text{g}/\text{m}^3$. The maximum predicted on-site value is $191 \mu\text{g}/\text{m}^3$.

The quantity of PM that would be deposited on the ground and other surfaces in the vicinity of the GLE construction site were predicted using the AERMOD wet and dry deposition algorithms. **Figures R-4 through R-6** show that the AERMOD predicted annual dry, wet, and total deposition rates around the GLE construction site due to the construction activities would be very small. The total maximum annual deposition flux of PM_{10} predicted at the property fenceline is $0.3 \text{ g}/\text{m}^2/\text{year}$, which occurs to the northeast (37.5-degree radial) from the center of the source. The on-site predicted maximum annual deposition flux is $0.7 \text{ g}/\text{m}^2/\text{year}$. The maximum predicted 24-hour dry deposition flux at the property fenceline is $0.02 \text{ g}/\text{m}^2/\text{day}$, which occurs to the northeast (52-degree radial). Onsite, the maximum dry deposition flux value is $0.02 \text{ g}/\text{m}^2/\text{day}$.

Table R-2 also presents the maximum ambient air concentrations at the Wilmington Site property boundary (i.e., fenceline) predicted by the AERMOD modeling for gaseous air emissions from the Proposed GLE Facility on-site construction activities (i.e., carbon monoxide, nitrogen dioxide, volatile organic compounds, and sulfur dioxide exhausted from off-road construction equipment and other motor vehicles traveling on-site). All of the predicted concentrations are multiple orders of magnitude lower than the level of the ambient air quality standard used for comparison.

[This page intentionally left blank.]

Tables

Table R-1. AERMOD Site-Specific Input Parameter Values Used for Proposed GLE Facility Construction Ambient Air Dispersion Modeling

Proposed GLE Facility Sector Orientation ^a and Land Cover Percentages ^b	Season	AERMET Input Parameter Values ^c		
		Surface Roughness Length (meters)	Albedo	Wet Bowen Ratio
Sector 1 - East of site 6% Developed land 10% Cultivated land/pasture 31% Forest 36% Woody wetlands <1% Open water 16% Other	Winter	0.62	0.41	0.47
	Spring	0.68	0.14	0.23
	Summer	0.72	0.15	0.24
	Fall	0.67	0.16	0.31
Sector 2 – Southeast of site 19% Developed land 16% Cultivated land/pasture 31% Forest 17% Woody wetlands <1% Open water 16% Other	Winter	0.56	0.45	0.47
	Spring	0.62	0.14	0.28
	Summer	0.67	0.16	0.33
	Fall	0.60	0.16	0.42
Sector 3 – Southwest of site 4% Developed land 1% Cultivated land/pasture 19% Forest 53% Woody wetlands 15% Open water 8% Other	Winter	0.62	0.32	0.44
	Spring	0.67	0.13	0.16
	Summer	0.68	0.13	0.16
	Fall	0.67	0.15	0.20
Sector 4 – Northwest and North of site <1% Developed land 1% Cultivated land/pasture 18% Forest 75% Woody wetlands 1% Open water 4% Other	Winter	0.73	0.32	0.47
	Spring	0.80	0.12	0.15
	Summer	0.80	0.14	0.14
	Fall	0.79	0.15	0.16

^a Sector orientation in AERMOD set up as Sector 1 (15° to 75°), Sector 2 (75° to 180°), Sector 3 (180° to 255°), and Sector 4 (255° to 15°) where 0 degrees is North.

^b Approximate sector land cover percentages within 3 kilometer-radius around Proposed GLE Facility identified using 2001 National Land Cover Dataset (NLCD).

^c Value listed is proportional average by land cover percentage in sector of the applicable *AERMET User's Guide* land cover category seasonal values cross-matched to the corresponding NLCD land cover categories identified for the sector.

**Table R-2. AERMOD Predicted Maximum Fenceline Air Pollutant Concentrations
Due to Proposed GLE Facility Onsite Construction Activities**

Air Pollutant	Averaging Time	AERMOD predicted maximum fenceline concentration ($\mu\text{g}/\text{m}^3$)	Comparable Ambient Air Quality Standard level^{a,b} ($\mu\text{g}/\text{m}^3$)
Carbon monoxide (CO)	Annual average	0.6	No ambient standard
	8-hour	34	10,000
	1-hour	158	40,000
Nitrogen dioxide (NO ₂)	Annual average	0.1	100
Particulate matter (PM ₁₀)	Annual average	3.5	50
	24-hour	114	150
Sulfur dioxide (SO ₂)	Annual average	0.0007	78
	24-hour	0.01	364
	3-hour	0.04	1,300
Volatile organic compounds (VOC)	Annual average	0.08	No ambient standard ^d

^a Compliance with ambient air quality standards is determined by long term ambient air quality monitoring at predetermined monitoring station locations using methods and analysis procedures established by the regulatory agencies. These ambient standards are not intended to be used for direct assessment of localized ambient air pollutant concentrations from temporary emission sources such as those construction projects. The comparison of the predicted AERMOD concentrations with ambient air quality standards presented in this table is intended to provide an order-of-magnitude measure of the potential incremental contribution to ambient pollutant levels in the vicinity of emissions of the Proposed GLE Facility produced by on-site construction activities.

^b Standards listed are the federal National Ambient Air Quality Standards (NAAQS), which the State of North Carolina has adopted as state standards with the exception of the annual average standard for PM. The federal annual average NAAQS has been revoked but the level is still maintained as a North Carolina state standard.

^c No federal or State annual average air quality standard for this pollutant.

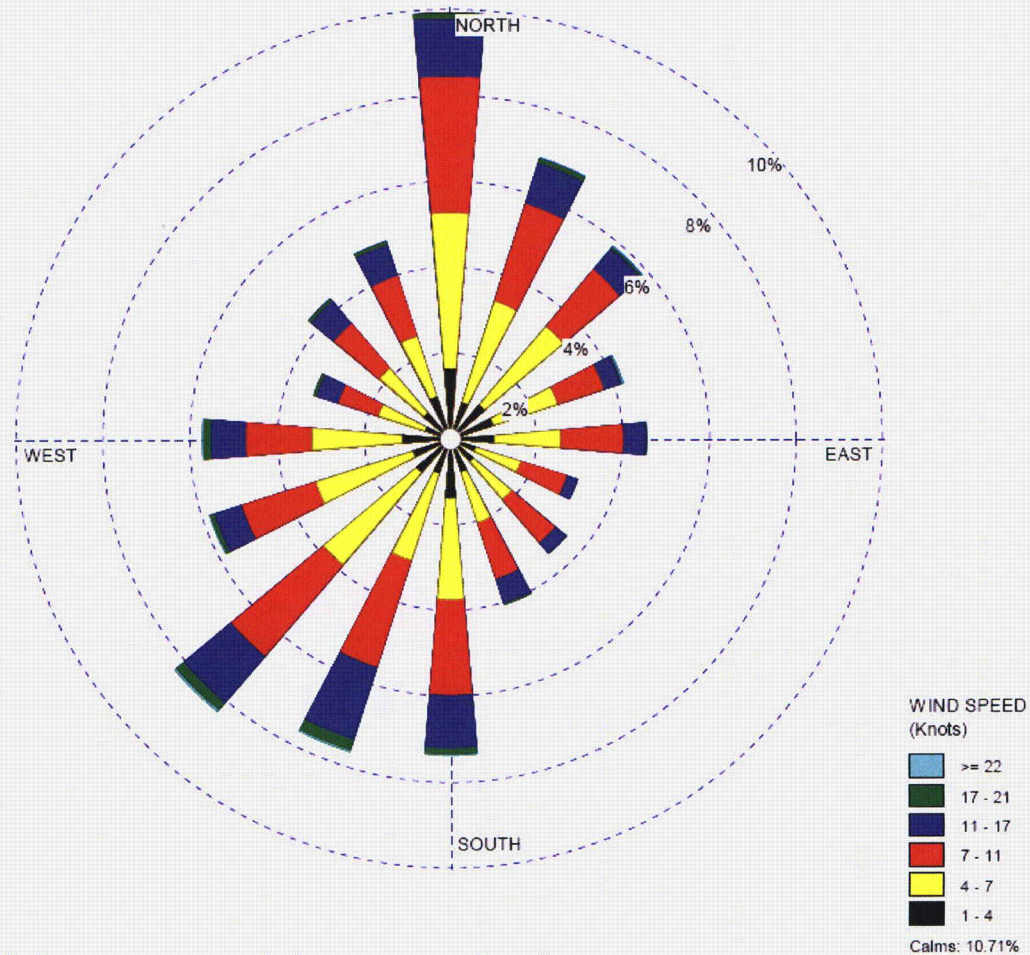
^d No air quality standards are established specifically for VOCs. VOC is a precursor pollutant involved in the atmospheric photochemical formation of ozone for which ambient air quality standards have been established.

Figures

WIND ROSE PLOT:

Station #13748 - WILMINGTON/NEW HANOVER COUNTY, NC

DISPLAY:

Wind Speed
Direction (blowing from)

COMMENTS:

Source of Data: DS-3505.

DATA PERIOD:

1992-1996
Jan 1 - Dec 31
00:00 - 23:00

CALM WINDS:

10.71%

AVG. WIND SPEED:

7.13 Knots

TOTAL COUNT:

42911 hrs.

DATE

1/2/2008

PROJECT NO.:

WRPLOT View - Lakes Environmental Software

Figure R-1. Wind rose for Wilmington International Airport based on 1992 through 1996 meteorological data used in construction dispersion modeling.

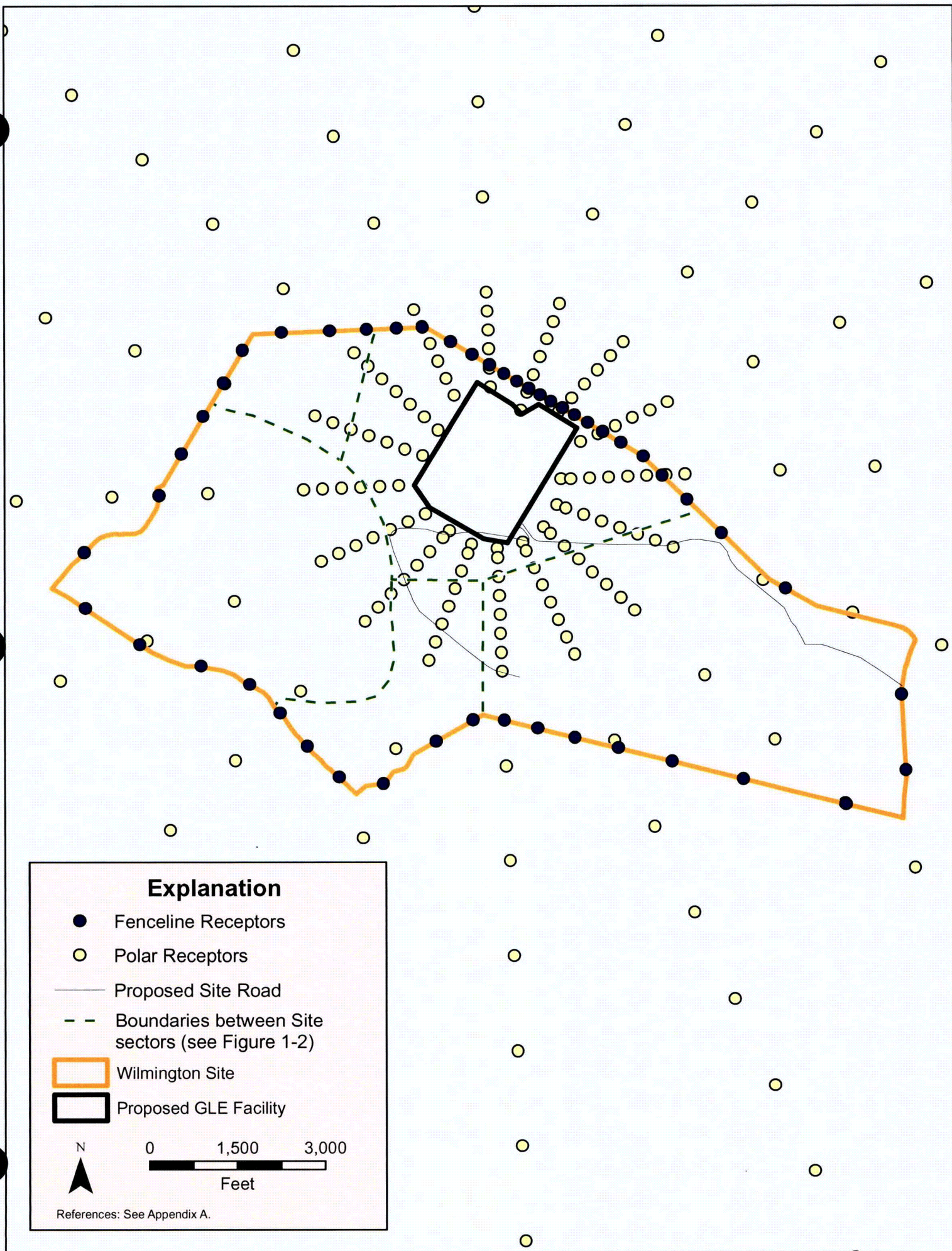


Figure R-2. Receptor grid patterns used for AERMOD modeling of the air emissions due to construction activities.

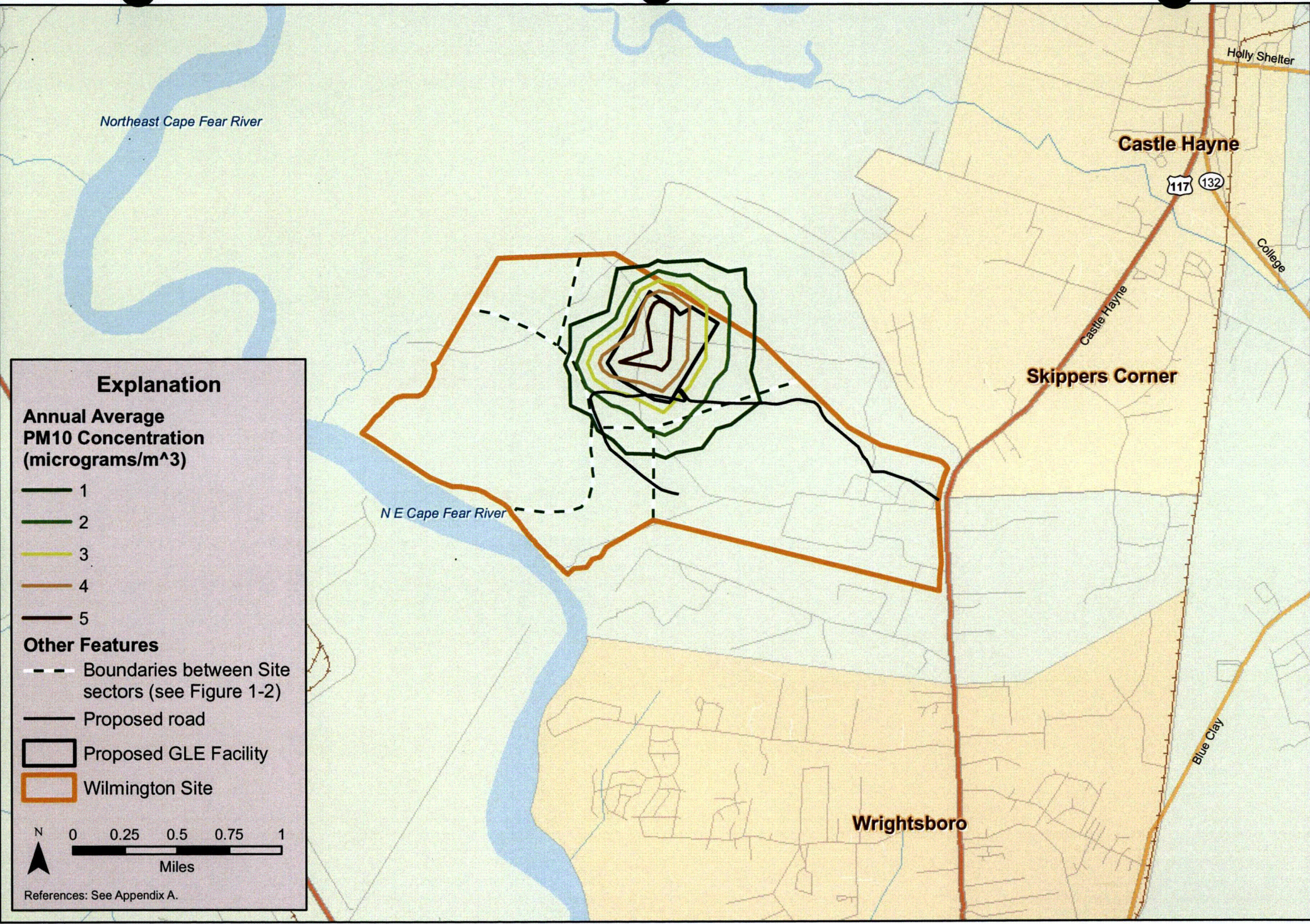


Figure R-3. Annual average concentration isopleths for PM₁₀ due to construction activities.

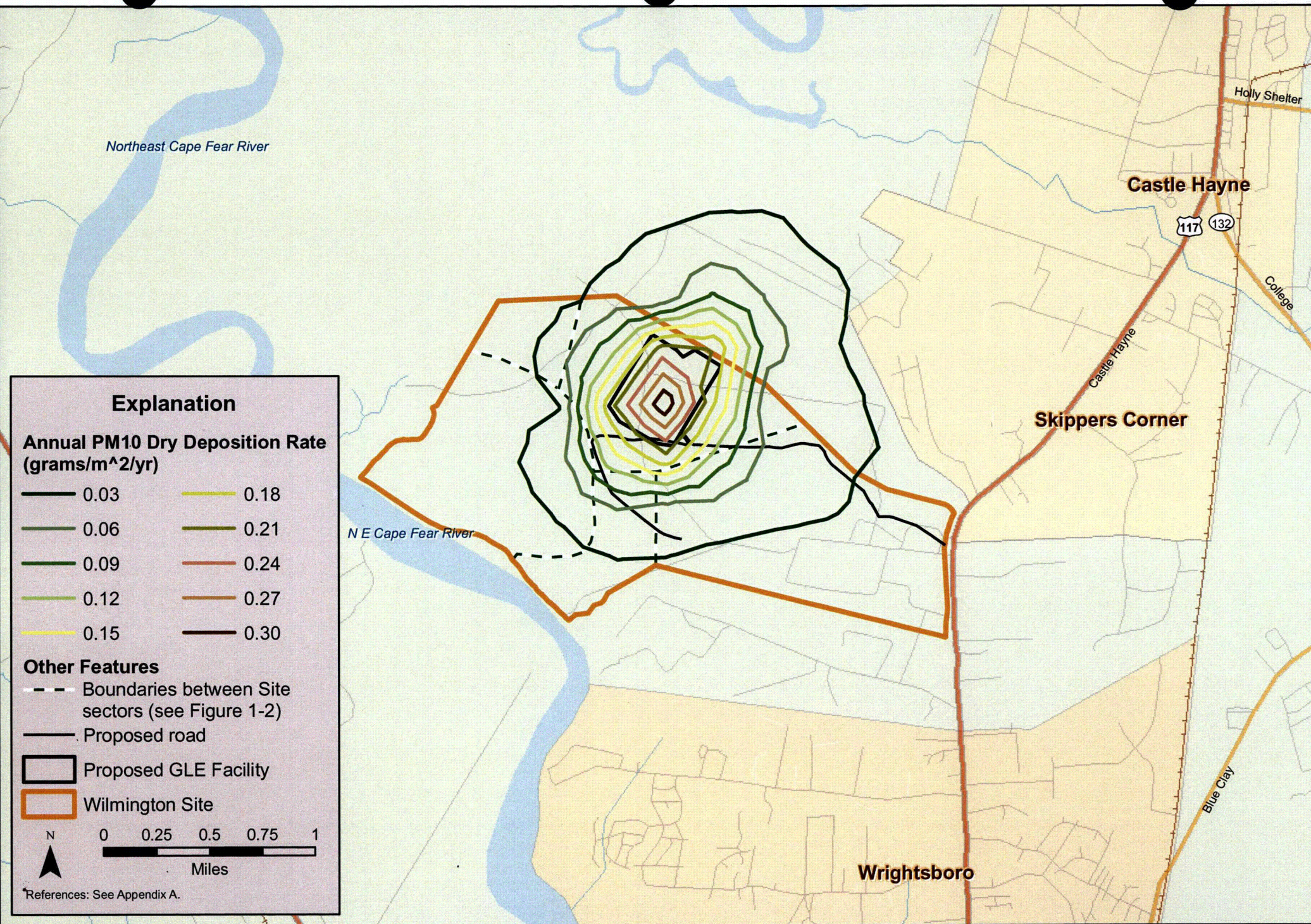


Figure R-4. Annual dry deposition rate isopleths for PM₁₀ due to construction activities.

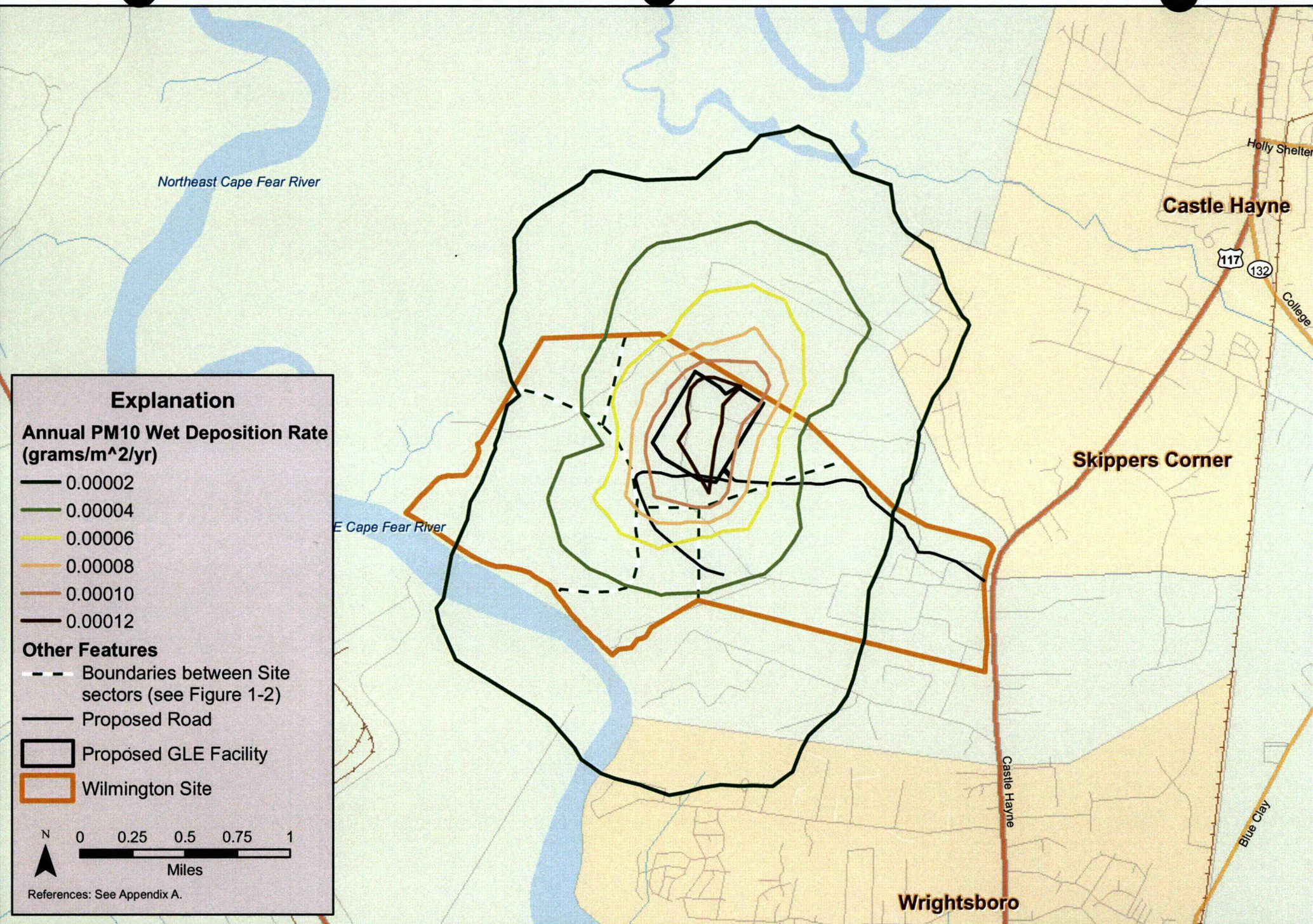


Figure R-5. Annual wet deposition rate isopleths for PM₁₀ due to construction activities.

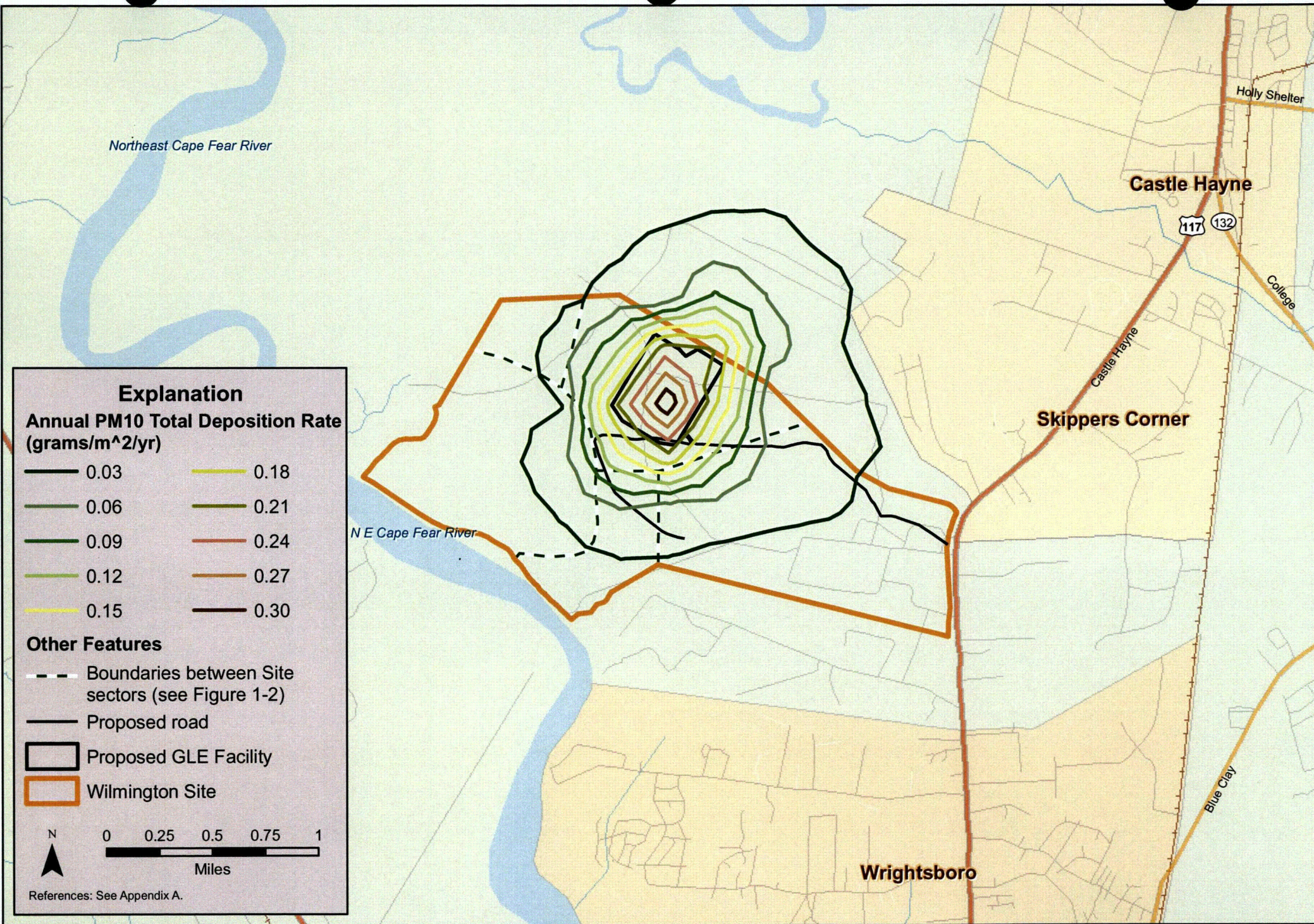


Figure R-6. Annual total deposition rate isopleths for PM₁₀ due to construction activities.

Table of Contents

S.1	Operation Air Quality Impacts	S-1
S.2	XOQDOQ Meteorological Data	S-1
S.3	XOQDOQ Emission Source Model Assumptions.....	S-1
S.4	XOQDOQ Receptor Grid Layout.....	S-2
S.5	XOQDOQ Modeling Results.....	S-2
S.6	Operation Air Quality Impacts	S-3

List of Tables

S-1	Stack/Vent Characteristics Used for Proposed GLE Facility Operation Ambient Air Dispersion Modeling
S-2	Total Uranium and Uranium Isotope Emission Rates Used for Proposed GLE Facility Operation Ambient Air Dispersion Modeling
S-3	Predicted Unitized Concentration (Chi/Q) and Relative Deposition (D/Q) for Selected Receptors from Proposed GLE Facility Operation Air Emissions
S-4	Predicted Unitized Concentration (Chi/Q) for Receptors Close to the Proposed GLE Facility (<5 miles)
S-5	Predicted Unitized Concentration (Chi/Q) for Receptors Far from the Proposed GLE Facility (5 mi – 50 miles)
S-6	Predicted Relative Deposition (D/Q) for Receptors Close to the Proposed GLE Facility (<5 miles)
S-7	Predicted Relative Deposition (D/Q) for Receptors Far from the Proposed GLE Facility (5 mi – 50 miles)

List of Figures

S-1	Approximate relative location of stack groups used in XOQDOQ modeling.
S-2	Annual average concentration of radioisotopes from all stacks at the Wilmington Site.
S-3	Annual deposition rate of radioisotopes from all stacks at the Wilmington Site.

[This page intentionally left blank.]

Appendix S

Air Emissions Dispersion Modeling for Operation of the Proposed GLE Facility Using XOQDOQ Model

S.1 Operation Air Quality Impacts

Air emissions dispersion modeling was performed using the XOQDOQ model in NRCDOSE (version 2.3.9) to estimate the normalized concentration ($\text{Chi}[\chi]/Q$) and/or relative deposition rate (D/Q) of uranium particle air emissions from the Proposed GLE Facility during normal operations at selected receptor locations (RSICC, 2007). The XOQDOQ model assumes that air emissions released into the atmosphere follow a Gaussian (normal) distribution around the plume centerline. Results may be calculated to a distance of 50 miles (80 kilometers [km]) from the source considering radioactive decay and depletion of the plume. The model assumes that the plume follows a straight-line trajectory between the source and all receptors (i.e., no plume meander); this approach produces conservative estimates. The XOQDOQ model also can calculate χ/Q and D/Q at user-defined locations.

S.2 XOQDOQ Meteorological Data

The XOQDOQ model requires joint frequency distributions for wind speed and direction by stability class. To generate these model input distributions, meteorological data were used for the years 1988 through 1992, collected at the Wilmington International Airport station (WebMET.com, 2002). These data were gathered in Met144 format and transformed to CD144 format using the U.S. Environmental Protection Agency's (EPA's) MET144 program. This data transformation was necessary to make them compatible with EPA's Stability Array (STAR) program, which generates the joint frequency distributions. The most recent data that could be found in the correct format for use with the STAR program were for calendar year 1992.

S.3 XOQDOQ Emission Source Model Assumptions

The main GLE operations building is planned to be vented through an emissions control system that discharges to the atmosphere through a single roof stack. The Fuel Manufacturing Operation (FMO) facility has multiple roof vents. In addition, separate FMO sources with stacks are located away from the main FMO building. Each source stack with the potential to emit uranium isotopes was included in XOQDOQ model as an individual source with an individual emission rate. The stacks were then grouped by geographic position into three stack groups to allow stacks that are in close proximity to each other to have their emissions contribution directly added at each receptor. The total contributions of each stack group were then spatially summed using geographic information systems (GIS) tools.

Figure S-1 shows the approximate location of the three stack groups used for the XOQDOQ modeling of the Proposed GLE Facility and FMO. Stack Group A represents the Proposed GLE Facility sources and is the location of the main GLE operations building's single stack. For the modeling analysis, Stack Group A is positioned approximately 1.1 miles (1.7 km) from the FMO building. Stack Group C represents the main FMO building roof stacks and other nearby separate sources with stacks within approximately 400 feet (ft; 122 meters [m]) of the main building. Stack Group B represents the two FMO sources with stacks that are too far away from the main building to be included in Stack Group C. Stack Group B is located between the main GLE operations building and the main FMO building approximately 0.7 mi (1.1 km) away from the Stack Group A and approximately 0.4 mi (0.6 km) away from Stack Group C. **Table S-1** lists the stack and vent gas-stream physical characteristics for the stacks in each stack group used for XOQDOQ dispersion modeling. All of the stacks are assumed to have a round cross section.

The total uranium and uranium isotopes (uranium-234 [^{234}U], uranium-235 [^{235}U], uranium-236 [^{236}U], and uranium-238 [^{238}U]) emission rates used for the XOQDOQ dispersion modeling were developed based on stack monitoring data for the existing FMO operations. The total uranium and uranium isotope emission rates used for each FMO stack are listed in **Table S-2**. The SILEX (Separation of Isotopes by Laser Excitation) laser process is a new technology for which air emissions monitoring data presently are not available. To model the stack air emissions from the main GLE operations building, total uranium and individual uranium isotope emission rates for Stack Group A were selected through a review of the FMO stack monitoring data; the modeling source term was based on data from one of the various FMO stacks judged to be most similar to sources expected for Proposed GLE Facility operations. The selected emission rate is considered to be a conservative assumption (i.e., the uranium and uranium isotope emission rates used for the XOQDOQ dispersion modeling are higher than the actual emissions expected from Proposed GLE Facility operations).

S.4 XOQDOQ Receptor Grid Layout

The XOQDOQ model uses a receptor grid for a standard set of receptor locations spaced along 16 radial directions beginning at 0.25 miles (0.4 km) and continuing to a distance of 50 miles (80 km) from the emission source. To this standard receptor grid, additional receptor locations for schools and hospitals in the vicinity of the Proposed GLE Facility were added to the model. Receptor locations were also added at points along the Wilmington Site fenceline to assess the highest off-site χ/Q and D/Q values.

S.5 XOQDOQ Modeling Results

The XOQDOQ modeling results were examined in two different ways to assess the air quality impact of the Proposed GLE Facility operations. First, the air emissions from the Proposed GLE Facility (Stack Group A) were examined for χ/Q and D/Q values at selected locations, as required by NUREG-1748, *Environmental Review Guidance for Licensing Actions Associated with NMSS (Nuclear Material Safety and Safeguards) Programs* (NRC, 2003). Second, the cumulative air quality impact due to air emissions from both the Proposed GLE Facility (Stack Group A) and the existing FMO (Stack Groups B and C) were evaluated. Only the χ/Q values predicted by the XOQDOQ model without decay and without depletion were considered further for several reasons. Assuming no decay or depletion occurs during the dispersion of the plume provides the most conservative (i.e., highest) concentration values. Secondly, the uranium isotopes that would be released have an extremely long half-life compared to the plume transport time or even the lifetime of the Proposed GLE Facility. Also, default values that are used in the XOQDOQ model for decay and depletion result in only slightly lower values, but represent isotopes of other elements with very short decay times compared to the uranium isotopes.

The predicted unitized concentrations (χ/Q) and relative depositions (D/Q) from Proposed GLE Facility air emissions for selected receptor locations are presented in **Table S-3**. The highest on-site χ/Q value is $1.3\text{E-}06 \text{ sec/m}^3$ and is predicted to occur at 0.25 miles (402 m) to the northeast of the main GLE operations building stack location. The highest off-site χ/Q occurs at the Wilmington Site fenceline at 0.3 miles (0.5 km) to the northeast with a value of $1.3\text{E-}06 \text{ sec/m}^3$. The nearest resident is located at 0.9 miles (1.5 km) to the east-southeast and has a χ/Q value of $2.7\text{E-}07 \text{ sec/m}^3$. Each of the specified schools and hospitals are significantly farther away than these locations, ranging from 3.4 miles (5.4 km) away to 29.8 miles (48 km) away. χ/Q values for the schools and hospitals are approximately one to two orders of magnitude lower than that for the nearest resident. **Tables S-4 through S-7** list the χ/Q and D/Q values predicted by the XOQDOQ model for all sectors to a distance of 50 miles (80 km).

Cumulative impacts of air emissions from both the Proposed GLE Facility and existing FMO were calculated by multiplying the χ/Q and D/Q values predicted by the XOQDOQ model for each stack by that stack's emission rates in Ci/sec listed in **Table S-2**. Because the stack groups were far enough away

from each other that they could not be considered to be collocated, the predicted concentration and deposition values for each stack group were spatially summed together using GIS software. The predicted cumulative annual average ambient concentrations of uranium isotopes emitted from the Proposed GLE Facility and the existing FMO facility are presented in **Table 4.6-5**. The predicted cumulative annual average deposition rates of uranium isotopes emitted from Proposed GLE Facility and the existing FMO facility are presented in **Table 4.6-6**.

Figures S-2 and S-3 show the predicted cumulative annual average ambient concentrations and deposition rates of uranium isotopes for the combination of Stack Groups A, B, and C. Most of the contribution for this maximum off-site point of impact is from the currently operating FMO stacks. The maximum off-site annual average concentration of uranium isotopes from the combined stacks is $8.4\text{E-}13 \mu\text{Ci}/\text{m}^3$ and occurs 1.2 miles (2 km) to the south-southeast of the proposed GLE stack, or 0.1 mi (0.2 km) from the south fenceline near the FMO facility. Nearby, the point of maximum off-site deposition occurs with a value of $4.1\text{E-}07 \mu\text{Ci}/\text{m}^2/\text{year}$, which is at a distance of 1.2 miles (1.9 km) to the south-southeast of the proposed GLE stack, or 158 feet (42 m) south of the fenceline near the operating FMO facility. Neither of these points occurs directly at a residence.

The maximally exposed existing residence has an annual average concentration of uranium isotopes from the combined stacks of $7.6\text{E-}13 \mu\text{Ci}/\text{m}^3$ and is at a distance of 1.4 mi (2.2 km) from the main GLE building operations stack, or 0.2 miles (0.3 km) south of the fenceline near the operating FMO building. The combined deposition rate at this residence is $2.1\text{E-}07 \mu\text{Ci}/\text{m}^2/\text{year}$. The nearest residence to the proposed GLE stack is 0.9 mi (1.5 km) to the ESE of the stack, or about 0.03 mi (50 m) from the fenceline of the Wilmington Site. The combined annual average concentration at this residence is $5.8\text{E-}13 \mu\text{Ci}/\text{m}^3$, while the combined deposition rate is $1.5\text{E-}07 \mu\text{Ci}/\text{m}^2/\text{year}$.

S.6 Operation Air Quality Impacts

The laser uranium-enrichment technology that would be used for the Proposed GLE Facility would not emit carbon monoxide, nitrogen oxides, sulfur dioxide, or volatile organic compounds. There is a potential for small gaseous releases associated with operation of the process that could contain uranium isotopes, hydrogen fluoride, and particulate uranyl fluoride. Any such gaseous releases would be contained within the main GLE operations building and routed to a high-efficiency, multi-stage emissions control system. The public health and ecological impacts associated with exposure to the cumulative ambient air uranium isotope concentrations predicted by XOQDOQ model for the Proposed GLE Facility with the existing FMO are discussed respectively in **Section 4.12, Public and Occupational Health**, and **Section 4.5, Ecological Resources Impacts**.

The operation of the Proposed GLE Facility would also result in small amounts of nonradioactive air emissions consisting of CO, NO_x, PM, VOCs, and SO₂ from the intermittent operation of auxiliary diesel electric generators and miscellaneous sources. The incremental air quality impacts from the operation of these sources at the Proposed GLE Facility are predicted to be SMALL and would not substantially change the ambient air quality in the vicinity of the Proposed GLE Facility.

[This page intentionally left blank.]

Tables

**Table S-1. Stack/Vent Characteristics Used for Proposed GLE Facility Operation
Ambient Air Dispersion Modeling**

Stack Group	Facility Stack ID#	Stack		Vented Gas Stream		
		Diameter m (in)	Release Height m (ft)	Velocity m/sec (ft/sec)	Flow Rate m ³ /sec (ft ³ /min)	Temperature
GLE Stack Group A	1	1.20 (47)	15.24 (50.0)	12.30 (40.4)	13.90 (29,452)	Ambient
FMO Stack Group B	5	0.25 (10)	3 (9.8)	11.50(37.7)	0.58 (1,235)	Ambient
	29	0.51 (20)	7 (23.0)	18.56 (60.9)	3.76 (7,970)	Ambient
FMO Stack Group C	1	1.12 (44)	20 (65.6)	14.43(47.3)	14.16 (30,000)	Ambient
	2	1.07 (42)	17 (55.8)	5.89 (19.3)	5.26 (11,155)	Ambient
	3	0.81 (32)	17 (55.8)	10.08(33.1)	5.23 (11,081)	Ambient
	4	0.30 (12)	17(55.8)	4.59 (15.1)	0.34 (710)	Ambient
	6	0.91 (36)	21(68.9)	9.65 (31.7)	6.34 (13,424)	Ambient
	7	0.64 (25)	18 (59.1)	15.21(49.9)	4.82 (10,204)	Ambient
	8	0.61 (24)	16 (52.5)	5.66 (18.6)	1.65 (3,501)	Ambient
	9	0.46 (18)	16.(52.5)	10.41 (34.2)	1.71 (3,621)	Ambient
	10	1.52 (60)	20 (65.6)	7.26 (23.8)	13.24 (28,064)	Ambient
	11	1.52 (60)	20 (65.6)	7.26 (23.8)	13.24 (28,064)	Ambient
	12	0.81 (32)	18 (59.1)	3.00 (9.8)	1.55 (3,294)	Ambient
	13	0.56 (22)	16 (52.5)	15.99 (52.5)	3.92 (8,311)	Ambient
	14	0.76 (30)	16 (52.5)	6.27 (20.6)	2.86(6,059)	Ambient
	15	0.56 (22)	17 (55.8)	15.28 (50.1)	3.75 (7,942)	Ambient
	16	0.46(18)	13 (42.7)	13.50 (44.3)	2.22(4,710)	(a)
	17	0.61 (24)	16 (52.5)	9.14 (30.0)	2.67 (5,652)	Ambient
	18	0.56 (22)	16 (52.5)	0.80 (2.6)	0.20 (417)	Ambient
	19	0.76 (30)	15 (49.2)	12.31 (40.4)	5.62 (11,898)	Ambient
	20	0.76 (30)	15 (49.2)	10.92 (35.8)	4.98 (10,553)	Ambient
	21	0.76 (30)	20 (65.6)	15.56 (51.0)	7.10 (15,038)	Ambient
	31	0.51 (20)	17 (55.8)	10.89 (35.7)	2.21 (4,677)	Ambient
	32	0.76 (30)	15 (49.2)	4.98 (16.3)	2.27 (4,808)	Ambient
	33	1.22 (48)	19 (62.3)	12.13 (36.8)	14.16 (30,000)	Ambient
	34	0.30 (12)	13 (42.7)	19.40 (63.6)	1.42 (3,000)	Ambient

^a Vent gas stream is from waste incinerator. Gas stream temperature assumed to be 100°F (37.8°C).

**Table S-2. Total Uranium and Uranium Isotope Emission Rates Used for
Proposed GLE Facility Operation Ambient Air Dispersion Modeling**

Stack Group	Facility Stack ID#	Uranium Isotope Emission Rate				
		Total U	²³⁴ U	²³⁵ U	²³⁶ U	²³⁸ U
		Ci/sec	Ci/sec	Ci/sec	Ci/sec	Ci/sec
GLE Stack Group A	1	1.47E-13	1.25E-13	4.88E-15	5.49E-17	1.77E-14
FMO Stack Group B	5	8.88E-16	7.52E-16	2.93E-17	3.30E-19	1.07E-16
	29	4.50E-15	3.81E-15	1.49E-16	1.68E-18	5.42E-16
FMO Stack Group C	1	1.47E-13	1.25E-13	4.88E-15	5.49E-17	1.77E-14
	2	9.89E-15	8.37E-15	3.27E-16	3.68E-18	1.19E-15
	3	1.58E-14	1.33E-14	5.23E-16	5.90E-18	1.90E-15
	4	2.85E-16	2.42E-16	9.42E-18	1.06E-19	3.42E-17
	6	2.19E-14	1.85E-14	7.23E-16	8.15E-18	2.63E-15
	7	1.65E-14	1.40E-14	5.45E-16	6.15E-18	1.99E-15
	8	2.70E-15	2.28E-15	8.91E-17	1.01E-18	3.23E-16
	9	2.76E-15	2.33E-15	9.10E-17	1.03E-18	3.33E-16
	10	9.39E-14	7.93E-14	3.10E-15	3.49E-17	1.13E-14
	11	5.30E-14	4.47E-14	1.75E-15	1.97E-17	6.34E-15
	12	2.63E-15	2.23E-15	8.69E-17	9.80E-19	3.16E-16
	13	4.66E-14	3.93E-14	1.53E-15	1.73E-17	5.58E-15
	14	2.51E-15	2.12E-15	8.28E-17	9.32E-19	3.01E-16
	15	6.94E-15	5.87E-15	2.30E-16	2.59E-18	8.34E-16
	16	4.44E-14	3.76E-14	1.46E-15	1.78E-17	5.34E-15
	17	3.87E-15	3.27E-15	1.28E-16	1.44E-18	4.66E-16
	18	3.84E-15	3.23E-15	1.27E-16	1.43E-18	4.60E-16
	19	1.14E-15	9.67E-16	3.77E-17	4.25E-19	1.37E-16
	20	7.07E-15	5.99E-15	2.34E-16	2.64E-18	8.50E-16
	21	1.46E-14	1.24E-14	4.85E-16	5.45E-18	1.76E-15
	31	3.03E-14	2.56E-14	1.00E-15	1.13E-17	3.65E-15
	32	3.52E-15	2.98E-15	1.16E-16	1.31E-18	4.22E-16
	33	1.67E-13	1.41E-13	5.52E-15	6.22E-17	2.00E-14
	34	9.01E-15	7.61E-15	2.98E-16	3.36E-18	1.08E-15

Table S-3. Predicted Unitized Concentration (Chi/Q) and Relative Deposition (D/Q) for Selected Receptors from Proposed GLE Facility Operation Air Emissions

Receptor Location	Direction From Proposed GLE Facility	Distance From Proposed GLE Facility	Chi/Q sec/m³	D/Q 1/m²
Highest on-site impact	NE	0.25 mi (0.4 km)	1.3E-06	1.9E-08
Highest off-site impact (fenceline)	NE	0.3 mi (0.5 km)	1.3E-06	1.6E-08
Nearest resident ^a	ESE	0.9 mi (1.5 km)	2.7E-07	1.3E-09
Writesboro Elementary School	SSE	3.4 mi (5.4 km)	2.1E-07	1.8E-10
Emma B. Trask Middle School	ESE	4.7 mi (7.5 km)	9E-08	9.9E-11
Emsley A. Laney High School	SE	5.2 mi (0.4 km)	9.6E-08	9.3E-11
New Hanover Regional Medical Center	S	9.0 mi (14.5 km)	1.9E-07	1.1E-10
Pender Memorial Hospital	N	14.9 mi (24.0 km)	6.9E-08	4.4E-11
Brunswick Community Hospital ^a	SW	29.8 mi (48.0 km)	2.0E-08	1.3E-11

^a Not specified in model as a discrete receptor. Value calculated using geographic information systems (i.e., GIS) spatial averaging techniques.

Table S-4. Predicted Unitized Concentration (Chi/Q) for Receptors Close to the Proposed GLE Facility (< 5 miles)

NO DECAY, UNDEPLETED ANNUAL AVERAGE CHI/Q (SEC/METER CUBED) SECTOR	DISTANCE IN MILES FROM THE SITE										
	.250	.500	.750	1.000	1.500	2.000	2.500	3.000	3.500	4.000	4.500
S	1.206E-06	9.578E-07	8.763E-07	8.957E-07	8.545E-07	7.513E-07	6.493E-07	5.630E-07	4.925E-07	4.351E-07	3.880E-07
SSW	1.082E-06	8.107E-07	6.245E-07	5.345E-07	4.216E-07	3.411E-07	2.819E-07	2.377E-07	2.040E-07	1.777E-07	1.568E-07
SW	9.261E-07	7.319E-07	5.948E-07	5.358E-07	4.486E-07	3.735E-07	3.137E-07	2.672E-07	2.310E-07	2.023E-07	1.792E-07
WSW	6.122E-07	4.990E-07	4.484E-07	4.457E-07	4.133E-07	3.595E-07	3.090E-07	2.671E-07	2.332E-07	2.057E-07	1.832E-07
W	7.466E-07	5.516E-07	5.176E-07	5.562E-07	5.584E-07	5.012E-07	4.378E-07	3.821E-07	3.357E-07	2.975E-07	2.659E-07
WNW	5.178E-07	3.550E-07	3.300E-07	3.571E-07	3.622E-07	3.266E-07	2.861E-07	2.501E-07	2.200E-07	1.952E-07	1.746E-07
NW	6.104E-07	4.200E-07	3.758E-07	3.915E-07	3.844E-07	3.429E-07	2.988E-07	2.604E-07	2.286E-07	2.025E-07	1.809E-07
NNW	6.656E-07	4.648E-07	3.917E-07	3.816E-07	3.515E-07	3.057E-07	2.630E-07	2.274E-07	1.986E-07	1.752E-07	1.561E-07
N	9.495E-07	7.537E-07	6.626E-07	6.477E-07	5.920E-07	5.121E-07	4.391E-07	3.789E-07	3.304E-07	2.913E-07	2.593E-07
NNE	1.091E-06	8.064E-07	6.561E-07	6.080E-07	5.304E-07	4.506E-07	3.828E-07	3.286E-07	2.855E-07	2.510E-07	2.231E-07
NE	1.328E-06	9.797E-07	7.858E-07	7.065E-07	5.927E-07	4.943E-07	4.156E-07	3.544E-07	3.065E-07	2.686E-07	2.380E-07
ENE	1.057E-06	7.642E-07	6.407E-07	5.921E-07	5.076E-07	4.265E-07	3.599E-07	3.075E-07	2.664E-07	2.337E-07	2.072E-07
E	1.031E-06	7.092E-07	5.869E-07	5.444E-07	4.710E-07	3.979E-07	3.368E-07	2.884E-07	2.501E-07	2.196E-07	1.949E-07
ESE	5.752E-07	3.837E-07	2.991E-07	2.696E-07	2.292E-07	1.924E-07	1.624E-07	1.388E-07	1.202E-07	1.054E-07	9.349E-08
SE	5.880E-07	4.190E-07	3.378E-07	3.110E-07	2.690E-07	2.273E-07	1.924E-07	1.647E-07	1.428E-07	1.254E-07	1.113E-07
SSE	5.946E-07	4.303E-07	3.777E-07	3.794E-07	3.583E-07	3.141E-07	2.711E-07	2.349E-07	2.054E-07	1.814E-07	1.617E-07

Table S-5. Predicted Unitized Concentration (Chi/Q) for Receptors Far from the Proposed GLE Facility (5 mi – 50 miles)

NO DECAY, UNDEPLETED											
ANNUAL AVERAGE CHI/Q (SEC/METER CUBED)											
SECTOR	5.000	7.500	10.000	15.000	DISTANCE IN MILES FROM THE SITE						
					20.000	25.000	30.000	35.000	40.000	45.000	50.000
S	3.492E-07	2.273E-07	1.649E-07	1.034E-07	7.372E-08	5.654E-08	4.545E-08	3.776E-08	3.214E-08	2.786E-08	2.452E-08
SSW	1.399E-07	8.874E-08	6.353E-08	3.929E-08	2.782E-08	2.123E-08	1.701E-08	1.409E-08	1.196E-08	1.035E-08	9.092E-09
SW	1.603E-07	1.026E-07	7.379E-08	4.583E-08	3.254E-08	2.489E-08	1.996E-08	1.656E-08	1.407E-08	1.219E-08	1.072E-08
WSW	1.646E-07	1.068E-07	7.728E-08	4.834E-08	3.445E-08	2.641E-08	2.122E-08	1.762E-08	1.500E-08	1.300E-08	1.144E-08
W	2.397E-07	1.569E-07	1.141E-07	7.178E-08	5.129E-08	3.939E-08	3.169E-08	2.634E-08	2.243E-08	1.946E-08	1.713E-08
WNW	1.575E-07	1.032E-07	7.505E-08	4.720E-08	3.373E-08	2.591E-08	2.084E-08	1.733E-08	1.476E-08	1.280E-08	1.127E-08
NW	1.630E-07	1.065E-07	7.733E-08	4.855E-08	3.467E-08	2.661E-08	2.140E-08	1.779E-08	1.515E-08	1.314E-08	1.157E-08
NNW	1.404E-07	9.109E-08	6.595E-08	4.128E-08	2.944E-08	2.258E-08	1.815E-08	1.508E-08	1.283E-08	1.113E-08	9.792E-09
N	2.330E-07	1.509E-07	1.092E-07	6.825E-08	4.860E-08	3.724E-08	2.991E-08	2.483E-08	2.113E-08	1.831E-08	1.611E-08
NNE	2.001E-07	1.290E-07	9.305E-08	5.795E-08	4.117E-08	3.149E-08	2.527E-08	2.096E-08	1.782E-08	1.543E-08	1.357E-08
NE	2.131E-07	1.366E-07	9.822E-08	6.099E-08	4.328E-08	3.308E-08	2.653E-08	2.200E-08	1.870E-08	1.619E-08	1.424E-08
ENE	1.857E-07	1.194E-07	8.601E-08	5.356E-08	3.808E-08	2.915E-08	2.340E-08	1.942E-08	1.652E-08	1.431E-08	1.259E-08
E	1.747E-07	1.125E-07	8.108E-08	5.051E-08	3.593E-08	2.751E-08	2.209E-08	1.834E-08	1.560E-08	1.352E-08	1.189E-08
ESE	8.377E-08	5.388E-08	3.885E-08	2.422E-08	1.724E-08	1.321E-08	1.061E-08	8.813E-09	7.498E-09	6.500E-09	5.719E-09
SE	9.979E-08	6.432E-08	4.643E-08	2.898E-08	2.063E-08	1.580E-08	1.269E-08	1.054E-08	8.961E-09	7.767E-09	6.832E-09
SSE	1.455E-07	9.468E-08	6.868E-08	4.307E-08	3.073E-08	2.358E-08	1.895E-08	1.575E-08	1.340E-08	1.162E-08	1.023E-08

Table S-6. Predicted Relative Deposition (D/Q) for Receptors Close to the Proposed GLE Facility (< 5 miles)

***** RELATIVE DEPOSITION PER UNIT AREA (M**2) AT FIXED POINTS BY DOWNWIND SECTORS *****											
DIRECTION FROM SITE	DISTANCES IN MILES										
	.25	.50	.75	1.00	1.50	2.00	2.50	3.00	3.50	4.00	4.50
S	1.774E-08	8.869E-09	4.880E-09	2.922E-09	1.477E-09	9.027E-10	6.148E-10	4.514E-10	3.512E-10	2.865E-10	2.430E-10
SSW	1.509E-08	8.005E-09	4.442E-09	2.652E-09	1.341E-09	8.169E-10	5.538E-10	4.041E-10	3.119E-10	2.520E-10	2.116E-10
SW	1.317E-08	6.787E-09	3.748E-09	2.239E-09	1.131E-09	6.897E-10	4.686E-10	3.432E-10	2.662E-10	2.165E-10	1.830E-10
WSW	9.222E-09	4.491E-09	2.458E-09	1.470E-09	7.415E-10	4.532E-10	3.088E-10	2.270E-10	1.769E-10	1.447E-10	1.230E-10
W	1.183E-08	5.532E-09	3.011E-09	1.804E-09	9.101E-10	5.569E-10	3.794E-10	2.784E-10	2.160E-10	1.755E-10	1.480E-10
WNW	9.125E-09	3.727E-09	1.969E-09	1.172E-09	5.858E-10	3.582E-10	2.443E-10	1.794E-10	1.393E-10	1.132E-10	9.539E-11
NW	1.069E-08	4.339E-09	2.286E-09	1.360E-09	6.783E-10	4.145E-10	2.826E-10	2.077E-10	1.614E-10	1.314E-10	1.109E-10
NNW	1.113E-08	4.770E-09	2.544E-09	1.515E-09	7.583E-10	4.632E-10	3.155E-10	2.315E-10	1.796E-10	1.460E-10	1.231E-10
N	1.405E-08	6.952E-09	3.815E-09	2.280E-09	1.150E-09	7.026E-10	4.784E-10	3.514E-10	2.737E-10	2.238E-10	1.902E-10
NNE	1.514E-08	8.147E-09	4.526E-09	2.699E-09	1.363E-09	8.295E-10	5.621E-10	4.104E-10	3.173E-10	2.570E-10	2.165E-10
NE	1.895E-08	9.444E-09	5.177E-09	3.084E-09	1.552E-09	9.457E-10	6.430E-10	4.720E-10	3.676E-10	3.005E-10	2.557E-10
ENE	1.696E-08	6.918E-09	3.648E-09	2.167E-09	1.081E-09	6.615E-10	4.531E-10	3.360E-10	2.650E-10	2.200E-10	1.901E-10
E	1.718E-08	7.134E-09	3.774E-09	2.242E-09	1.118E-09	6.828E-10	4.660E-10	3.434E-10	2.684E-10	2.202E-10	1.877E-10
ESE	9.228E-09	4.045E-09	2.167E-09	1.291E-09	6.467E-10	3.949E-10	2.687E-10	1.970E-10	1.526E-10	1.237E-10	1.041E-10
SE	8.568E-09	4.088E-09	2.228E-09	1.331E-09	6.703E-10	4.095E-10	2.788E-10	2.046E-10	1.591E-10	1.297E-10	1.098E-10
SSE	9.038E-09	4.324E-09	2.360E-09	1.411E-09	7.118E-10	4.350E-10	2.960E-10	2.169E-10	1.682E-10	1.365E-10	1.151E-10

Table S-7. Predicted Relative Deposition (D/Q) for Receptors Far from the Proposed GLE Facility (5 mi – 50 miles)

***** RELATIVE DEPOSITION PER UNIT AREA (M ⁻²) AT FIXED POINTS BY DOWNWIND SECTORS *****											
DIRECTION FROM SITE	DISTANCES IN MILES										
	5.00	7.50	10.00	15.00	20.00	25.00	30.00	35.00	40.00	45.00	50.00
S	2.136E-10	1.318E-10	9.392E-11	5.516E-11	3.544E-11	2.411E-11	1.746E-11	1.323E-11	1.039E-11	8.413E-12	6.972E-12
SSW	1.843E-10	1.100E-10	7.699E-11	4.444E-11	2.836E-11	1.923E-11	1.387E-11	1.047E-11	8.182E-12	6.595E-12	5.434E-12
SW	1.604E-10	9.810E-11	6.955E-11	4.064E-11	2.605E-11	1.768E-11	1.276E-11	9.642E-12	7.539E-12	6.081E-12	5.015E-12
WSW	1.084E-10	6.744E-11	4.826E-11	2.847E-11	1.832E-11	1.247E-11	9.031E-12	6.844E-12	5.368E-12	4.345E-12	3.597E-12
W	1.292E-10	7.759E-11	5.450E-11	3.170E-11	2.042E-11	1.400E-11	1.022E-11	7.812E-12	6.175E-12	5.036E-12	4.200E-12
WNW	8.302E-11	4.931E-11	3.446E-11	2.005E-11	1.304E-11	9.035E-12	6.665E-12	5.147E-12	4.095E-12	3.364E-12	2.821E-12
NW	9.673E-11	5.788E-11	4.062E-11	2.373E-11	1.544E-11	1.069E-11	7.877E-12	6.073E-12	4.824E-12	3.955E-12	3.310E-12
NNW	1.073E-10	6.412E-11	4.495E-11	2.618E-11	1.696E-11	1.169E-11	8.575E-12	6.578E-12	5.204E-12	4.248E-12	3.540E-12
N	1.677E-10	1.045E-10	7.487E-11	4.416E-11	2.839E-11	1.928E-11	1.393E-11	1.053E-11	8.244E-12	6.660E-12	5.504E-12
NNE	1.893E-10	1.146E-10	8.085E-11	4.696E-11	2.998E-11	2.029E-11	1.462E-11	1.102E-11	8.610E-12	6.939E-12	5.722E-12
NE	2.258E-10	1.414E-10	1.016E-10	6.004E-11	3.858E-11	2.616E-11	1.885E-11	1.422E-11	1.109E-11	8.931E-12	7.352E-12
ENE	1.699E-10	1.108E-10	8.132E-11	4.913E-11	3.196E-11	2.184E-11	1.584E-11	1.201E-11	9.405E-12	7.604E-12	6.279E-12
E	1.655E-10	1.031E-10	7.392E-11	4.387E-11	2.850E-11	1.957E-11	1.427E-11	1.089E-11	8.564E-12	6.955E-12	5.766E-12
ESE	9.052E-11	5.367E-11	3.746E-11	2.172E-11	1.405E-11	9.683E-12	7.096E-12	5.437E-12	4.295E-12	3.500E-12	2.910E-12
SE	9.637E-11	5.905E-11	4.193E-11	2.459E-11	1.583E-11	1.079E-11	7.828E-12	5.938E-12	4.657E-12	3.769E-12	3.116E-12
SSE	1.005E-10	6.046E-11	4.250E-11	2.472E-11	1.590E-11	1.087E-11	7.908E-12	6.025E-12	4.745E-12	3.856E-12	3.204E-12

[This page intentionally left blank.]

Figures

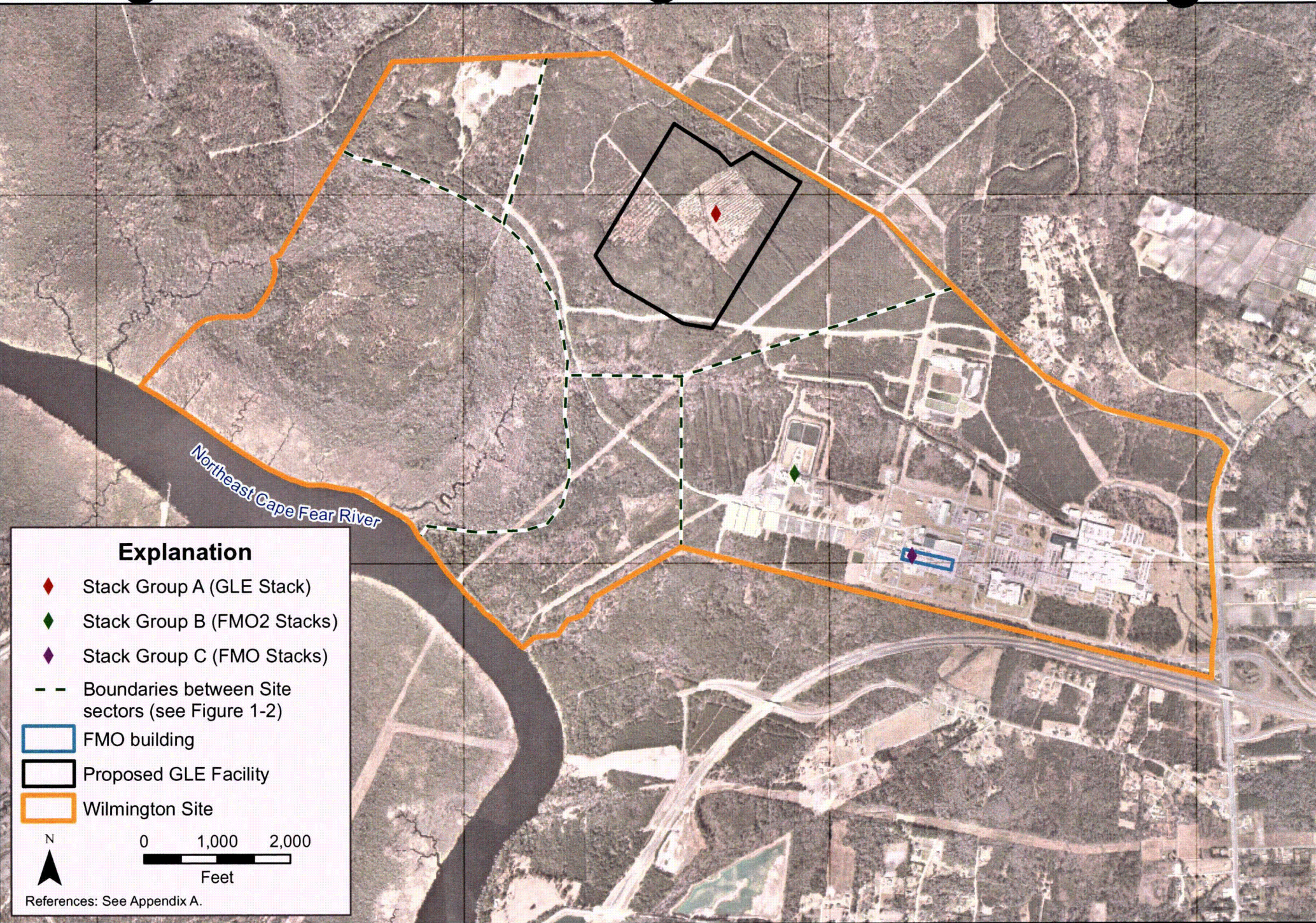


Figure S-1. Approximate relative location of stack groups used in XOQDOQ modeling.

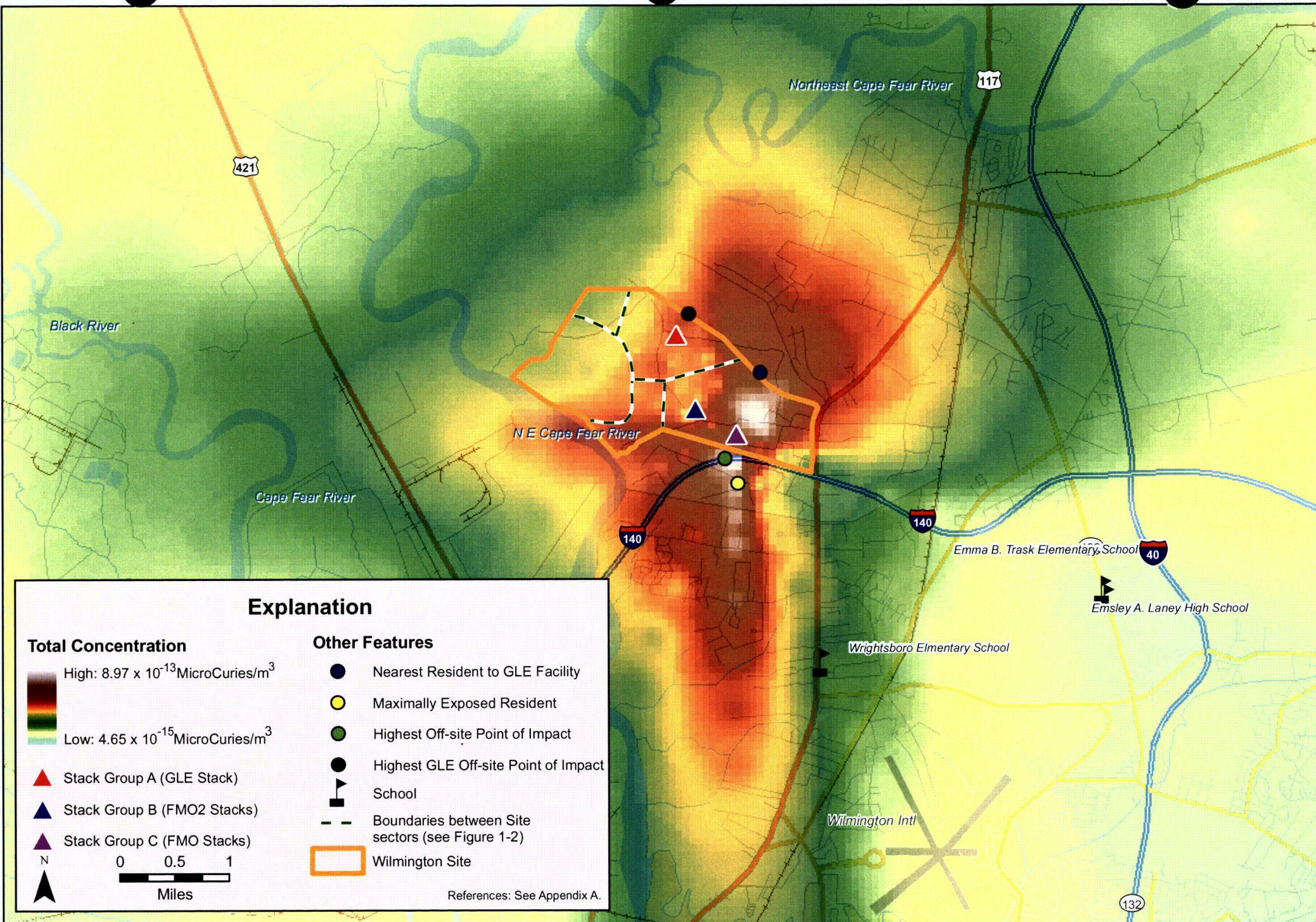


Figure S-2. Annual average concentration of radioisotopes from all stacks at the Wilmington Site.

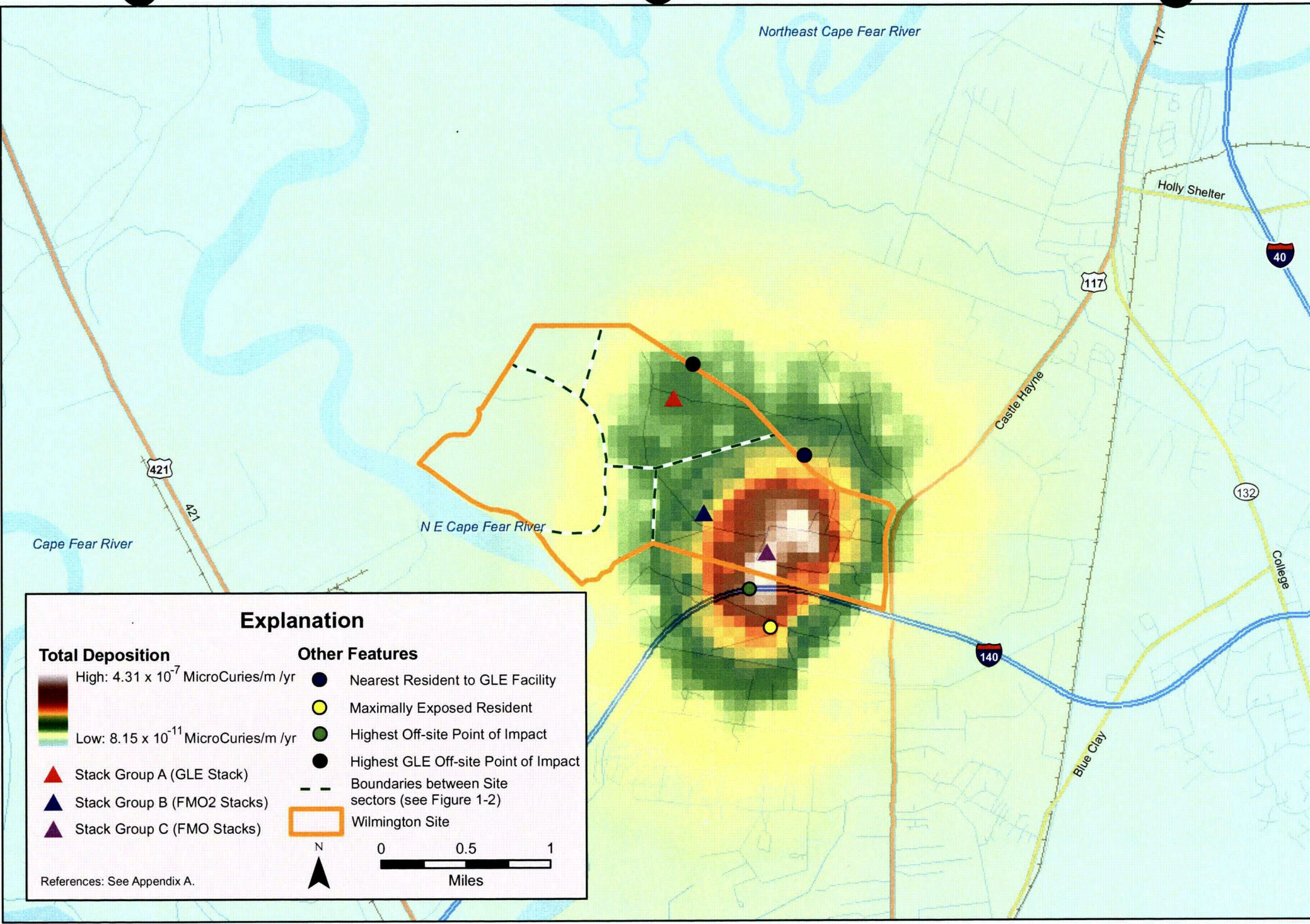


Figure S-3. Annual deposition rate of radioisotopes from all stacks at the Wilmington Site.

Table of Contents

T.1	Geometry Elements	T-1
T.2	Road Construction Noise Sources	T-1
T.3	Site Preparation Noise Sources.....	T-1
T.4	Facility Operations Noise Sources	T-2

[This page intentionally left blank.]

Appendix T

Facility-Specific Data Input and Assumptions Required for the Cadna/A[®] Noise Model

T.1 Geometry Elements

- Topography: Acquired for New Hanover County. The site was slightly modified to represent the flat terrain where the Proposed GLE Facility would be located.
- Existing Buildings: Determined from aerial photos and observations during site visit.
- Future Buildings (used only in study of Facility Operations): Acquired from proposed site plan.

T.2 Road Construction Noise Sources

- Dozers: 4 per day
- Graders: 2 per day
- Loader: 4 per day
- Rollers: 2 per day
- Excavator: 1 per day
- Water Truck: 1 per day

These sources were positioned on the plan for the North Road portion of the GLE Study Area, which includes a proposed new road segment, and defined as a moving source with a speed of 1 mile per hour to represent road-building operations. The source levels for the construction equipment (built circa 1995) were based on sound levels measured from construction equipment outfitted with standard muffler and noise-control devices (no special noise control was considered). The source level for the water truck was based on the sound levels obtained from the Federal Highway Administration Traffic Noise Model[®] (FHWA TNM[®]) program (Federal Highway Administration, 1998). The operating hours of these sources were defined between 7 a.m. and 6 p.m.

T.3 Site Preparation Noise Sources

- Dozers: 4 per day
- Graders: 2 per day
- Loader: 4 per day
- Rollers: 2 per day
- Excavator: 1 per day
- Water truck: 1 per day
- Passenger vehicles: 375 per day
- Hauling vehicles: 35 per day

The heavy construction sources were positioned around the GLE Study Area in static locations to represent the average locations where this equipment may be during GLE Facility site preparation operations. The vehicles (i.e., hauling trucks and passenger vehicles) were located in the model along the

line of the new road segment in the North Road portion of the GLE Study Area. The source levels for the construction equipment were based on sound levels measured from construction equipment (built circa 1995) outfitted with standard muffler and noise-control devices (no special noise control was considered). The source levels for the water truck, hauling trucks, and passenger vehicles were based on the sound levels obtained from FHWA TNM program (Federal Highway Administration, 1998). The operating hours of these sources were defined between 7 a.m. and 6 p.m.

T.4 Facility Operations Noise Sources

- Passenger vehicles: 375 per day
- Hauling vehicles: 6 per day
- Cylinder hauling vehicles dedicated to Proposed GLE Facility: 4 per day
- Hauling vehicles using the western connector to existing facility: 2 per day
- Air handling units: 4
- Scrubber exhaust^a: 1
- Cooling tower: 2
- Heat pumps: 2 per service building (6 total)
- Pump/lift station (25 horsepower [hp]): 2
- Electrical substation (60,000 kilovolt-amperes [kVA]): 1

The hauling vehicles and passenger vehicles were located in the model along the line of the new road segment. The hauling vehicles dedicated to the Facility were located to the southwest of the Facility for moving cylinders. The hauling vehicles using the existing south road that will connect the Proposed GLE Facility to the existing Wilmington Site facilities were located along this access road. The source levels for the hauling trucks and passenger vehicles were based on the sound levels obtained from FHWA TNM program (Federal Highway Administration, 1998). The operating hours of the passenger vehicle sources were defined to be spread evenly over a 24-hour period. The operating hours of all the hauling vehicles sources were defined with 90% of traffic occurring during daytime hours and 10% occurring during evening hours.

The air handling units, scrubber exhaust^a, and cooling towers are located on the rooftop of the proposed GLE operations building. Heat pumps are located on each of the service buildings. The two pump/lift stations and electrical substation are positioned to the southeast of the Proposed GLE Facility, near the vehicular entrance. All of this equipment is modeled as operating for 24 hours per day. The source levels of the pumps were estimated based on the horsepower of the pump motor (Hoover and Keith, 1996). The sound levels of the transformer were based on this being an outdoor, forced-air-cooled, immersed oil transformer of standard design with a capacity of 60,000 kVA (Ver and Anderson, 1977; National Electrical Manufacturers Association, 2000).

^a Although scrubber exhaust noise was considered in this impacts assessment, the scrubber subsequently was removed from the Proposed GLE Facility design. Therefore, this is a conservative assessment of noise impacts from the operations phase of the Proposed Action.